ONE DIMENSIONAL SITE RESPONSE ANALYSIS OF A POWER PLANT SITE BEFORE AND AFTER GROUND IMPROVEMENT

ANAN DAS BRISTI

MILITARY INSTITUTE OF SCIENCE AND TECHNOLOGY

2020

ONE DIMENSIONAL SITE RESPONSE ANALYSIS OF A POWER PLANT SITE BEFORE AND AFTER GROUND IMPROVEMENT

ANAN DAS BRISTI

(*MSc Engineering, MIST*)

A THESIS SUBMITTED FOR THE DEGREE OF MASTER OF ENGINEERING

DEPARTMENT OF CIVIL ENGINEERING
MILITARY INSTITUTE OF SCIENCE AND TECHNOLOGY

2020

The thesis titled ONE DIMENSIONAL SITE RESPONSE ANALYSIS OF A POWERPLANT SITE BEFORE AND AFTER GROUND IMPROVEMENT Submitted by Anan Das Bristi, Roll No: 1016110008, Session: 2016-18 has been accepted as satisfactory in partial fulfillment of the requirement for the degree of Msc in Civil Engineering on 10th June, 2020.

BOARD OF EXAMINERS

1. Chairman
Dr. Mehedi Ahmed Ansary
Professor, Department of CE, BUET

2. Member
Dr. Md. Zoynul Abedin
Professor, Department of CE, MIST

3. Member
Brig Gen Wahidul Islam, SUP, ndc, psc (Ex-officio)
Professor, MIST
Head of the Department, Department of CE, MIST

4. External Member
Dr. Syed Abdul Mofiz
Professor, Department of CE, RUET

"*Declaration*

I hereby declare that this thesis is my original work and it has been written by me in its entirety. I have duly acknowledged all the sources of information which have been used in the thesis. The thesis (fully or partially) has not been submitted for any degree or diploma in any university or institute previously."

Date:

_____

Author

Acknowledgment

I would like to express my gratitude and appreciation to Dr. Mehedi Ahmed Ansary, Professor, Department of Civil Engineering, Bangladesh University of Engineering & Technology (BUET), Dhaka, whose guidance, support and encouragement has been invaluable throughout this study. The author wishes to express his profound gratitude and sincere appreciation to her supervisor, Dr. Mehedi Ahmed Ansary, It would not be possible for the author to carry out this study without his continuous guidance and inspiration.

Table of Contents

List of Figures

List of Tables

Abstract

The purpose of this research is to measure amplification factor of a power plant site before and after ground improvement. Eight earthquakes with different frequency content (ChiChi, Coyote, Kobe, Loma Girloy, Nahani, Northridge, Mammoth, & Parkfield earthquakes) were selected to do the analysis. The analyses were mainly based on shear wave velocity. Soil parameters and other data were collected from the Power Plant Site. In this location Ground Improvement was done by deep mixing with cement.

Soil model before ground improvement mainly considered as silty fine sand with shear wave velocity of 160 m/s at ground level to 640 m/s at 120m depth. Similarly, after ground improvement shear wave velocity was 1100 m/s at ground level to 640 m/s at 120m depth. For estimating site amplification factor, computer program DEEPSOIL was used. With soil layer depth, unit weight (γ) and shear wave velocity (Vs) as inputs, soil amplification by equivalent linear analysis was estimated. Amplitude ratio versus frequency (Hz), Peak Ground Acceleration (PGA) versus depth, Acceleration versus time, normalized Peak Surface Acceleration (PSA) versus period were plotted both for the above two models.

After combining all the earthquakes, the mean value amplitude ratio decreased from almost 12 before ground improvement to 9 after ground improvement though the frequency was the

same. PSA value decreased from 0.6 to 0.3 within the same period of time. We cannot find any significant change in the normalized PSA value. After ground improvement the mean PGA value of all the earthquakes decreased to 0.15g from 0.30g which is a significant amount.

CHAPTER ONE
INTRODUCTION

1.1 General

Predicting site response is an important part of geotechnical earthquake engineering. Site response analyses are performed to evaluate the influence of the local soil deposit on strong ground shaking, with the resulting surface response spectrum being used in seismic design. The traditional approach is to perform one-dimensional (1D) site response analyses for multiple 1D profile. Increasing number of Nuclear Power Plant (NPP) has increased the concern for safety. Earthquake is one of the important factors that can cause catastrophic structural damage to nuclear reactors. About one-fifth of the operating nuclear plants are located in seismically activity zones. Hence, robust modelling techniques and stringent design methodologies should be ensured for the nuclear plant structures situated in seismic regions. With increasing energy demand, use of nuclear energy has increased worldwide, which in turn led to construction of more number of nuclear power plants (NPP). In order to estimate site response we propose a method to estimate site amplification factors of seismic intensity which are obtained using shear wave velocity of different soil layers.

Effect of Shear wave velocity (V_S) contrast in ground response analysis V_S is an important parameter of seismic site response analysis. This has been a wide spread practice in the community for decades as this simplification is advantageous to the day-to-day geotechnical engineering related computations (both analytical and numerical). Site response analysis provides surface acceleration time series, surface acceleration response spectra, and spectral amplification factors based on the dynamic response of

local soil conditions. In most cases, 1D site response analysis is performed to assess the effect of soil conditions on ground shaking because vertically propagating and horizontally polarized shear waves dominate the earthquake ground motion wave field. Frequency domain (FD) equivalent linear (EQL) are the most common approaches used to perform 1D seismic site response analysis.

1.2 Objectives with Specific Aims

The objective of the study is to compare the site amplification factors before and after ground improvement. Local site response analyses will be carried out after the one-dimensional stratigraphic model is completely defined.

1.3 Outline of Methodology

Dynamic behavior of soils is quite complex and requires models which characterize the important aspects of cyclic behavior, but need to be simple, rational models.

The procedure applied herein to propose site-dependent amplification factors is shown below:

(i) Estimation of soil stratification, shear wave profile, shear modulus degradation curves, damping ratio, through in-situ and laboratory testing.
(ii) Development of 1D soil models before and after soil improvement.
(iii) Perform 1D site response analysis for different ground motion.

1.4 Organization of the Thesis

The thesis consists of five chapters. Chapter one describes the background of the current research, its scopes, objectives, and methodology. Chapter two presents the geology and geomorphology, seismic zonation, Past research of site response and also different softwares for analyzing, numerical data have been described. Chapter three describes the methodology of the analysis. Chapter four is the main part of this research which represents site data collection and analysis, various effects on the result, Comparison of the results and their interpretation. Chapter five is the conclusions and recommendations. The results and different graphical explanation have been summarized in this chapter. Some recommendations for future work has also been described in this chapter.

CHAPTER TWO
LITERATURE REVIEW

2.1 General

The local soil conditions have a profound influence on ground response during earthquakes. The recent destructive earthquakes have again demonstrated that the topography, nature of the bedrock and nature and geometry of the depositional soils are the primary factors that influence local modifications to the underlying motion. Site response analysis is commonly performed to account for local site effects on ground motion propagation during an earthquake. Earthquakes in the last 50 years have demonstrated the role of site effects in the distribution and magnitude of the damages associated with a seismic event to be paramount. In 1985 an 8.1 magnitude earthquake caused significant casualties and extensive damage in Mexico city. The occurrence of damage in a city located 350 km from the earthquake epicenter has been attributed to the amplification of seismic waves throughout the city's unconsolidated lacustrine deposit. Seismic events such as the Loma Prieta 1989, Northridge 1994 Kobe 1995, and Chi-Chi 1999 earthquakes have corroborated the significance of local geologic and geomorphologic conditions on the seismic ground response. The changes in the intensity and the frequency content of the motion due to the propagation of the seismic waves in soil deposits and the presence of topographic features, commonly referred to as site effects, have a direct impact on the response of structures during each of these earthquake events. The behavior of soil under cyclic loading is often non-linear and depends on several factors including amplitude of loading, number of cycles, soil type and in situ confining pressure.

In order to carry out site response analyses, with the aim of determining the amplification of seismic motion through the profile, a simplified model of the profile is needed. In particular, the definition of a one-dimensional soil profile, as adopted in this study, requires an identification of layers, i.e. homogeneous soil areas to which a single value of a certain number of geotechnical parameters is associated.

2.2 Regional Tectonics

Plate tectonics provide a physically simple mechanism for large-scale horizontal motions of separate portions of the earth's crust. One of the central concepts of plate tectonics is that a small number of large plates of high strength lithosphere, move rigidly with respect to one another at rates of 1 to 20 cm/year over the low-strength asthenosphere. For the past 40 million years the Indian subcontinent has been pushing northward against the Eurasian plate at a rate of 5 cm/year, giving rise to the severest earthquakes and most diverse land forms known. Figure 2.1 estimated slip potential along the Himalaya and Figure 2.2 showed India's northward drift over the last 70 million years.

The region of northeastern India, northern Burma and Southwestern China is tectonically and seismically one of the most interesting active plate boundaries. The region comprises the Himalayas, the Indo-Burma Ranges, the Tripura folded belt, the Bengal Basin, the Shillong Plateau and the Assam Valley. Figure 2.3 shows the generalized tectonic map of Bangladesh and adjoining areas (BNBC, 1993). It is a rifted eastern marginal basin of Indian plate that is gradually shortening due to the subduction of the Indian plate and overriding of the Burmese plate from the east.

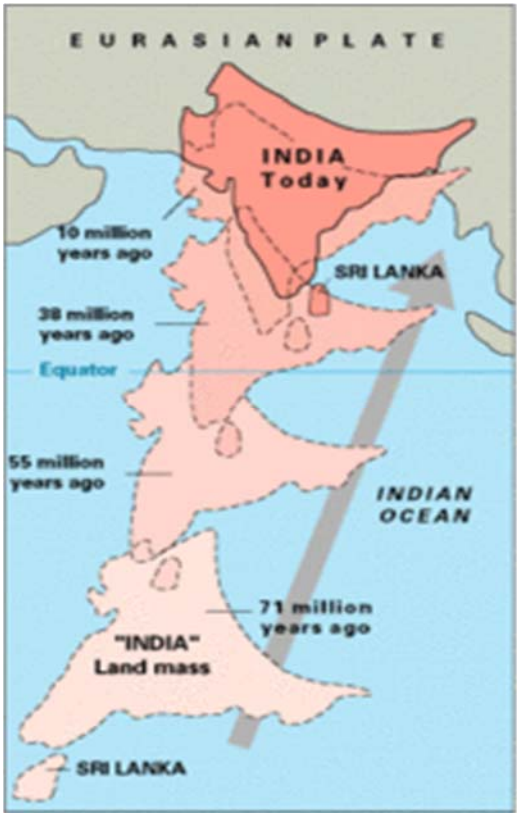

Fig. 2.1 India's northward drift over the last 70 million years

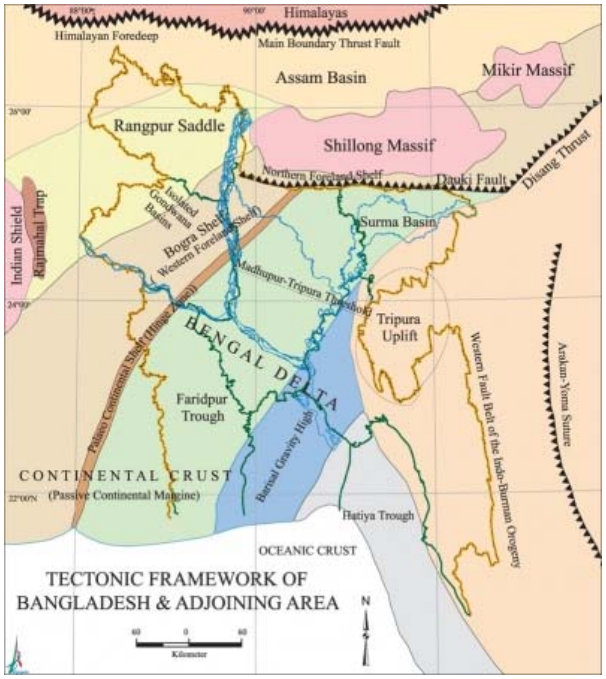

Fig. 2.2 Generalized tectonic map of Bangladesh and adjoining areas (After GSB, 1991)

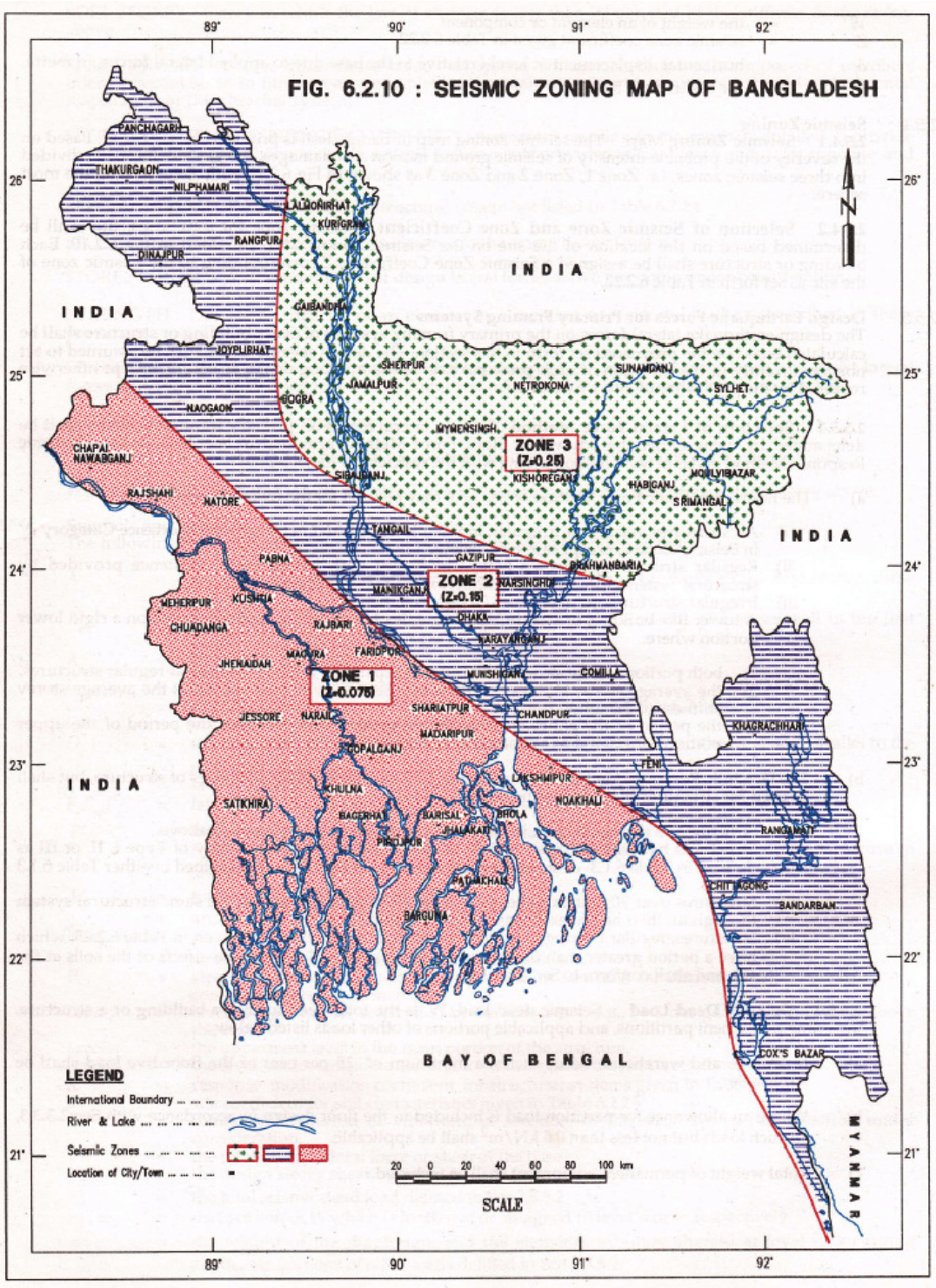

Fig. 2.3 Seismic zoning map of Bangladesh (after BNBC, 1993)

2.3 Seismotectonic Setup

Bangladesh is divided into three major tectonic zones: (i) The Shelf zone: It consists of mainly the northwestern part of the country including the districts of Rangpur, Dinajpur and Bogra; (ii) The Hinge zone: It passes through Calcutta, Pabna, Mymensingh and extend further NE across the Dauki fault and (iii) The Bengal Foredeep zone: It comprises of the rest of area of the country and occupies the area between the Shelf zone in the west and Arakan-Yoma Hill range in the east. The deep basin area of the foredeep is composed of the Surma Basin or Sylhet Trough, Faridpur Trough and the Hatia Trough.

The junction between the platform and the foredeep running southwest from Mymensingh to Calcutta (the Hinge line) is considered to be a zone of weakness. However, no association of the hinge with earthquakes has so far been established. The Foredeep is terminated in the northeast by a major fault, the Dauki fault at the southern margin of the Shillong Plateau. Some major earthquakes can be related to this fault. There are numerous faults particularly in the eastern part of the folded flank of the Foredeep. Here again there is no association with any major earthquake. Most recorded earthquakes had epicenter further east in Burma.

The eastern margin of the Indian plate is supposed to run through Myanmar, not far from the Bangladesh border, and northeast Assam (Arunachal Pradesh) is considered to be a corner of the northern and eastern margins of the plate.

The Himalayan arc can be regarded as one of the most intensely active seismic regions of the world. In northeast India, the Shillong plateau and adjacent syntaxis between the two arcuate structures is one of the most unstable regions in the Alpine-Himalayan belt and

faced three major earthquakes of magnitude greater than 8.0 within the last two hundred years (1897, 1934, and 1950).

At present, the southernmost thrusting in the Himalaya-Shillong Plateau region could be taking place along the southern fringe of the plateau coinciding with the Dauki fault. Currently, it is believed that the Shillong plateau has a thrust plane beneath it and is undergoing southward thrusting against a concept of vertical tectonism along the Dauki fault.

The Shillong plateau and its adjoining region including the northeastern part of Bangladesh have high seismic status. The seismic activity along the Dauki-Haflong fault zone is comparatively lower and a seismic gap has been postulated along this fault zone.

The major earthquakes that have affected Bangladesh since the middle of the last century are presented in Table 2.1.

Table 2.1 Great historical earthquakes in and around Bangladesh

Date	Name	Epicentre	Magnitude (M)
10-1-1869	Cachar Earthquake	Jantia Hill, Assam	7.5
14-7-1885	Bengal Earthquake	Sirajgonj, Bangladesh	7.0
12-6-1897	Great Indian Earthquake	Shilong Plateaue	8.7
18-7-1918	Srimongol Earthquake	Srimongol, Sylhet	7.6
2-7-1930	Dhubri Earthquake	Dhubri, Assam	7.1
15-1-1934	Bihar, Nepal Earthquake	Bihar, India	8.3

2.4 Major Seismic Sources

The seismic hazard is typically determined using a combination of seismological, morphological, geological and geotechnical investigations, combined with the history of earthquake in the region. Bolt (1987) analyzed different seismic sources in and around Bangladesh and arrived at conclusions related to maximum likely earthquake magnitude

(Bolt, 1987). Bolt identified the following four major sources: Assam fault zone; Tripura fault zone; Sub- Dauki fault zone, and Bogra fault zone. A brief description of geology, tectonics of the individual fault zone is given below:

Assam Fault Zone

The east-west fault separates the Assam fault zone from sub-Dauki fault zone. This zone consists of Archaean Proterozoic basement complex and characterized by the maximum concentration earthquake events. The hypocenter beneath the Shillong plateau is shallow focus in origin and are scattered. Only a few epicenters appear on or close to Dauki fault indicate that this fault is relatively seismically inactive during the recent time. But it was active since the Jurassic and was the main architect for the evolution of Shillong plateau. The great earthquake of 1897 originated in the Assam fault zone. Number morphotectonic lineaments have been identified from the study of the satellite imagery. Most of the lineaments trend NE-SW with a few trending N-S. The N-S trending Brahmaputra fault is present along the course of Brahmaputra River. The fault dips steeply to the north. This zone is characterized by scattered shallow depth earthquake probably due to prevalent upward forces existing below the Shillong Plateau.

Tripura Fault Zone

This zone is characterized by high concentration of earthquake events. A number of morphotectonic lineaments have been identified. Among these the Kopili lineament trending NW-SE is remarkable and is geologically recent in origin. Seismic section reveals that this lineament is the surface expression of deep-seated subvertical fault and termed as the Kopili fault, which belongs to the category of high angle reverse fault. At the north of this zone Halflong-Dissang thrust is present. Morphotectonic lineaments around the Halflong-Dissang thrust zone trend NE-SW, E-W and NW-SE. Mikir hill is

present to the northeast corner of the Halflong-Dissang thrust, which separates the Shillong plateau by Kopili fault.

Sub-Dauki Fault Zone

This zone covers the southern part of Dauki fault and eastern part of Bogra fault zone and bounded by longitude 90°E and 92°E. The morphotectonic lineaments trend NNW- SSE and NW-SE. The Sylhet plain covers the area and comprises the vast alluvial tract and the linear belts of folded Tertiary rocks trending N-S and NNE-SSW. Sylhet lineament of 180 km long trending NE-SW is the subsurface expression of deep seated high angle reverse fault having a dip of about 70° towards southeast and as named as Sylhet fault. A number of epicenters fall on or close to this fault and some of them were of damaging character. Among them the earthquake of 1845 and Srimangal earthquake of 1918 are remarkable.

Bogra Fault Zone

This is the westernmost area bounded by latitude 20°N and 28°N, and longitude 87°E and 90°E. The area is covered with thick deposits of alluvium. The main boundary fault of Himalayan ranges occurs in the north of this fault zone. A number of morphotectonic lineaments have been identified from the study of satellite imagery. These are mostly oriented NW/ NNW- SE/SSE. One such lineament is Teesta lineament. Gupta and Nandi seismic activity in the Garo-Rajmahal gap is related to the activity along the Jamuna fracture which is the surface manifestation of apparently deep-seated sub-vertical fault. Most of the earthquakes along this fault are shallow in depth. But one earthquake had a depth of hypocentre of 100 km. The 1885 earthquake of magnitude 7.0 was originated in this fault.

The magnitudes of earthquake suggested by Bolt (Table 2.2) are the maximum magnitude generated in these blocks as recorded in the historical seismic catalogue. The historical seismic catalogue of the regions covers approximately 250 years of (starting 1762) recent seismicity of the region and such a meagre database does not provide true picture of seismicity of the tectonic provinces. For example, the Assam and Tripura fault zones contain significant faults capable of producing magnitude 8.6 and 8.0 earthquakes respectively in future. Similarly maximum magnitude of 7.5 in Sub- Dauki fault zone an Bogra fault zones are not unlikely event.

After a thorough review of available data, Ali and Choudhury (1992) recommended magnitudes of Operational Basis Earthquakes and Maximum Credible Earthquakes in Table.2.3.

Reliable historical data for seismic activity affecting Indian subcontinent is available only for the last 450 years. Recently developed earthquake catalogue for Bangladesh and surrounding area (Sharfuddin, 2001) showed that 66 earthquakes with Ms≥4.0 occurred from 1885 to 1995 within a 200 km radius of Dhaka City. The most prominent historical earthquakes affecting of Bangladesh was listed in Table 2.4

Table 2.2 Significant Seismic Sources and Maximum Likely Earthquake Magnitude in Bangladesh (After Bolt, 1987)

Location	Maximum likely earthquake magnitude
A. Assam fault zone	8.0
B. Tripura fault zone	7.0
C. Sub Dauki fault zone	7.3
D. Bogra fault zone	7.0

Table 2.3 Operational Basis Earthquake, Maximum Credible Earthquake and Depth of Focus of Earthquakes for Different Seismic Sources (After Ali and Chowdhury, 1992)

Location	Operational basis earthquakes (Richter)	Maximum credible earthquakes	Depth of focus (km)
A. Assam fault zone	8.0	8.7	0-70
B. Tripura fault zone	7.0	8.0	0-75
C. Sub-Daukifault zone	7.3	7.5	0-75
D. Bogra fault zone	7.0	7.5	0-70

Table 2.4 Magnitude, EMS Intensities and distances of some major historical earthquakes around Dhaka

Name of Earthquake	Magnitude	Intensity at Dhaka	Distance (km)
1869 Cachar Earthquake	7.5	V	250
1885 Bengal	7.0	VII	70
1897 Great Indian Earthquake	8.7	VIII+	230
1918 Srimangal Earthquake	7.6	VI	150
1930 Dhubri Earthquake	7.1	V+	250

2.5 Seismic Zoning Map of Bangladesh

The seismicity zones and the zone coefficients may be determined from the earthquake magnitude for various return periods and the acceleration attention relationship. It is required that for design or ordinary structures, seismic ground motion having 10% probability of being exceeded in design life of a structure (50 years) is considered critical.

An earthquake having 200 years return period originating in sub-Dauki zone have epicentral acceleration of more than 1.0g but at 50 kilometer the acceleration shall be reduced to as low as 0.3g.

Tectonic frame work of Bangladesh adjoining areas indicate that Bangladesh is situated adjacent to the plate margins of India and Eurasia where devastating earthquake have occurred in the past. Non-availability of earthquake, geology and tectonic data posed great problem in earthquake hazard mapping of Bangladesh in the past. The first seismic map which was prepared in 1979 was developed considering only the epicentral location of past earthquake and isoseismic map of very few of them. During preparation of National Building Code of Bangladesh in 1993, substantial effort was given in revising the existing seismic zoning map using geophysical and tectonic data, earthquake data, ground motion attenuation data and strong motion data available from within as well as outside of the country. Geophysical and tectonic data were available from Geological survey of Bangladesh. Earthquake data were collected from NOAA data files and geodetic survey, US. Dept. of commerce.

Seismic zoning map for Bangladesh has been presented in Bangladesh National Building code (BNBC) published in 1993. The pattern of ground surface acceleration contours having 200 year return period from the basis of this seismic zoning map. There are three zones in the map- zone 1, zone2, zone3. The seismic coefficients of the zones are 0.075g, 0.15g and 0.25g for zone 1, zone 2 and zone 3 respectively. Bangladesh National building Code (1993) placed Dhaka city area in seismic zone 2. however, the seismic zones in the code are not based on the analytical assessment of seismic hazard and are mainly based on the location of historical data.

The first seismic zoning map of the subcontinent was compiled by the Geological Survey of India in 1935. The Bangladesh Meteorological Department adopted a seismic zoning map in 1972. In 1977, the Government of Bangladesh constituted a Committee of Experts to examine the seismic problem and make appropriate recommendations. The Committee proposed a zoning map of Bangladesh in the same year.

According to Bangladesh National Building Code (BNBC, 1993), Bangladesh is divided into 3 earthquake zones and proposed updating seismic zoning Map of Bangladesh as shown in Figure 2.3.

(i) **Zone-I** comprising the southwestern part of Bangladesh is seismically quiet, with an estimated basic seismic zoning co-efficient of 0.075.

(ii) **Zone-II** comprising the central part of Bangladesh represents the regions of recent uplifted Pleistocene blocks of the Barind and Madhupur Tracts, and the western extension of the folded belt. The zone extends to the south covering Chittagong and Cox's Bazar. Seismic zoning coefficient for Zone II is 0.15.

(iii) **Zone-III** comprising the northern and eastern regions of Bangladesh with the presence of the Dauki Fault system of eastern Sylhet and the deep seated Sylhet Fault, and proximity to the highly disturbed southeastern Assam region with the Jaflong thrust, Naga thrust and Disang thrust, is a zone of high seismic risk with a basic seismic zoning co-efficient of 0.25. Northern Bangladesh comprising greater Rangpur and Dinajpur districts is also a region of high seismicity because of the presence of the Jamuna Fault and the proximity to the active east-west running fault and the Main Boundary Fault to the north in India. The Chittagong-Tripura Folded Belt experiences frequent

earthquakes, as just to its east is the Burmese Arc where a large number of shallow depth earthquakes originate.

Bangladesh National Building Code (1993) placed Dhaka (Latitude; 23.8°N, Longitude; 90.3°E) in Seismic zone 2. The seismic zones in the code are not based on the analytical assessment of seismic hazard and are mainly based on the location of historical data. Based on the philosophy behind the seismic zoning and experience from recent earthquakes, it can reasonably be assumed that a major earthquake event in Dhaka region is capable of higher damage than that assumed in the existing zoning map (BNBC 1993).

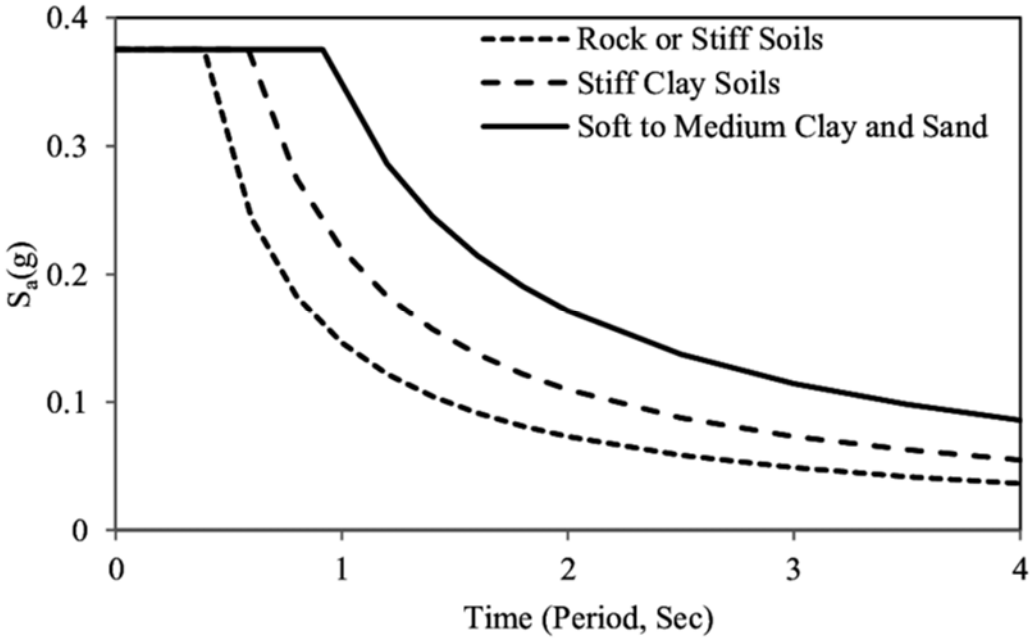

Fig. 2.4. Design Response Spectra, BNBC 1993

Figure 2.4 shows the response spectra diagram of rock, stiff and soft clays.

2.6 Site-Response Analysis

After a fault rupture takes place (i.e. initiation of an earthquake event), body waves spread in every directions and propagate through different layers of geologic materials while reflections and refractions at the layer interfaces define their travel path to the ground surface. Generally speaking, waves propagate with decreasing velocity as they approach to the ground surface, causing the waves to refract at the horizontal layer interfaces until the wave path becomes near vertical. This is the basis for the approximation of one-dimensional site response analysis in the case of horizontally layered soil deposit where vertical shear-wave propagation from the underlying bedrock to the ground surface is assumed (Kramer,1996)

2.7 Introduction to Different Software for Site Response Analysis

There are different softwares which are used to run the site response analysis. Some are presented below:

(i) SHAKE2000: It is a Windows based, user-friendly computer program that will help geotechnical earthquake engineers and researchers with the analysis of site-specific response and the evaluation of earthquake effects on soil deposits. Hence, the main objective in the development of SHAKE2000 was to add new features to transform SHAKE and SHAKE91 into an analysis tool for seismic analysis of soil deposits and earth structures. As such, the governing philosophy in developing this new version of SHAKE was to lay before the user a suite of tools designed to answer questions of interest to both academia and the consulting professional. SHAKE2000 will have a dual role in geotechnical earthquake engineering. First, it will be used as a learning tool for students of geotechnical engineering. Second, it will serve practitioners of geotechnical

earthquake engineering as a scoping tool to provide a first approximation of the dynamic response of a site. Depending upon the prediction of site response, the practitioner will judge whether more sophisticated dynamic modeling is warranted.

SHAKE2000 is a software package that integrates ShakEdit and SHAKE. ShakEdit was originally developed as a 16-bit, Windows 3.1 application that provided a graphical interface for SHAKE. It was originally conceived as an aid to the user in the creation of the input file and the graphical display of the program's numeric output. It accomplished the first step by incorporating user-friendly screens to assist in entering the arcane input data for the differing SHAKE options. The second step required the development of routines for the processing and error checking of output data, and for displaying that output in forms familiar to the geotechnical engineer. SHAKE was developed at the University of California, Berkeley, by H. Bolton Seed, John Lysmer and Per B. Schnabel. SHAKE computes the response in a system of homogeneous, viscous-elastic layers of infinite horizontal extent subjected to vertically traveling shear waves. The program is based on the continuous solution to the wave-equation adapted for use with transient motions through the Fast Fourier Transform algorithm. The nonlinearity of the shear modulus and damping is accounted for by the use of equivalent linear soil properties using an iterative procedure to obtain values for modulus and damping compatible with the effective strains in each layer.

(ii) DEEPSOIL: It is a unified 1D equivalent linear and nonlinear site response analysis platform. Main features include, Strength-controlled nonlinear model, Frequency-independent damping formulation, Porewater pressure generation and dissipation models, Graphical user interface, Parallel-processing capability.

(iii) PLAXIS 3D: It is a powerful and user friendly finite element package intended for three-dimensional analysis of deformation and stability in geotechnical engineering and rock mechanics. PLAXIS is used worldwide by top engineering companies and institutions in the civil and geotechnical engineering industry. Applications range from excavations, embankments and foundations to tunnelling, mining and reservoir geomechanics.

(iv) ProShake 2.0: A powerful, user-friendly program for one-dimensional, equivalent linear ground response analysis. ProShake 2.0 represents a major upgrade to ProShake. ProShake is currently being used by more than 200 of the world's top consulting firms and research institutions. ProShake 2.0 is a powerful, user-friendly computer program for one-dimensional, equivalent linear ground response analysis. Written completely from scratch, ProShake 2.0 includes numerous features to make data entry, analysis, viewing and documenting of results efficient and effective, including built-in modulus reduction and damping models, graphical display of soil profile and input motion parameters, graphical display of a wide variety of output parameters, and animation of ground response. ProShake 2.0 is organized into three "managers" - an Input Manager, a Solution Manager, and an Output Manager. The Input Manager allows entry of soil profile and input motion data. The Solution Manager performs iterative equivalent linear analyses while tracking the process of convergence toward strain-compatible soil properties. The Output Manager allows easy plotting of results in the form of time histories, response spectra, parameter profiles, and animations.

ProShake 2.0 - Educational Version, previously called EduShake, is a user-friendly, free computer program for one-dimensional, equivalent linear ground response analysis. ProShake 2.0 represents a major upgrade to ProShake 1.12. The Educational Version is

identical to and includes all of the features of the Professional Version but is limited to the use of 7 earthquake motion files that are included in the installation package. These features allow geotechnical earthquake engineering students to spend less time formatting data and plotting results and more time understanding seismic ground response.

2.8 Past Researches on Site Response Analysis

Brendon A. Bradley, professor of University of Canterbury researched on Accuracy and precision of 1D equivalent-linear site response analyses based on 100 KiK-net (a Japanese software) downhole array locations.

Site response, or local site effects, is well recognized to have a profound influence on surficial ground motions as a result of the variability in surficial geology, and the complexity in its characterization, particularly for nonlinear site response.

Bulletin of Earthquake Engineering, May 2017, Volume 15 published the results of a study that investigates potential revisions of the spectral shape factors used in standards in regions of low-to-moderate seismicity are presented here. Using an equivalent linear analysis, the investigation particularly focuses on the effects of seismic intensity associated with rare and very rare intraplate earthquake events on site response. The Pacific Earthquake Engineering Research Center ground motion database (PEER) is used in selecting appropriate acceleration-time histories for the intraplate region. The results are normalised for comparison with the current spectral shape factors given in the Australian Standards for Earthquake Actions AS 1170.4:2007, with some differences being observed. The records from the PEER ground motion database were also used for comparison with the results from this study, using a modified normalisation approach. The results from this study correlate well with the records from PEER.

Site response, or local site effects, is well recognized to have a profound influence on surficial ground motions as a result of the variability in surficial geology, and the complexity in its characterization, particularly for nonlinear site response.

Amplification characteristics of the shallow soil deposits are very important to evaluate ground motion distribution with seismometry network.

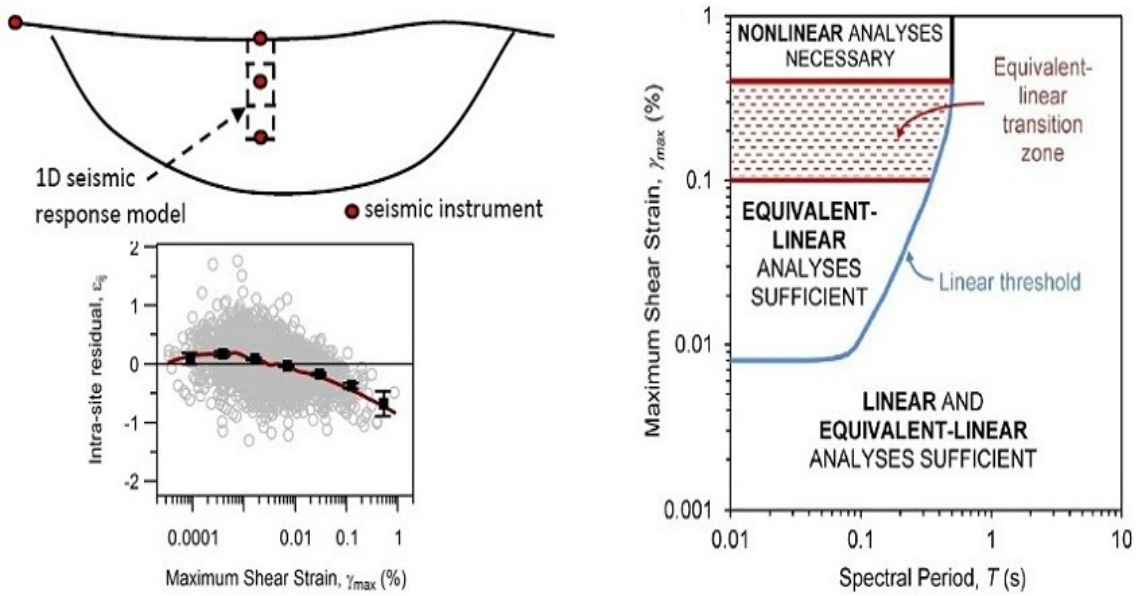

Fig. 2.5 1D Site Response Model

1) amplification factor during weak motion: Aw, 2) its limit input motion: X1, 3) upper limit: XL, 4) input motion reaching upper limit: X2. The upper limit of PGA, JMA seismic intensity scale and SI value are controlled by the shear strength of soil. Earthquake response analyses are carried out with many conditions and 4 parameters are decided. Topography classifications and a predominant period have been often used as ground parameter, but in late years the use of average S-wave velocity increases. Therefore, we connect average S-wave velocity to 20m or 30m deep with four parameters in order to apply to the urban city where borehole data are provided to high density.

Site response analysis is strongly influenced by the uncertainty associated to the definition of soil properties and model parameters. Deterministic, or even parametric analyses are unable to systematically assess such uncertainty, since the site characterization can hardly be sufficiently accurate for a deterministic prediction of site response and alternative approaches are hence needed. A fully stochastic procedure for estimating the site amplification of ground motion is proposed and applied to a case study in central Italy. The methodology allows to take into account the record-to-record variability in an input ground motion and the uncertainty in dynamic soil properties and in the definition of the soil model. In particular, their effect on response spectra at the ground surface is evaluated.

Comparison Study of 1D Site Response Analysis Methods by Chi-Chin Tsai M. EERI and Chun-Way Chen says The ground responses computed via frequency domain (FD) equivalent-linear (EQL) and time domain (TD) nonlinear (NL) methods can considerably differ because of the constitutional differences in numerical approaches, damping formulations, and modeling of nonlinear soil response. FD-EQL analysis is used in engineering practices to estimate seismic site response, although it models nonlinear soil behavior in a more simplified and approximate way compared to TD-NL. To systematically evaluate the two approaches, the current study performs a series of site response analyses that consider different input motions, intensities of input motion, depths of soil columns, and nonlinear properties. TD-NL, TD-EQL, and FD-EQL analyses are performed to identify the difference caused by each aspect. The way of modeling nonlinear soil behavior (EQL vs. NL) mostly contributes to the difference between TD-NL and FD-EQL, followed by the numerical approach (TD vs. FD) and the selection of the target frequency of Rayleigh damping. In general, the FD-EQL results envelop the TD-NL except for the period range between 0.05 and 0.3 s, where TD-NL

tends to predict higher response than FQ-EQL as the intensity of input motion increases. The RD in this period range is dependent on soil nonlinearity and damping. High soil nonlinearity (i.e. significant modulus reduction) tends to magnify the Rayleigh damping (RD) in this period range. However, high damping tends to mitigate such Rayleigh damping (RD). Therefore, the difference between TD-NL and FD-EQL for a site with high nonlinearity (e.g. sand) under a moderate shaking can be easily observed. The two methods show significant difference for the sandy site under moderate shaking because of sufficient modulus reduction but limited damping at the medium stain range. Under a strong shaking, the sandy site and the clay site both exhibit high modulus reduction and damping at large strain. Thus, TD-NL and FQ-EQL show similar RD at both sites. The two approaches exhibit more differences for shallow soil columns than for deep soil columns. The threshold intensity that causes the difference and the impact of such difference on engineering practice are furthered evaluated through surface acceleration (SA) of different periods and site amplification factors (AF)s. The PGA plots reveal highly significant differences. SA at 0.2 s exhibits an intermediate difference, whereas SA at 1.0 s exhibits little difference. Engineers should be cautious when selecting an analysis approach that depends on the period range of interest.

However, no clear threshold intensity that causes the NL result to deviate from that of EQL is found. The RD increases as the intensity of input motion increases (i.e. FD increases).

Lastly, AF by TD-NL exhibits more nonlinearity than that by FD-EQL, particularly for *Fv* because EQL adopts an equivalent (averaged) modulus, whereas NL actually models nonlinear behavior. Compared with the latest version of the NEHRP site factor, TD-NL

could be a better method than FD-EQL for modeling soil nonlinear behavior. Moreover, TD-NL leads to an accurate estimate of seismic site response.

In practice, spatial variability in Vs is modeled in 1D site response analyses by generating multiple 1D Vs profiles without any consideration of the horizontal correlation between velocities. The effect of this approach is investigated by generating multiple 1D Vs profiles using the Monte Carlo Simulation technique with σlnVs of 0.2, a vertical correlation distance (θz) of 80 m, and a horizontal correlation distance (θx) of 0 m (i.e., velocities are uncorrelated horizontally). Two hundred 1D Vs profiles were generated and 1D equivalent-linear site response analyses were performed for each profile using software program Strata (Kottke and Rathje, 2008). The results of the analyses are binned into 20 realizations of 10 profiles to have a comparable number of realizations as the 2D analyses. The values for the 1D analyses of the 1D random field range from 0.15 at short periods to peaks of 0.25 to 0.3 at periods of 0.15 s and 1.2 s. Here, the 1D analyses tended to predict larger standard deviations, particularly when the horizontal correlation between velocities is ignored. Additional work is required to explore how these differences are influenced by the size of the region of interest, the modeled correlation distances, the intensity of the input motion, and the characteristics of the input motion.

A study of the Effect of Soil Improvement Based on the Numerical Site Response Analysis of Natural Ground in Babol City by Asskar Janalizadechoobbasti, Mehran Naghizaderokni, Aida Talebi, Civil Engineering, Babol University of technology, Babol, Iran A series of numerical calculations have been performed to investigate the effect of soil improvement on seismic site response. Seismic site response analyses were also performed using data collected from a study area in Babol city. The improved site is a composite ground and has more or less different mechanical properties than the natural

ground. In this research, the influence of the elastic modulus of the pile, the pile distance ratio, ground motion input, distance to fault rupture, and PGA of the earthquakes on seismic response characteristics are especially investigated. The results reveal that the values of the PGA and amplification factor on the surface of the natural and improved grounds depend strongly on the fundamental period of the site, the predominant period, and the intensity of the ground motion input. The acceleration response spectra also are affected by the characteristics of ground motion input and soil layers.

Stochastic 1D site response analysis at a site in central Italy is focused at the seaport of Ancona (central Italy). The area of the port of Ancona was complex from a geological point of view, due to the significant tectonic activity of the region. From the boreholes carried out at the site, the following formations had been identified (from bottom to top):

Schlier formation (medium-lower Miocene), typical of the Ancona area, constituted by well consolidated marlstone, clayey marlstone and marly white limestone. This formation is present from a depth of 25–27 m, down to 40–50 m, which is the maximum explored depth. In this study, it was assumed that this formation extends to a larger depth and constitutes the bedrock.

On top of the Schlier formation, there are consolidated soil deposits of the upper Miocene, significantly varying for lithology and thickness. The so-called Gesso-Solfifera formation is constituted by clay, marlstone and diatomites, followed by marly. In order to characterize the site from a geotechnical point of view, some geotechnical and geophysical testing campaigns were carried out in 2006. In particular, the soil investigation campaign included:four boreholes, three of which down to 40 m depth and one down to 50 m; four cone penetration tests (CPT) down to depths varying between 23 and 25.4 m below the ground surface;

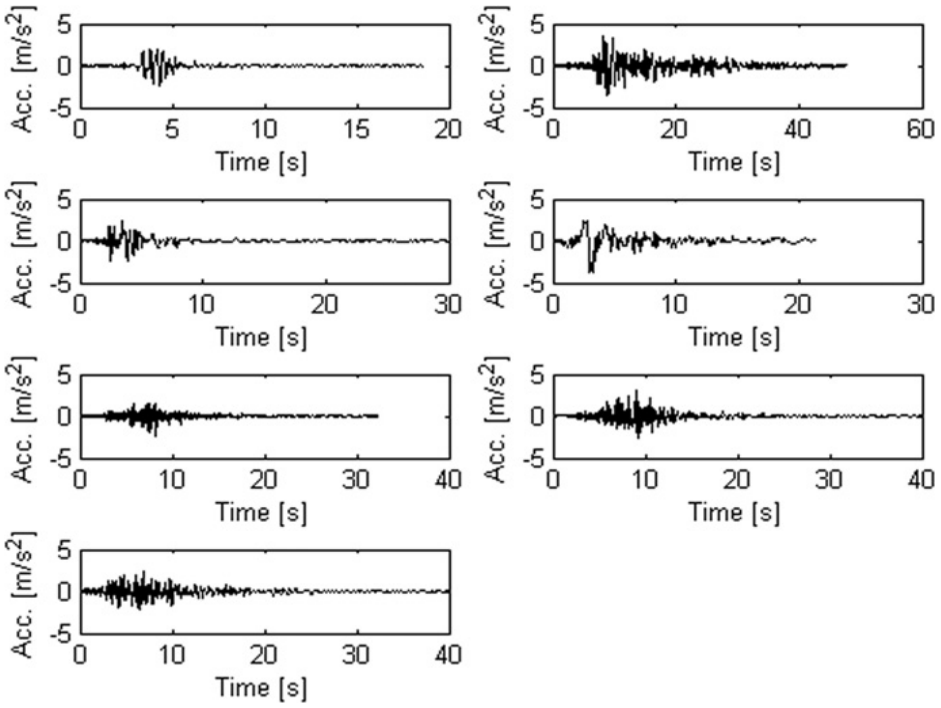

Fig. 2.6. Acceleration time histories of the seven selected real records, compatible with the EC8 code spectrum at the site of Ancona, for the 475 years return period.

four geophysical cross-hole tests, providing information on VP and Vs wave velocity profiles, down to 34, 39, 40 and 50 m; Geotechnical laboratory tests on undisturbed soil specimens. The main seismological characteristics of the seven spectrum- compatible real records, selected for a return period of 475 years. It should be noted that, since disaggregation was carried out for PGA and records were selected to be spectrum-compatible for a wider range of periods, the value of magnitude obtained from disaggregation (M¼ 5.55) is actually a lower bound of the magnitudes of the selected accelerograms. This is due to the fact that disaggregation for higher spectral ordinates would be likely to provide higher values of magnitude. Fig. 2.7 shows their plot and fig 2.8 shows their response spectra and their comparison with the average spectrum. It can be noted that the different accelerograms provide a contribution in the spectrum at different period ranges. Fig. 2.9 shows the comparison of the average response spectrum

of the seven accelerograms normalised to a PGA value of 0.25 g and the spectrum for the 475 year return period.

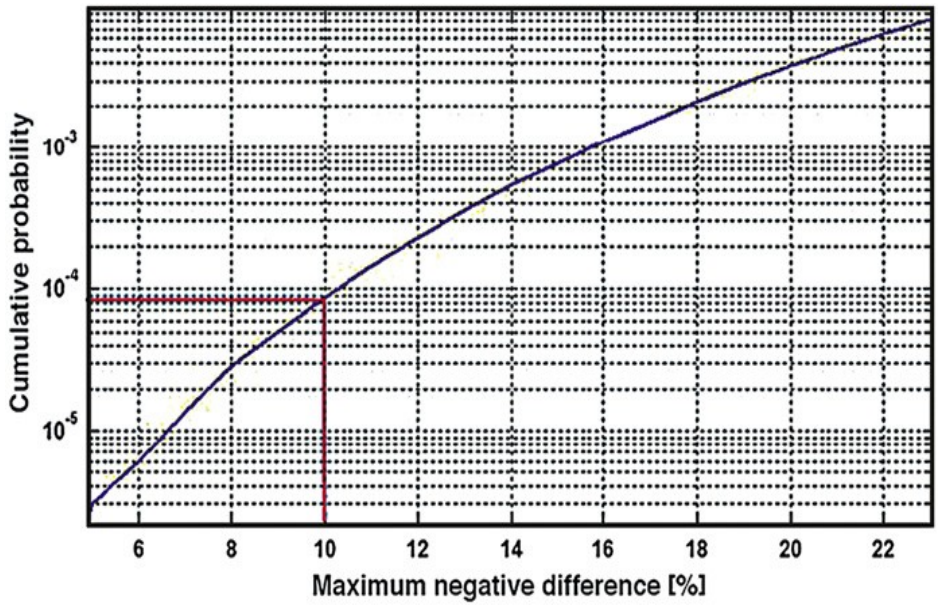

Fig. 2.7. Cumulative probability distribution of the maximum negative difference (in%) between the mean and the target spectra, obtained from the analysis of 5 ~ 108 groups of three accelerograms, randomly generated from the set of selected accelerograms.

Table 2.5 Seismological characteristics of the records selected for this study, for the 475 years return period.

S.L	Name of the record set	Epicentral distance [km]	Data	ML	MS	MW
1	Friuli (aftershock)	16	11/09/1976	5.7	5.52	5.6
2	Montenegro	16	15/04/1979	–	7.04	–
3	Kalamata (South Greece)	10	13/09/1986	5.5	5.75	–
4	Erzincan (Turkey)	13	13/03/1992	–	6.75	–
5	Ionian (Greece)	18	23/03/1983	5.5	6.16	–
6	Parkfield	11.6	28/09/2004	–	–	6.0
7	Parkfield	14	28/09/2004	–	–	6.0

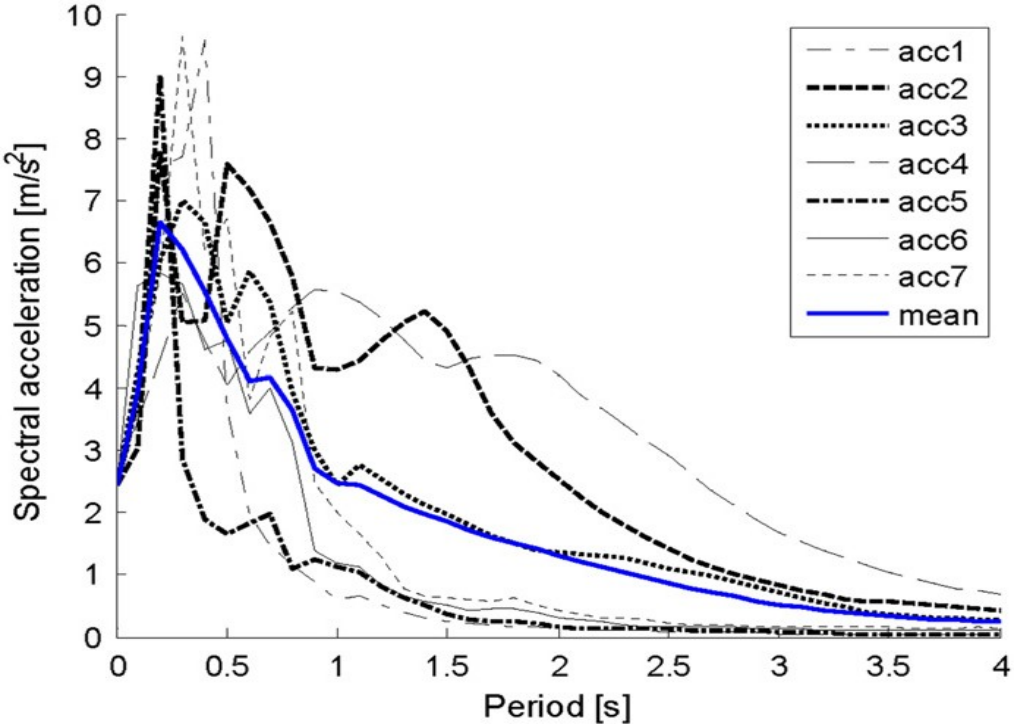

Fig. 2.8. Acceleration response spectra of the seven selected real accelerograms for Ancona, scaled to a PGA ¼ 0.25 g (475 years return period) and comparison with their mean response spectrum. Structural damping 5%.

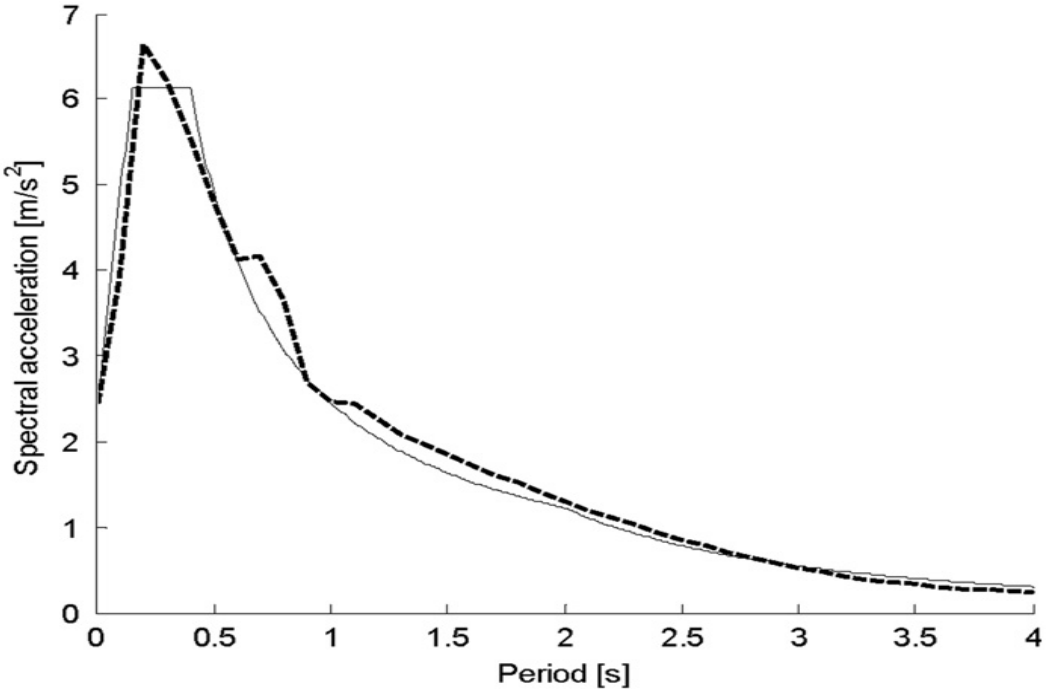

Fig. 2.9. Comparison between the mean response spectrum of the seven accelerograms selected for Ancona (dashed line) and the EC8 code spectrum for the 475 years return period (continuous line).

In the study the statistical distribution of the acceleration response spectra has been evaluated and the mean amplified accelerogram and mean spectra, for each of the seven seismic inputs, have been computed.

The results obtained also confirm that the variability of the seismic input is the most crucial source of uncertainty controlling the dispersion in the response.

Given the completeness of the study and the statistical reliability of the results obtained from the stochastic site response analyses, it has also been possible to select response spectra associated to arbitrary percentiles of the corresponding probability distribution.

Although authors are aware that 1D linear-equivalent soil response analyses have a number of limitations (e.g. 1D modelling fails to capture important site response aspects such as lateral soil variability and equivalent-linear soil modelling represents an approximation of nonlinear soil behavior), the proposed fully stochastic methodology has a significance that extends far beyond the specific application carried out in this study. In fact, it can be easily coupled with more advanced and accurate response analysis software and soil constitutive models.

2.9 Ground Improvement Technique

The ground can be improved by adapting certain ground improvement techniques. Vibro compaction increases the density of the soil by using powerful depth vibrators. Vacuum consolidation is used for improving soft soils by using a vacuum pump. Preloading method is used to remove pore water over time. Heating is used to form a crystalline or glass product by electric current. Ground freezing converts pore water to ice to increase their combined strength and make them impervious. Vibro-replacement stone columns

improve the bearing capacity of soil whereas Vibro displacement method displaces the soil. Electro osmosis makes water flow through fine grained soils.

Electro kinetic stabilization is the application of electro osmosis. Reinforced soil steel is used for retaining structures, sloping walls, dams etc. seismic loading is suited for construction in seismically active regions. Mechanically stabilized earth structures create a reinforced soil mass.

The geo methods like Geosynthetics, Geogrid etc. are discussed. Soil nailing increases the shear strength of the in-situ soil and restrains its displacement. Micro pile gives the structural support and used for repair/replacement of existing foundations.

Grouting is injection of pumpable materials to increase its rigidity. The jet grouting is quite advanced in speed as well as techniques when compared with the general grouting.

Ground improvement is carried out for various reasons to improve bearing capacity and reduce settlement of soft ground, prevent earthquake liquefaction, control groundwater, stabilize excavation bottom, prevent deformation of surrounding ground, or clean up contaminated ground.

Many causes including presence of peats and highly organic soils in construction projects increase the risk of foundation failure or inadmissible settlements due to low strengths, high compressibility, prolonged creep, and low permeability. As a result, foundations, embankments, excavations, and other ground works become very difficult and often require costly treatments. Possible solutions to this kind of problems include 1) strengthening foundations; 2) removing the problem soils; 3) treating the problem soils;

4) relocating the project. However, these existing options are often considered impractical or too expensive.

The Deep Mixing Method (DMM) has been used in RNPP site, also known in parts of the U.S. as soil mixing, is an insitu soil treatment and improvement technology mechanically blending the in situ soil with cementitious materials that are referred to as binders using a hollow stem auger and paddle arrangement. The intent of the soil mixing method is to achieve improved soil properties. The cemented material that is produced generally has a higher strength, lower permeability, and lower compressibility than the native ground, although total unit weight may be less. The properties obtained reflect the characteristics of the native soil, the mixing method, and the binder characteristics. Deep mixing technologies are usually categorized into "wet" mixing method and "dry" mixing method depending on how the binder is applied to the soil. In the wet mix method, a cementitious slurry is injected through large diameter to a specified depth. The common dry mix method is to rotate a mixing tool into the soil to break up the soil on the down stroke, and the dry reagent (quick lime or cement or a mixture of both) is pneumatically injected and blended with the soil by the mixing tool on the up stroke. The dry mix method is generally considered less expensive than the wet mix method. However, the strength of the final product is also considered less than the strength achieved for the same material with wet mix methods. Some methods are Groundwater control, Excavation support, Soil and foundation stabilization, Liquefaction mitigation, Vibration reduction, Fixation of contaminants, Passive and reactive in-ground barriers, Repair of defective soil-bentonite cut-off walls.

2.10 Concluding Remarks

Method of analysis has been discussed. Some past research about site response and ground improvement techniques have also been presented briefly. In this study no earthquake data have been used from our Bangladeshi subcontinent. The reason behind this is, there is lack of time history data. In this study, ground improvement technique has been applied for the top 20m of the soil. As a result, shear wave velocity has been increased from 210 m/s to 1100 m/s.

CHAPTER THREE

SITE RESPONSE ANALYSIS

3.1 General

Site response analysis provides surface acceleration time series, surface acceleration response spectra, and spectral amplification factors based on the dynamic response of local soil conditions.

Frequency domain (FD) equivalent linear (EQL) and time domain (TD) nonlinear (NL) analyses (e.g. Hashash and Park, 2001) are the most common approaches used to perform 1D seismic site response analysis. Equivalent linear analysis and elastic half space analysis method will be used in this study.

3.2 Methodology

To construct a stratigraphic 1D model, the first step is the definition of soil layers, with the corresponding depths and thicknesses. The stratigraphic model has been defined first, for each layer of thickness, shear wave velocity (Vs), unit weight of soil and degradation curves for the shear modulus and for the damping ratio. Once the one-dimensional stratigraphic model has been completely defined, local site response analyses have been carried out with a procedure allowing to consider in the model the uncertainties associated to the different geotechnical parameters. Hence, through a large number of numerical simulations, the influence of the variability of the single parameters and of their combination on the surface ground motion has been assessed. The method is based on consisting in the iterative calculation of a deterministic model, whose input parameters have been defined, at each iteration, by a set of random realizations. The input parameters

have been randomly generated according to previously defined probability distributions. The software performs automatically the deconvolution of the signal, transferring the seismic input to the top of the bedrock. The software performs the analysis in terms of total stresses and calculates stresses and deformations at the various layers as well as time histories of acceleration, velocity and displacement at the different depths. The implemented procedure consists the following steps:

The program performs automatically the deconvolution of the signal, transferring the seismic input to the top of the bedrock.

The software performs the analysis in terms of total stresses and calculates stresses and deformations at the various layers as well as time histories of acceleration, velocity and displacement at the different depths.

1D profile of them gives shear wave velocity V_S used in the simulation of local Ground amplification and the results of the analyses have been described in terms of surface acceleration time histories and surface elastic acceleration response spectra.

Method of analysis once the one-dimensional stratigraphic model has been completely defined local site response analyses has been carried out with a procedure allowing to consider in the model the uncertainties associated to the different geotechnical parameters. Hence, through a large number of numerical simulations, the influence of the variability of the single parameters and of their combination on the surface ground motion has been assessed the seismic input to the top of the bedrock.

Eight earthquakes analysis has been done to determine the correlation. Chi-Chi is one of them. Chi-Chi earthquake, also known as the 921 earthquake, is an earthquake in central

Taiwan. The earthquake happened on September 21, 1999 at 1:47 am local time (September 20 17:47 GMT). It measured 7.3 on the Richter scale.

Following flowchart in figure 3.1 showing the methods of the analysis in brief. And here Frequency independent method has been done. And figure 3.2 shows the final output from the analysis.

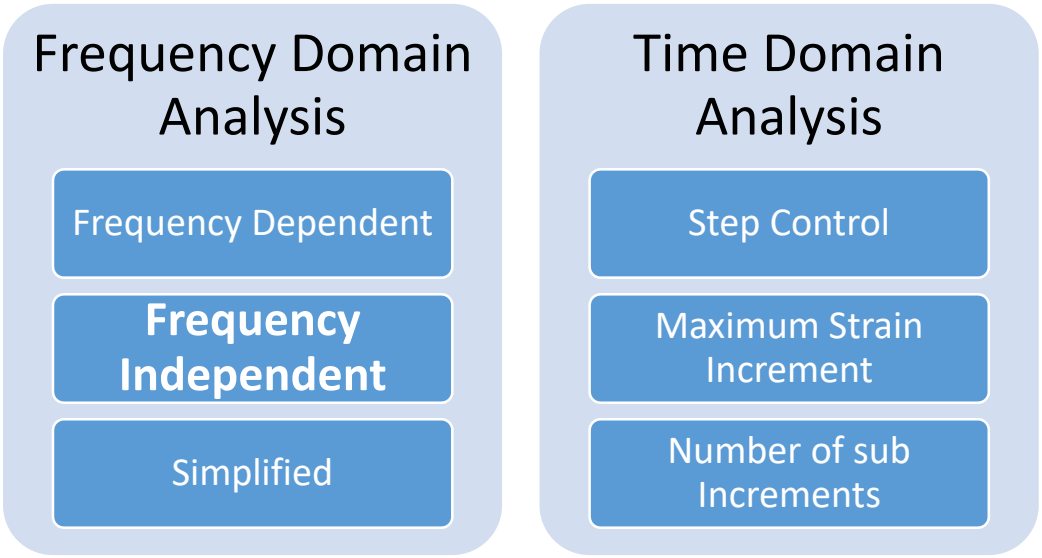

Fig 3.1: Flowchart of the analysis method

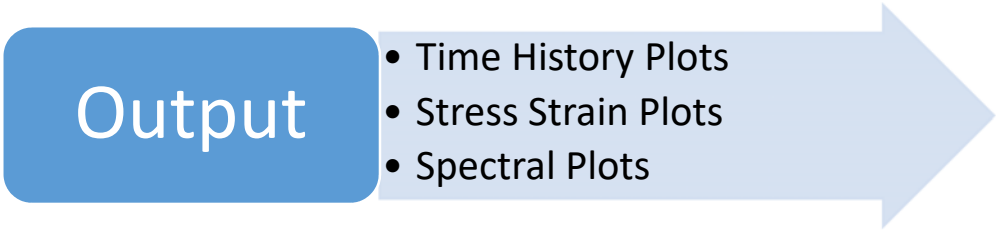

Fig 3.2 Output of the analysis

At relatively small strains, soils exhibit non-linear behavior. Thus it is necessary to incorporate soil non-linearity in any site response analysis. One dimensional site response analysis methods are widely used to quantify the effect of soil deposits on

propagated ground motions in research and practice. These methods can be divided into two main categories:

(1) Frequency domain analyses (including the equivalent linear method and (2) time domain analyses (including non-linear analyses).

Site response analysis methods in a linear site response analysis, the maximum soil stiffness and a constant damping ratio are considered throughout the entire time history. In an equivalent linear, frequency domain site response analysis, an equivalent soil stiffness and damping value are considered for each layer for the entire duration of a seismic event. This can lead to an over or under estimation of the damping and soil stiffness depending on the strain level the soil response is being analyzed. In a nonlinear, time domain analysis, the variation of soil shear modulus (G) and damping ratio (ξ) is considered in the material during shaking. In nonlinear site response analyses in DEEPSOIL, the soil column is discretized as a multi-degree-of-freedom (MDOF), lumped mass model, whereby each individual layer is represented by a corresponding mass, nonlinear spring, and a dashpot representing viscous damping. Lumping half of the mass of each of two consecutive layers at their common boundary forms the mass matrix, and the stiffness matrix is updated at each time increment to incorporate soil nonlinearity.

Input motions can be viewed/processed and it generates acceleration, velocity, and displacement and Arias intensity time histories, as well as the response spectrum and Fourier amplitude spectrum for the selected motion.

Motions which exhibit non-zero displacement time-histories for the latter part of the motion should be corrected with baseline correction. The corrected time-histories are

also calculated and presented. The response spectra and Fourier amplitude spectra for the original motion and baseline-corrected motion are also provided.

One of the most important factors to consider when evaluating ground motions is frequency content. The most common measure of frequency content is the Fourier amplitude spectrum, which indicates how the amplitude of the ground motion is distributed across different frequencies. Calculation of the spectrum requires a transformation of the ground motion from the time domain to the frequency domain. This transformation is called a Fourier transform. The transformation is completed using a Fast Fourier Transform (FFT).

3.2.1 The analysis method

The Analysis can be done in two ways, Frequency Domain and Time Domain. Frequency Domain is sub divided by linear and equivalent linear approach. Time domain is sub divided by linear and non-linear approach. The units to be used in analysis must be English and metric unit.

Shear Property is another important thing to identify. Shear modulus and shear wave velocity are two types of shear property. Shear wave velocity has been used in our analysis.

There are three types of pore water pressure control, No pore water pressure generation; Pore water pressure generation without dissipation (nonlinear only); and Pore water pressure generation and dissipation (nonlinear only)

For equivalent linear and non linear analysis there are different methods to define the soil curve, For Equivalent Linear method there are two systems, Discrete Points and any model supported for nonlinear analyses. For Nonlinear analysis, MRDF Pressure-

Dependent Hyperbolic Model, and MRDF General Quadratic/Hyperbolic Model. A number of techniques are available for ground response analysis. The methods differ in the simplifying assumptions that are made, in the representation of stress-strain relations of soil and in the methods used to integrate the equation of motion. The development of existing methods of dynamic response analysis has been a gradual evolutionary process stimulated by changing needs of practice and the increasing knowledge about the fundamental behavior of soils under cyclic loading derived from field observations and laboratory testing. The method can be broadly grouped in to the following three categories, Linear analysis, Equivalent linear analysis and Nonlinear analysis.

Linear analysis, because of its simplicity, has been extensively used to study analytically the dynamic response of soil deposits. Closed form analytical solutions have been derived for idealized geometries and soil properties, e.g. by assuming that the deposit consists of one uniform layer with soil stiffness either constant or varying with depth in a way which can be expressed by simple mathematical functions.

Non-linear analysis. A non-linear analysis is usually performed by using a discrete model such as finite element and lumped mass models and performing time domain step-by-step integration of equations of motion. For non-linear analysis to give meaningful results the stress strain characteristics of the particular soil must be realistically modeled.

3.2.2 Definition of a soil profile:

The following properties need to be defined for each layer:

(i) Thickness

(ii) Shear Wave Velocity (V_S) or Initial Shear Modulus (G_{max})

(iii) Damping Ratio (%)

(iv) Unit Weight

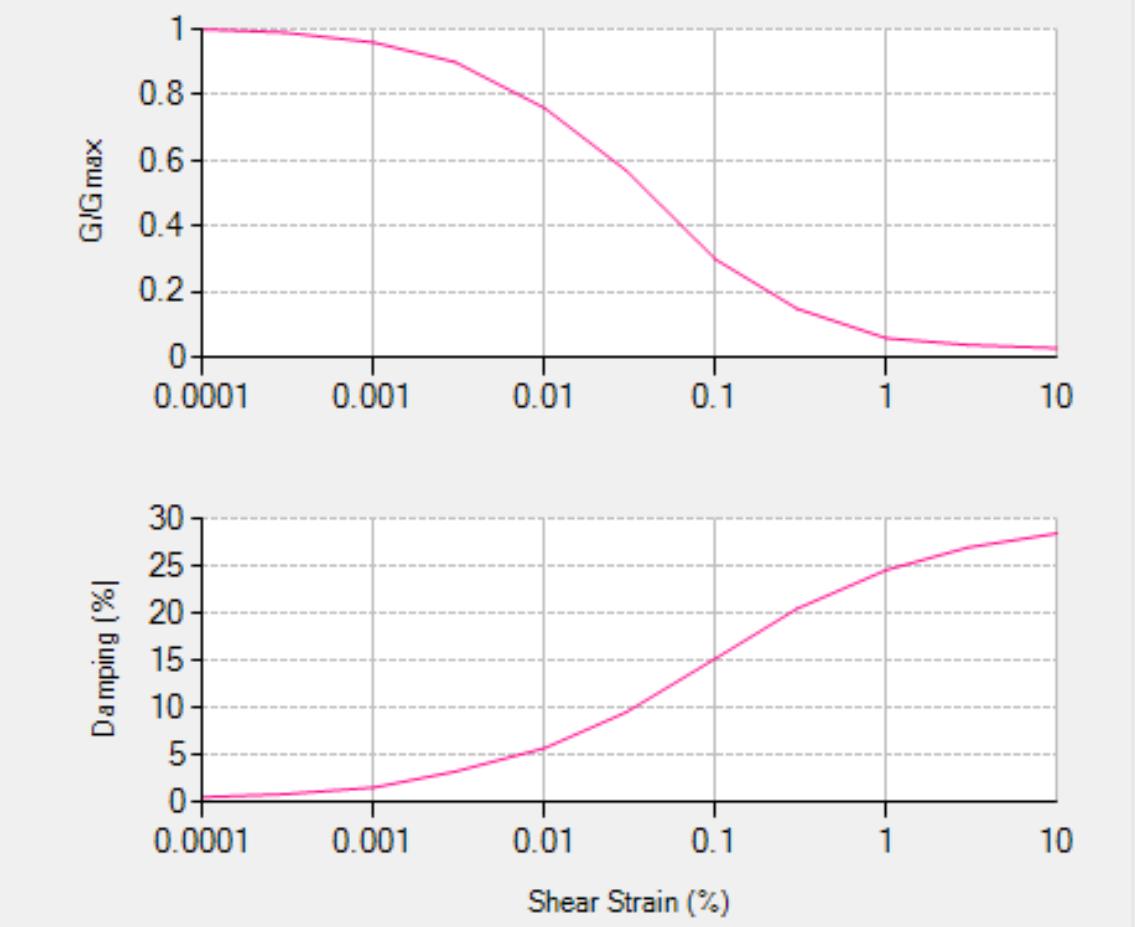

Fig 3.3 Shear Modulus and Damping ratio formulation

The **equivalent linear** method approximates the ground material nonlinearity as an equivalent linear material property. It employs an iterative procedure in the selection of the shear modulus and damping ratio.The option of defining the soil curves using discrete points is only applicable for the Equivalent Linear analysis. For this option, the shear modulus (G/G_{max}) and damping ratio (%) are defined as functions of shear strain (%). The software itself defines damping ratio and shear modulus. Figure 3.3 shows the generated graphs. Equivalent linear analysis is directly related with these factors.

3.2.3 Defining rock properties:

Rock properties include **Rigid Half-Space** and **Elastic Half-Space**. If a rigid half-space is being used, no input parameters are required. If an elastic half-space is being used, shear wave velocity (or modulus), unit weight, and damping ratio of the half-space must be applied. In general, the shear wave velocity of the bedrock should be greater than that of the overlying soil profile. It should be noted that the bedrock damping ratio has no effect in time domain analyses and only a negligible effect in frequency domain analyses regardless of the value specified by the user.

Appropriate rock motions (either natural or synthetic acceleration time histories) are selected to represent the design rock motion for the site. The rock motion should be associated with the specific seismo-tectonic structures, source areas or provinces that would cause most severe vibratory ground motion or foundation dislocation capable of being produced at the site under currently known tectonic framework. If natural time histories are used, it is preferable to use a set of natural time histories that have ground motion characteristics similar to those estimated for the design rock motions. That means the selected histories should have:

(i) Peak ground motion parameters

(ii) Response spectral content and

(iii)Duration of strong shaking

Most site response analyses involve horizontal ground motion, considering vertically propagating shear waves in horizontally layered systems. In reality, the ground is simultaneously subjected to shaking in both the horizontal and vertical directions during an earthquake. Field evidence from various recent earthquakes indicates though that

damage of concrete buildings and bridges can be attributed to high vertical ground motion Therefore there is a need for better establishing the site response to vertical ground motion. It is widely believed that vertical ground response is dominated by the propagation of compression waves (P-waves) and has been found to depend on the pore-fluid compressibility, permeability, soil stiffness and porosity. Saturated soils are two-phase materials consisting of a solid phase (soil skeleton) and a fluid phase (pore water filling the voids). Depending on the soil permeability, the rate of loading and the hydraulic boundary conditions, it is often necessary to employ coupled analysis to accurately model the two phase behavior of soils. The response of a uniform soil layer subjected to harmonic P-waves analytically and numerically, with dynamic coupled consolidation Finite Element (FE) analysis, aiming to highlight the importance of appropriately modeling the fluid-phase when vertical ground motion is considered. This is further emphasized in the second part of this study where the vertical seismic response of a ground profile is computed with different assumptions regarding the pore fluid compressibility (drained, undrained and coupled consolidation) and the results are compared with field measurements.

Earthquake engineering analyses often concentrate on the variability of soil properties when computing site specific ground motion. Conversely, the earthquake source is modeled as a simple modulated noise that fits a target response spectrum. The earthquake events like 1933 Long Beach, 1957 San Francisco,1967 Caracas, 1985 Mexico City, 1989 Loma Prieta, and 1994 Northridge are important examples of how local site conditions affect the characteristics of wave propagation through the top soil. The ground motion parameters such as amplitude, frequency content or the duration can be affected by the local site condition and may result in amplification or de amplification to the original

bedrock motion. The response spectra characteristic can very well be found from BNBC response spectra graph given in figure 2.4 in chapter two.

Therefore, the structures on the ground surface (or even the buried structures i.e. tunnels) can be seriously affected by such phenomena and need to be accounted for during the design phase. Quantification of site effects on ground motions is a challenging task. This dissertation is dedicated to improve the existing ground response quantification techniques and the related knowledge base.

3.3 Conclusions:

Different softwares for soil material modeling with linear, equivalent-linear or nonlinear stress-strain relationships can be used. Deepsoil is one of them. This software runs the analysis in a very simplified way described in the above articles. By only inputting the soil parameters (i.e unit weight, shear wave velocity etc.) the response spectra, PGA, amplitude ratio and other significant parameters of seismic site response analysis can be found.

CHAPTER FOUR

RESULTS AND DISCUSSIONS

4.1 General

Local site effects have long been recognized as an important factor contributing to variations in strong ground motions. This study is one of the most important goals of earthquake engineering. Seismic hazard evaluations are calculated over broad geographical areas; however, as more ground motion data are collected, the local geology condition is emerging as one of the dominant factors controlling the variation in ground motion and determination of the site-specific seismic hazard for a given earthquake. Observations from earthquakes over the past 40 years have shown that local soil conditions can significantly influence the characteristics of ground shaking during earthquakes. These site effects should be considered when specifying ground shaking levels for seismic designs to prevent earthquake damage. Site effects are quantified via site response analysis, which involves the propagation of earthquake motions from the base rock, through the overlying soil layers, to the ground surface.

4.2 Site Response Analysis Before Ground Improvement

Figure 4.1 shows the earthquake records of Chi-Chi on ground surface and in the bedrock. The figure shows PGA values 0.30g on ground surface and 0.18g in the bedrock.

Figure 4.1 shows the acceleration diagram at surface and at bedrock simultaneously before ground improvement. Table 4.1 shows the soil model used for the current analysis before the soil improvement. The top layer consists of silty fine sand of velocity 160 m/s

and the thickness of the layer is 12m. The other layers are also silty fine sand with different thickness and shear wave velocity shown in the table below. These data have been obtained from the report of Ruppur Nuclear Powerplant project.

Table 4.1 Soil Model Before Ground Improvement

Layer	Layer name	Depth(m)	Thickness (m)	Unit wt (KN/m^3)	Shear wave velocity (m/s)
1	Silty fine sand	0-12	12	15	160
2	Silty fine sand	12-20	8	15	210
3	Silty fine sand	20-40	20	16	250
4	Silty fine sand	40-64	24	16	360
5	Silty fine sand	64-89	25	16	360
6	Silty fine sand	89-103	14	17	410
7	Silty fine sand	103-120	17	18	640

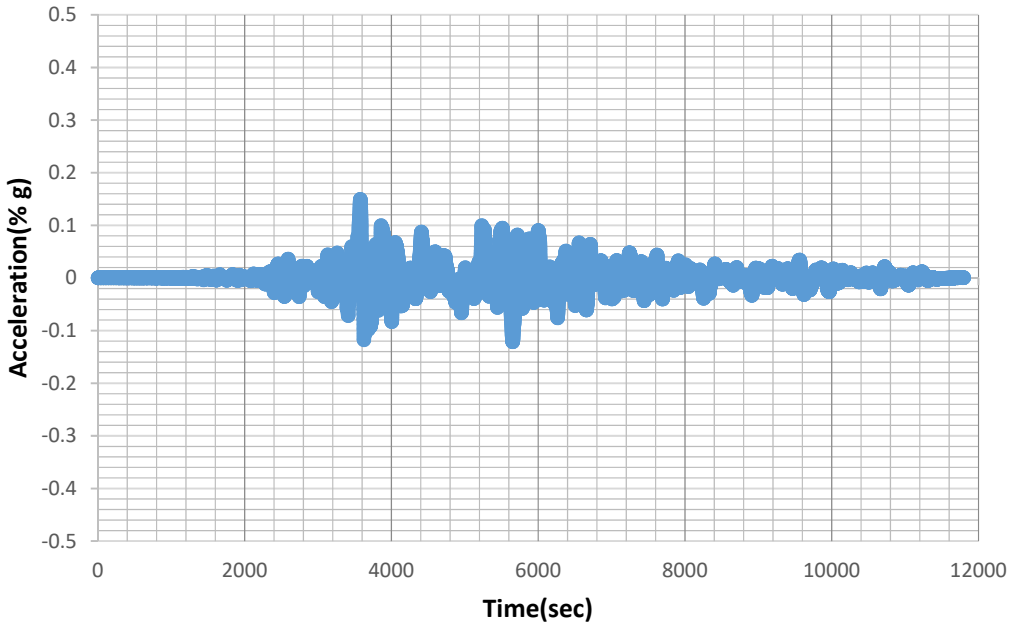

Fig 4.1(a) Time history records during Chichi earthquake at bedrock

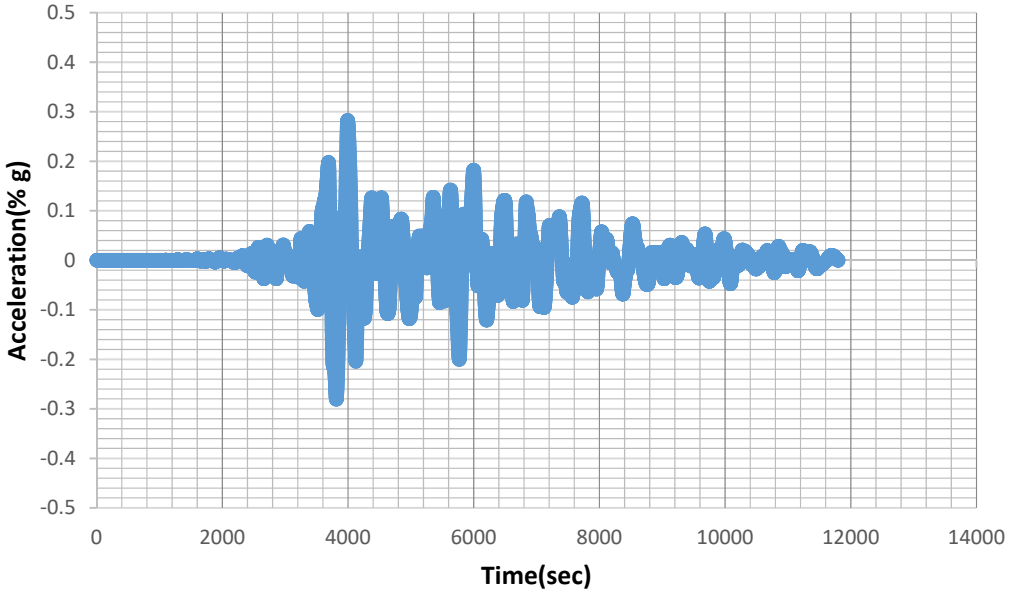

Fig. 4.1(b) Time history records during Chichi earthquake at surface

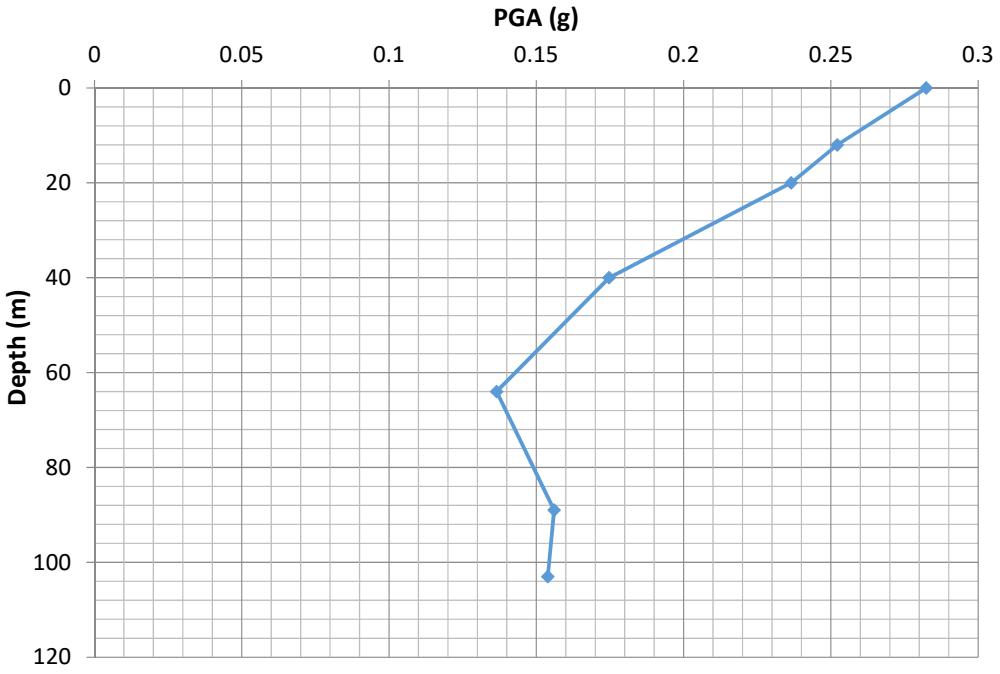

Fig. 4.2 PGA versus depth

4.2.1 Chi-Chi earthquake

This earthquake happened on Taiwan, China, 1991. On Sept. 21, 1999, at 1:47 a.m. (local time), central Taiwan experienced a destructive earthquake. As a result of this earthquake, more than 2,400 lives were lost, and more than 10,000 people were injured, according to the Taiwanese official report. Approximately 10,000 buildings and homes collapsed, and about 7,000 were severely damaged.

1D site response analysis had been carried out using the soil model as shown in Table 4.1 and using Chi-Chi earthquake (bedrock) as input. Figure 4.2 shows the graph of depth versus PGA. PGA value is gradually increasing from a depth of 120m. The value is 0.15g at 120 m which amplifies to 0.28g at the ground surface.

As seismic waves travel from bedrock to the surface, certain characteristics of the waves, such as amplitude and frequency content is changed as they pass through the soil deposits. This process can transfer large accelerations to structures causing large destruction, particularly when the resulting seismic wave frequency matches with the resonant frequencies of the structures. It can be seen from the figure 4.3 that the predominant frequency is around 0.5 Hz with amplitude ratio of almost 5. Normalized PSA value is below 4 at the period of 2 sec. Graph is presented in figure 4.4.

4.2.2 Coyote earthquake

The 1979 Coyote Lake earthquake occurred at 10:05:24 local time on August 6 with a moment magnitude of 5.7 and a maximum Mercalli Intensity of VII . Acceleration value of Coyote earthquake decreases from 0.4(surface) to 0.15 (bedrock) in figure 4.5.

.

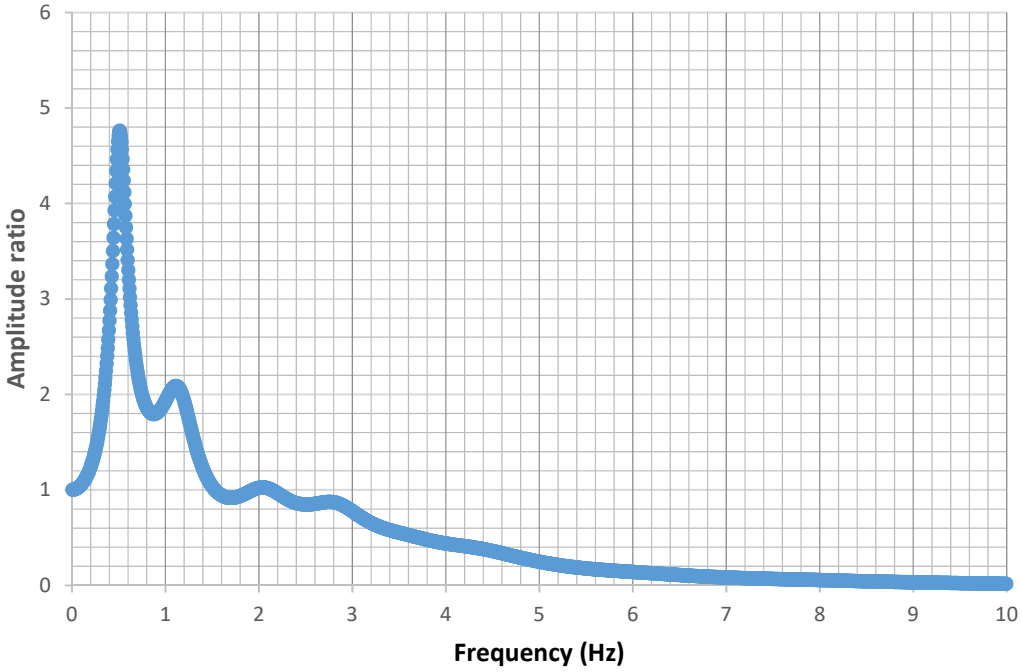

Fig. 4.3 Amplitude versus frequency curve

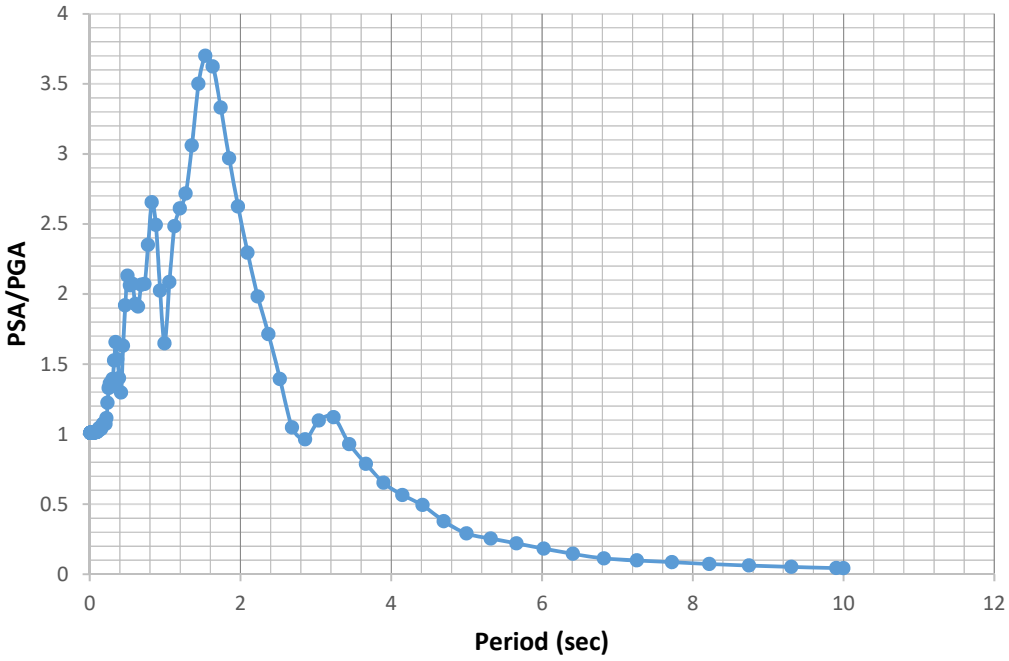

Fig. 4.4 Normalized PSA/PGA versus period relation

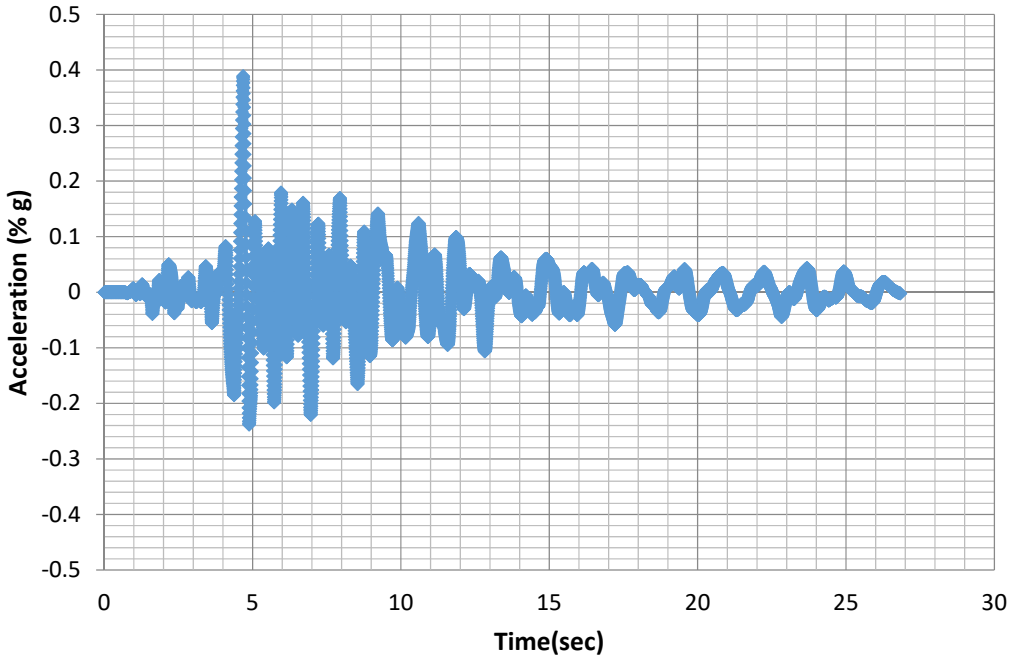

Fig. 4.5(a) Time history plots during Coyote earthquake at surface

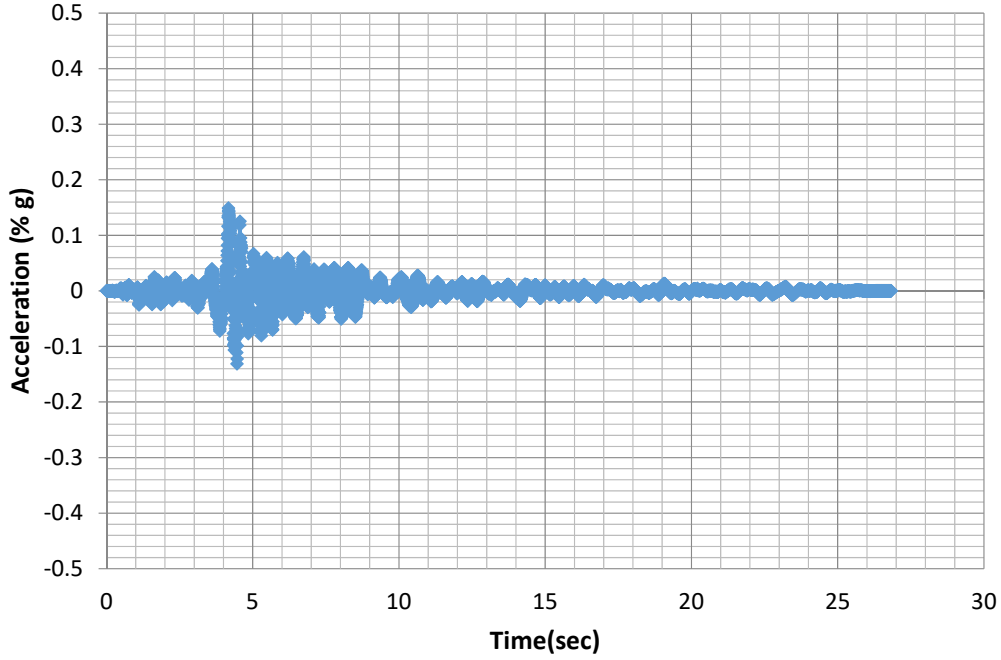

Fig 4.5(b) Time history plots during Coyote earthquake at bedrock

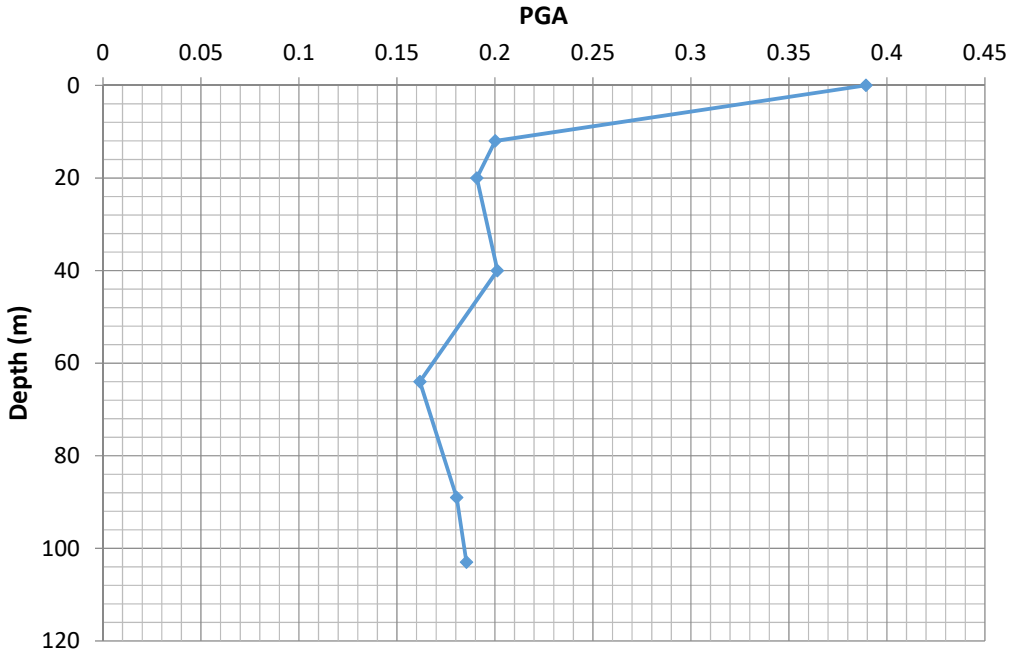

Fig 4.6 PGA versus depth

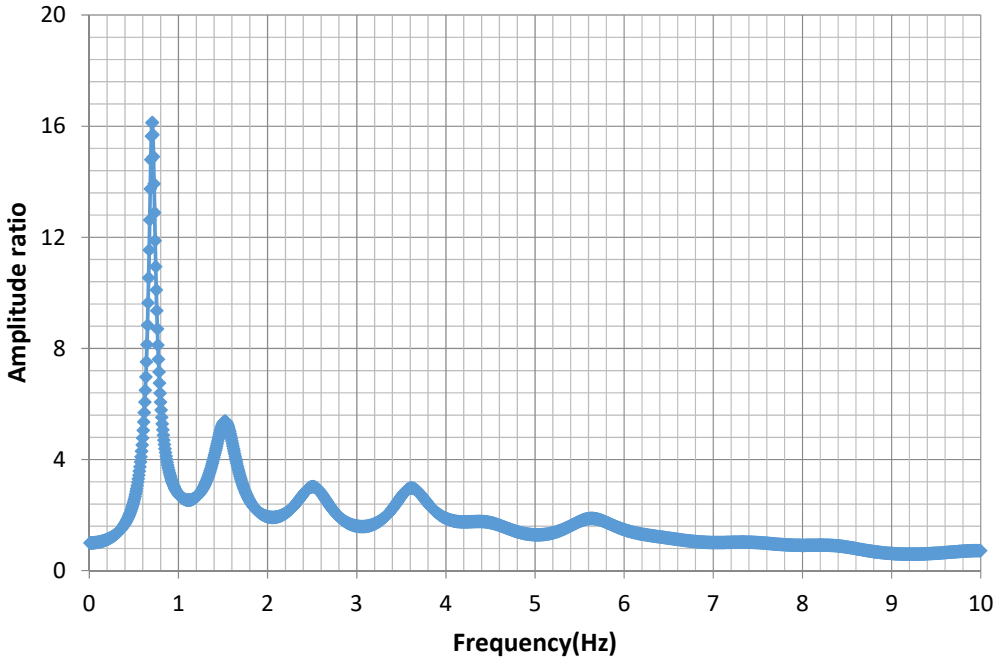

Fig. 4.7 Amplitude ratio versus frequency curve

Peak ground acceleration (PGA) is equal to the maximum ground acceleration that occurred during earthquake shaking. Here for Coyote earthquake the amplitude of the largest absolute acceleration recorded on an accelerogram is almost 0.4g shown in figure 4.6.

The predominant frequency is around 1 Hz in figure 4.7. In Coyote Earthquake normalized value is found in 0.5sec.

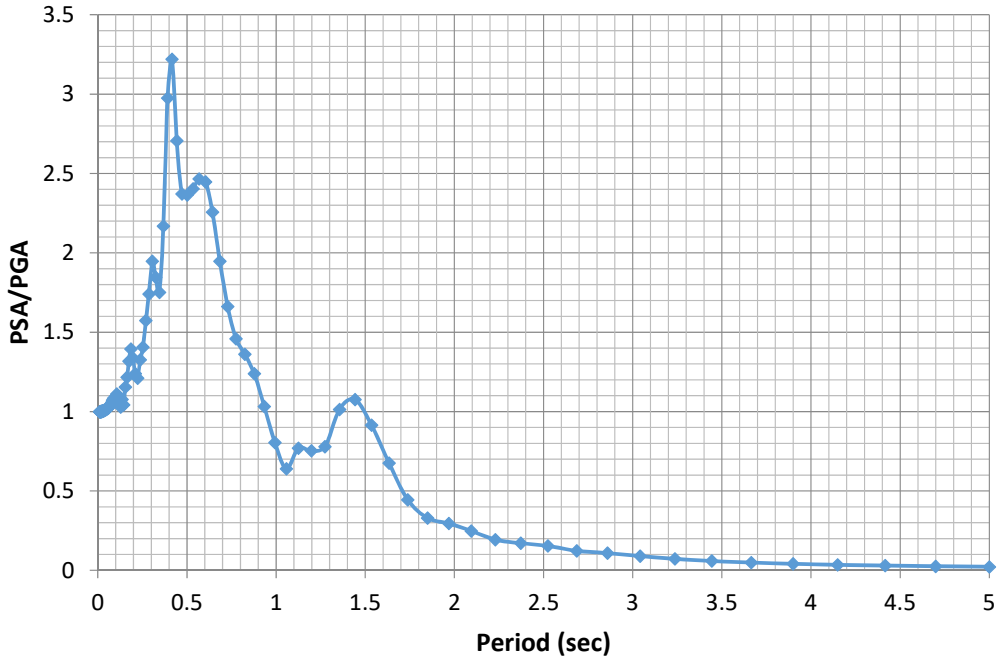

Fig. 4.8 Normalized PSA versus period relation

4.2.3 Kobe earthquake

The Great Hanshin earthquake or Kobe earthquake, occurred on January 17, 1995 at 05:46:53 JST (January 16 at 20:46:53 UTC) in the southern part of Hyōgo Prefecture, Japan, including the region known as Hanshin. The tremors lasted for approximately 20 seconds.

Figure 4.9 shows the earthquake records of Kobe earthquake on ground surface and in the bedrock. The figure shows acceleration value is 0.3 on ground surface and 0.18 in the bedrock.

The amplitude of the largest absolute acceleration recorded on an accelerogram for Kobe earthquake is almost 0.28g shown in figure 4.10.

The predominant frequency is again around 1 Hz for Kobe earthquake, but amplitude ratio decreases from Chichi earthquake from 16 to 5. Here period reaches around 1.5 sec for maximum PSA value shown in figure 4.12.

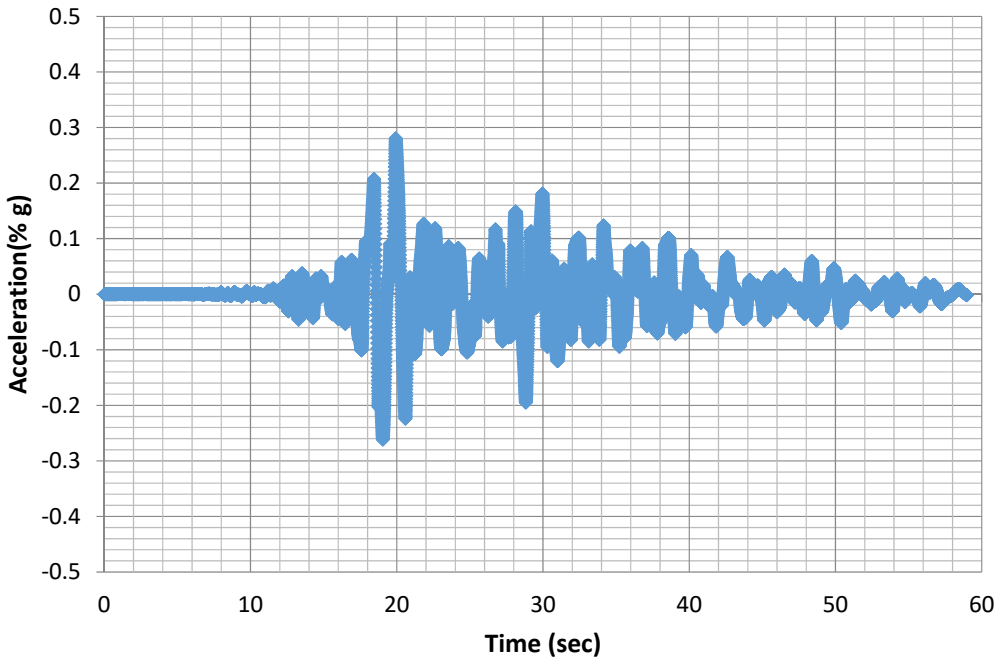

Fig 4.9(a) Time Histories of Kobe Earthquake at surface

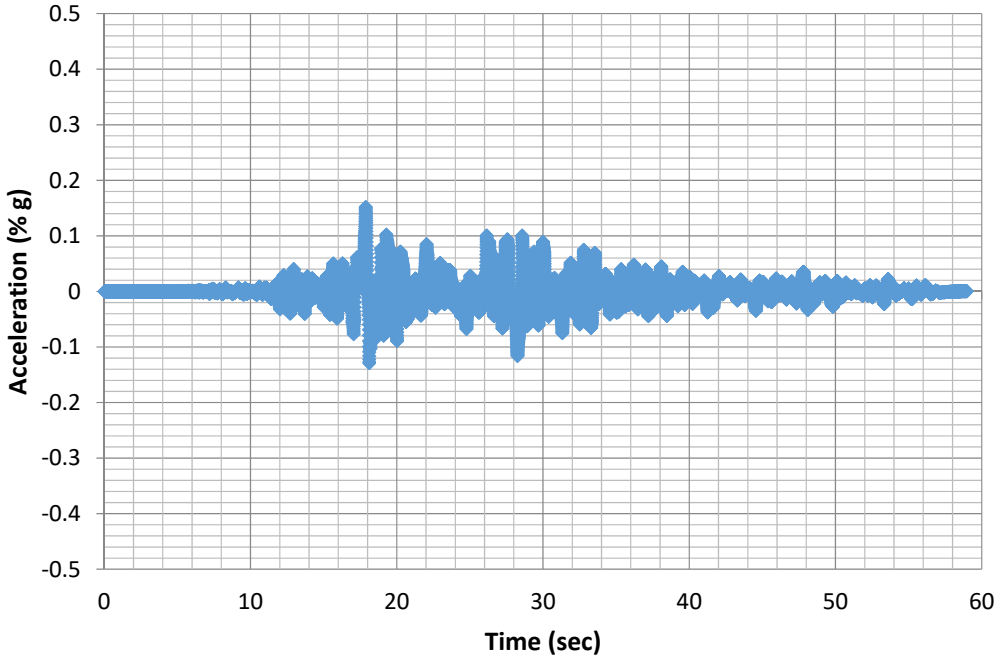

Fig 4.9(b) Time Histories of Kobe Earthquake at bedrock

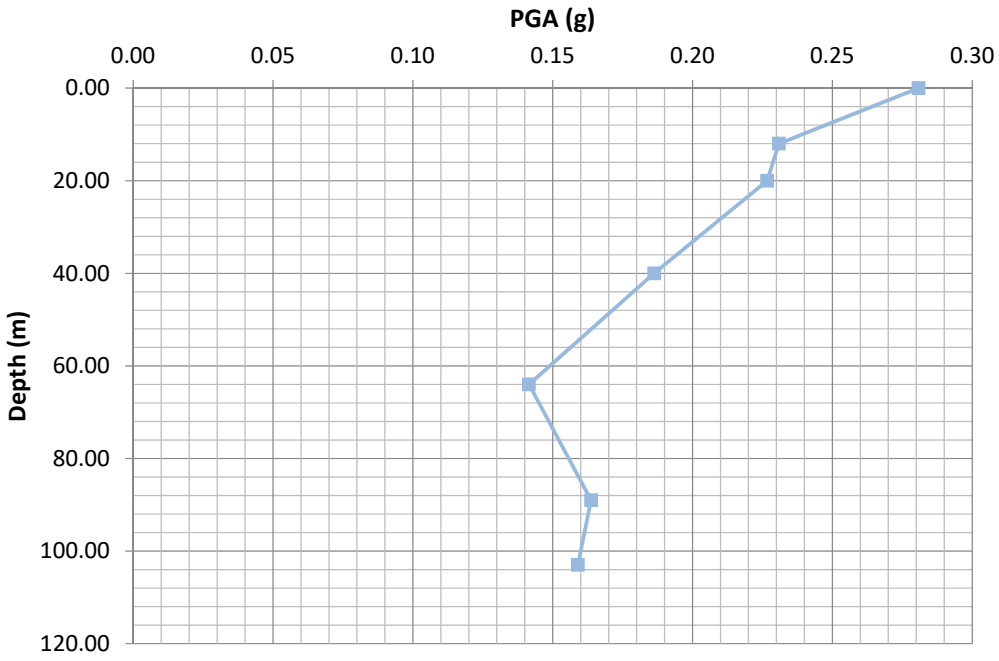

Fig 4.10 PGA versus depth

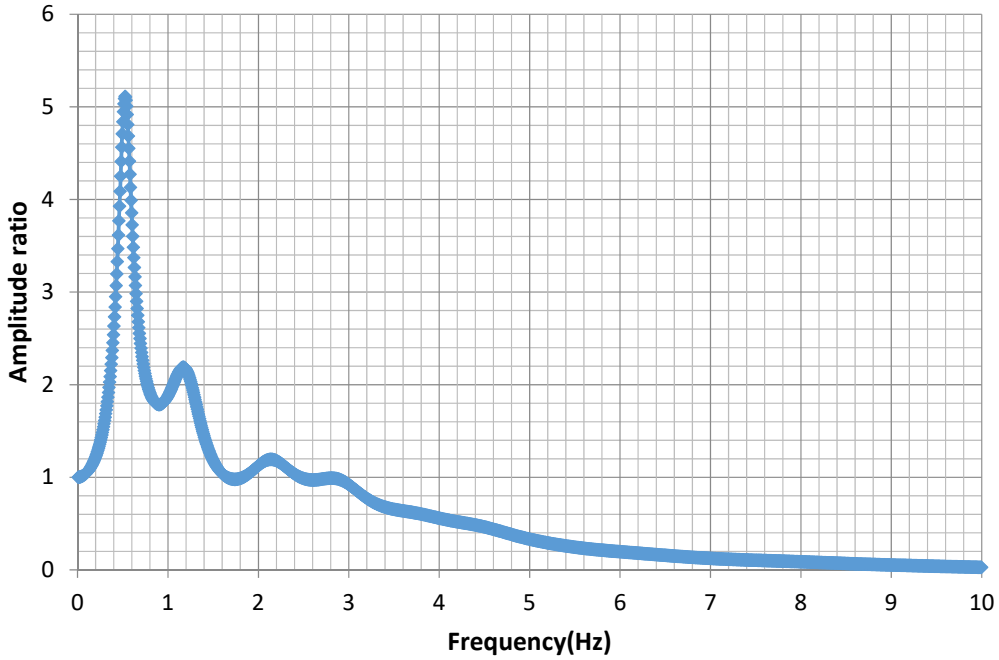

Fig 4.11 Amplitude ratio versus frequency curve

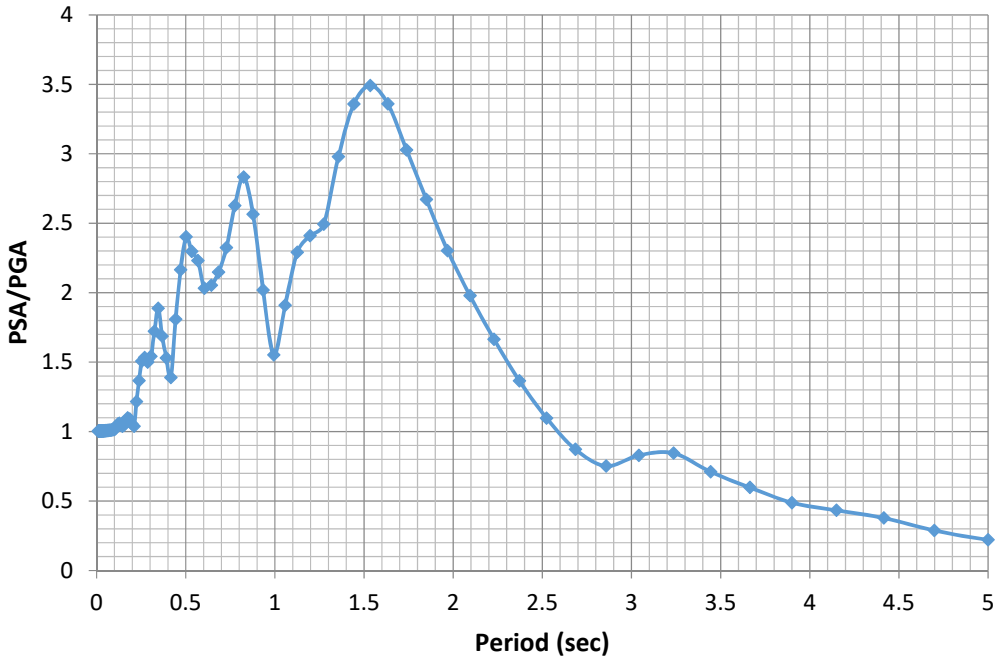

Fig 4.12 Normalized PSA versus period relation

4.2.4 Loma Girloy earthquake

Gilroy Quake is Vivid Reminder of '89 Shaker. Still, it is one of the strongest quakes in the area since the 1989 Loma Prieta quake, which has a magnitude of 6.9 And scientists say there is a 70% chance of a tremblor as strong as the 1994 Northridge quake striking the Bay Area by 2030.

Earthquake records of Loma Girloy on ground surface and in the bedrock is shown. Acceleration value of Loma Girloy earthquake is 0.30 on ground surface and 0.15 in the bedrock shown in figure 4.13.

PGA value in Loma Girloy earthquake reaches almost 0.3 and in Figure 4.15 amplitude ratio reaches to 8 and predominant frequency is around 1 Hz. Figure 4.16 shows normalized PSA versus period relation. Peak value is near 3.5.

4.2.5 Mammoth earthquake

On May 25, 1980 at 0933 Pacific Daylight Time (PDT) a magnitude 6.0 earthquake (all magnitudes are from Caltech Seismological Laboratory) occurred approximately 10.5 km east-southeast of Mammoth Lakes, California. During the next 16 minutes, four magnitude 4.1 - 5.0 shocks and one 5.5 shock occurred. This seismic activity was the beginning of an earthquake sequence that produced 72 magnitude 4.0 - 4.9 events, six magnitude 5.0 - 5.5 events and three events of magnitude 6.0 - 6.3 during the next 48 hours; thousands of magnitude < 3.9 earthquakes were generated during this same time period.

Earthquake records of Mammoth earthquake on ground surface and in the bedrock does not show any significant difference in figure 4.17.

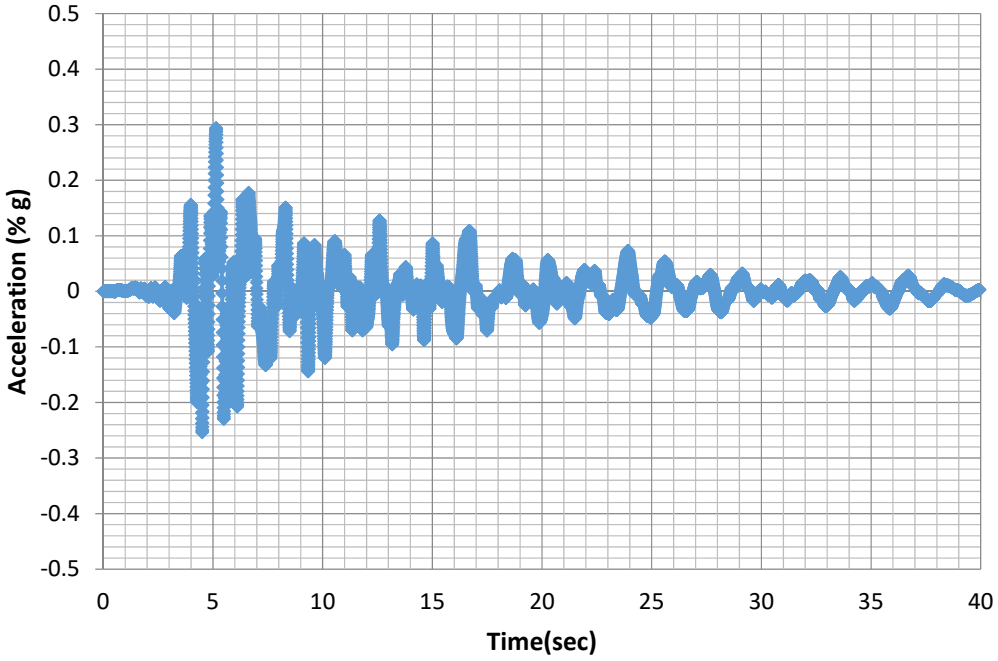

Fig 4.13(a) Time Histories of Loma Girloy Earthquake at surface

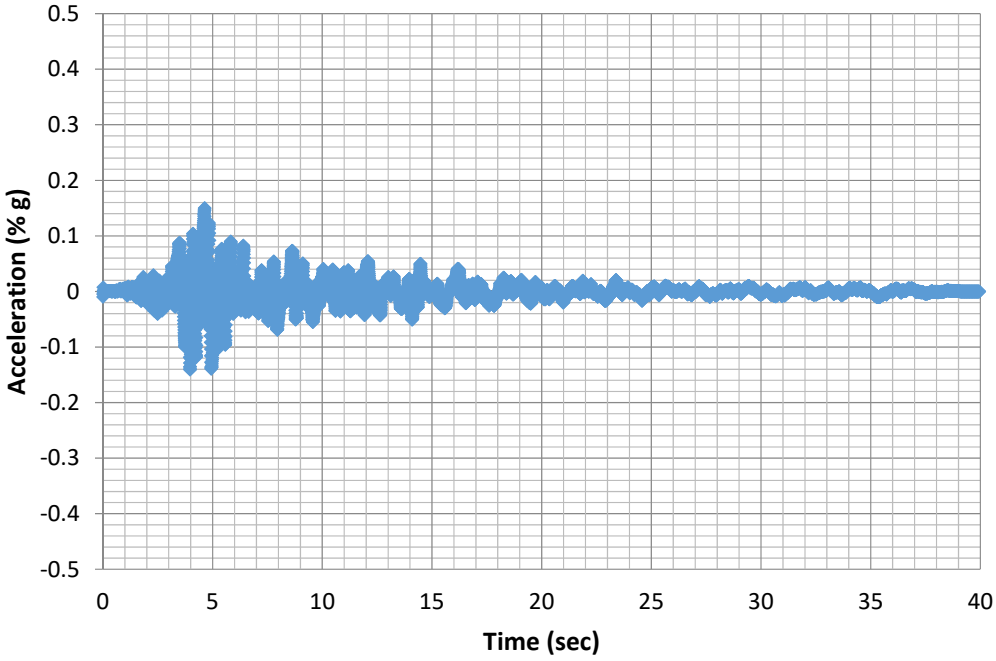

Fig 4.13(b) Time Histories of Loma Girloy Earthquake at bedrock

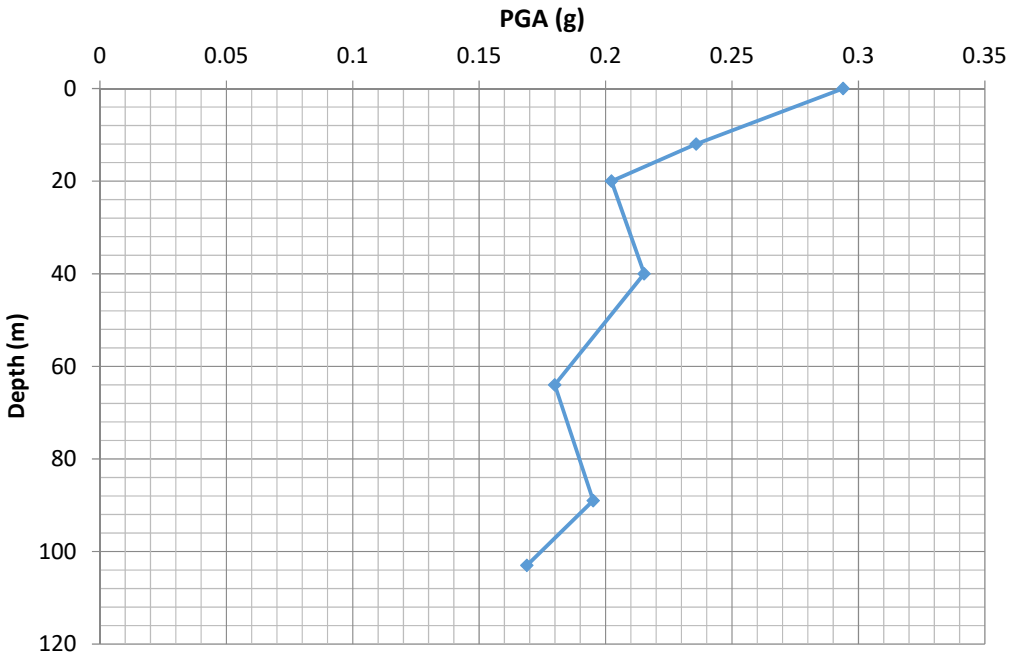

Fig 4.14 PGA versus depth

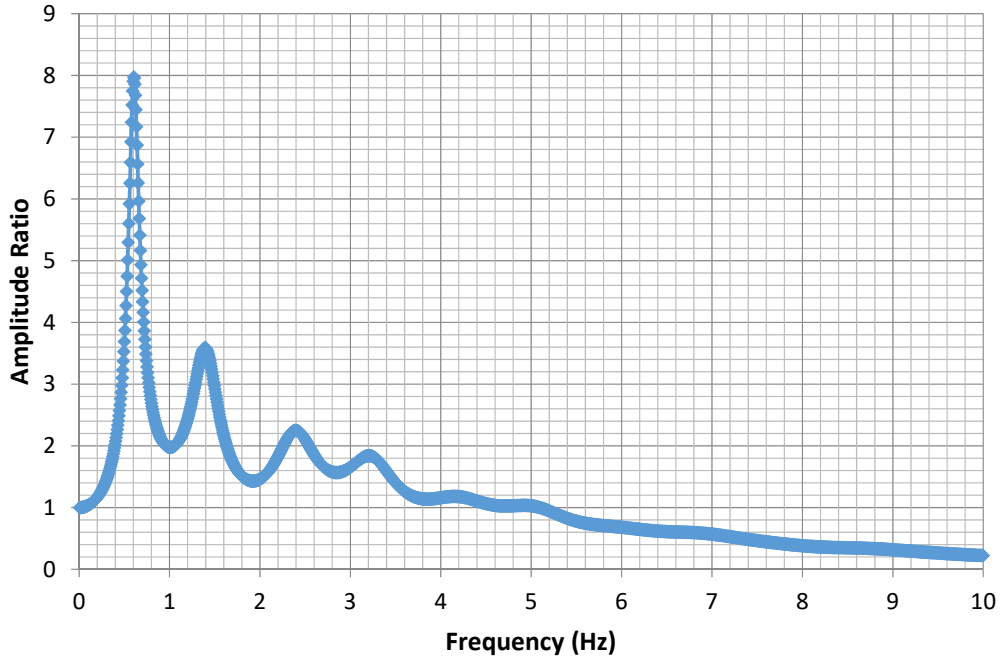

Fig 4.15 Amplitude versus frequency curve

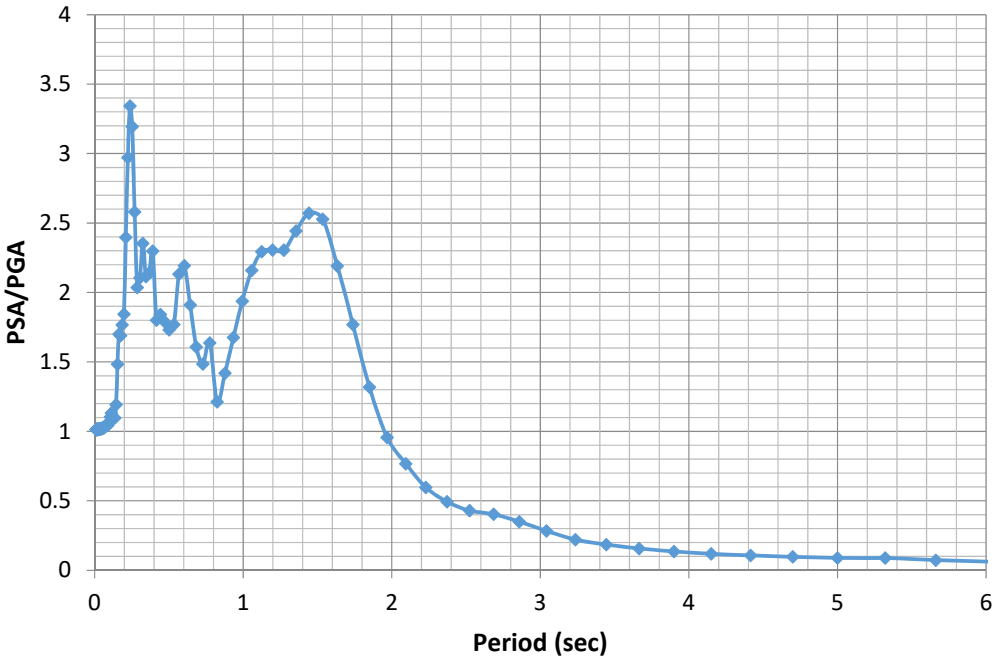

Fig 4.16 Normalized PSA versus period relation

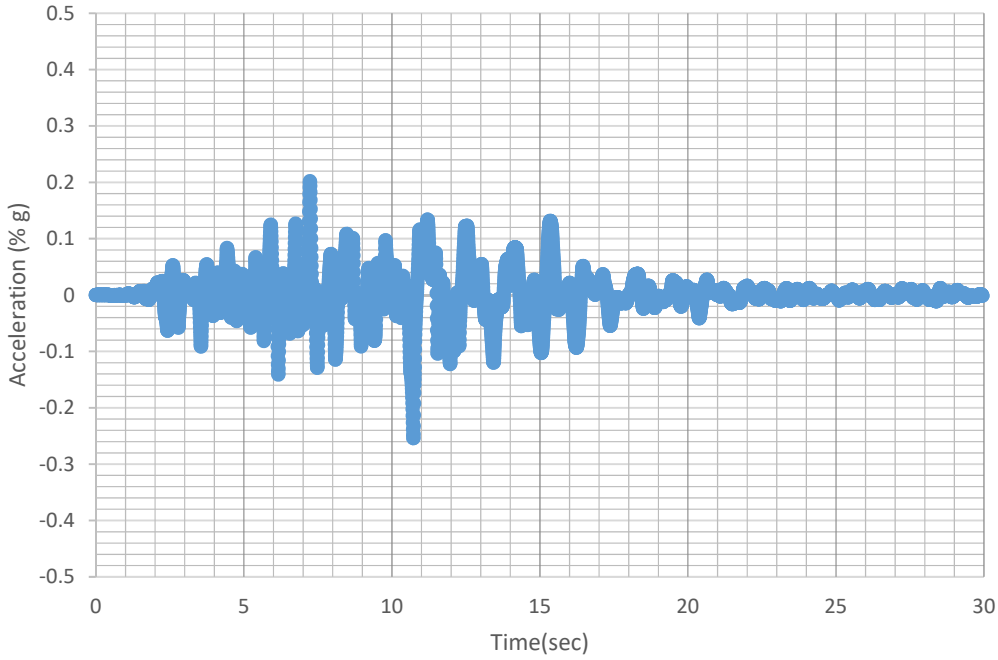

Fig 4.17(a) Time Histories of Mammoth Earthquake at surface

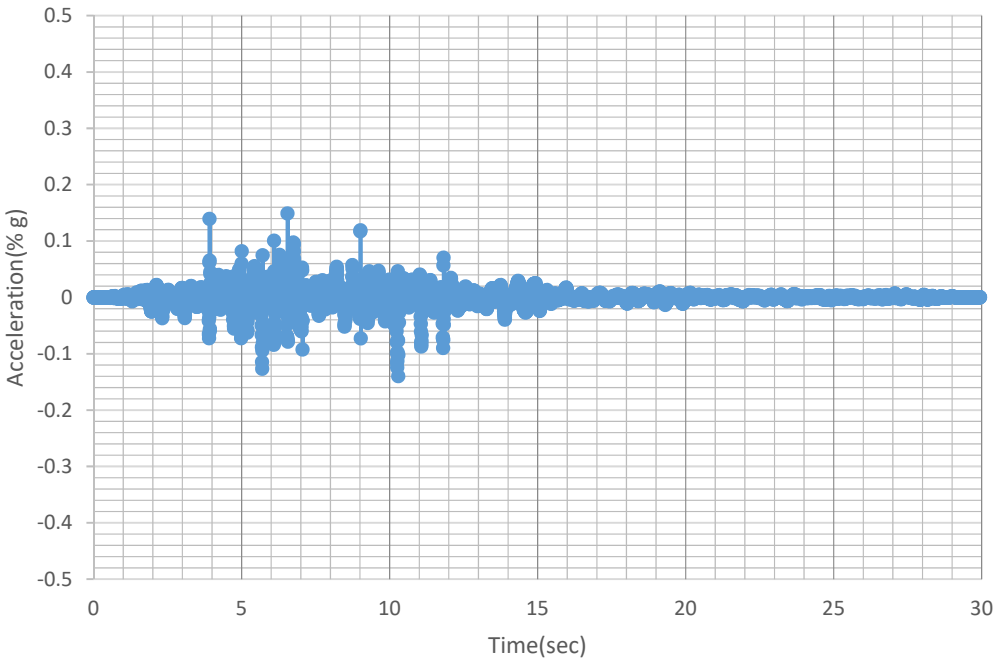

Fig 4.17(b) Time Histories of Mammoth Earthquake at bedrock

PGA value has reached to approximately 0.26g in figure 4.18 which is lesser than Loma Girloy earthquake.

The predominant frequency of Mammoth earthquake is around 1 Hz. At the same time figure 4.20 shows normalized PSA value is maximum when the period is 1.5 sec.

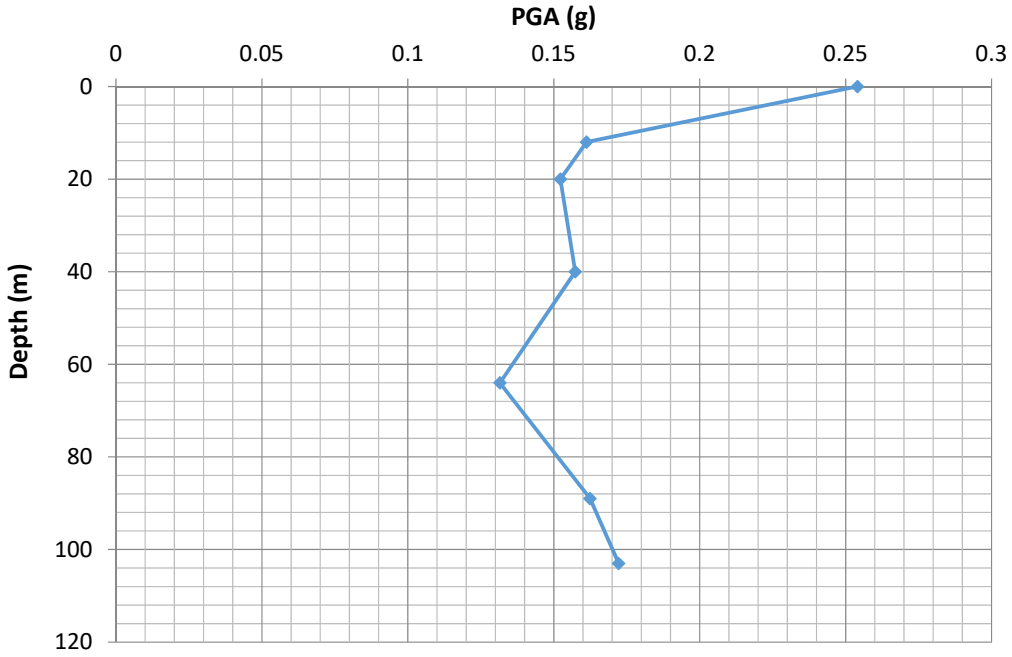

Fig 4.18 PGA versus depth

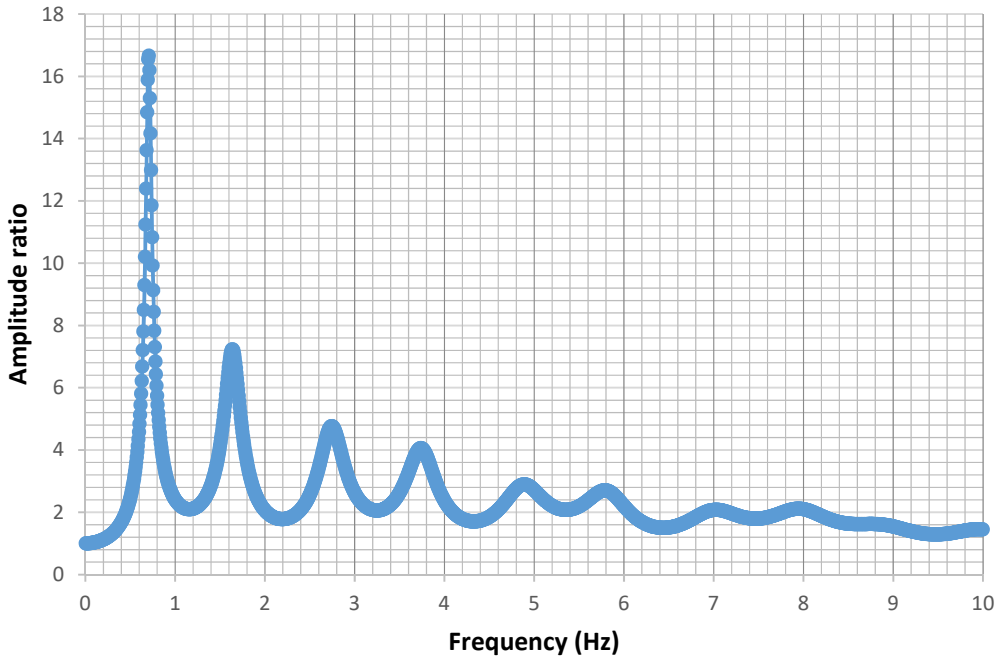

Fig 4.19 Amplitude versus frequency

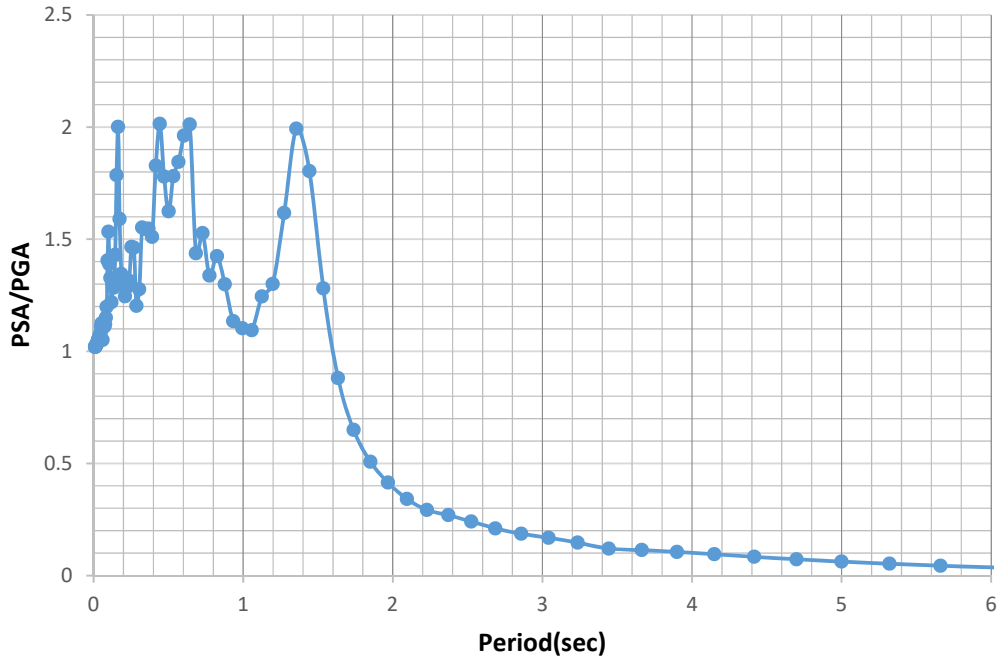

Fig 4.20 Normalized PSA versus period relation

4.2.6 Nahanni earthquake

The 1985 Nahanni earthquakes is the name for a continuous sequence of earthquakes that began in 1985 in the Nahanni region of the Northwest Territories, Canada. The largest of these earthquakes occurred on December 23, reaching 6.9 on the moment magnitude scale.

Acceleration value is almost same in surface and in bedrock for this earthquake.

PGA value has reached to approximately 0.21g. Figure 4.23 shows amplitude ratio versus frequency relation. From the figure, it can be seen that the predominant frequency is around 1 Hz. Figure 4.24 shows normalized PSA versus period relation.

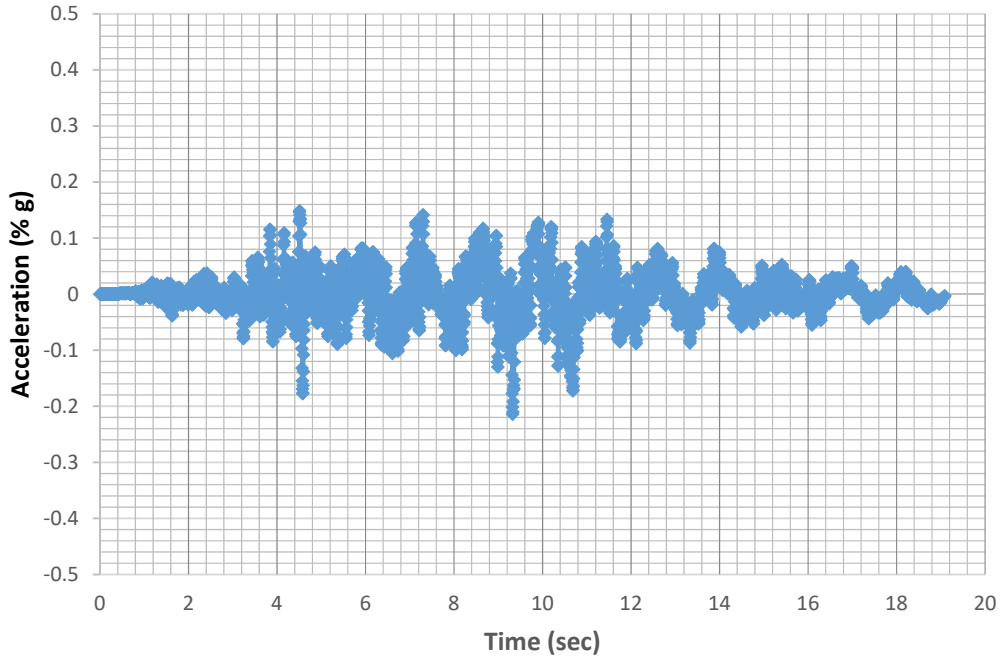

Fig 4.21(a) Time Histories of Nahanni Earthquake at surface

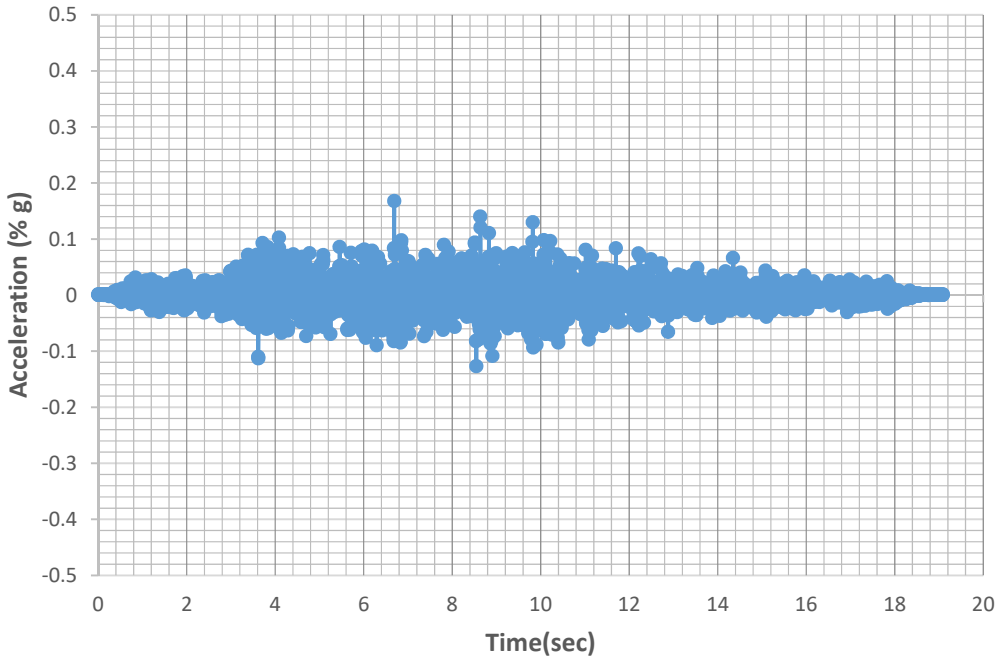

Fig 4.21(b) Time Histories of Nahanni Earthquake at bedrock

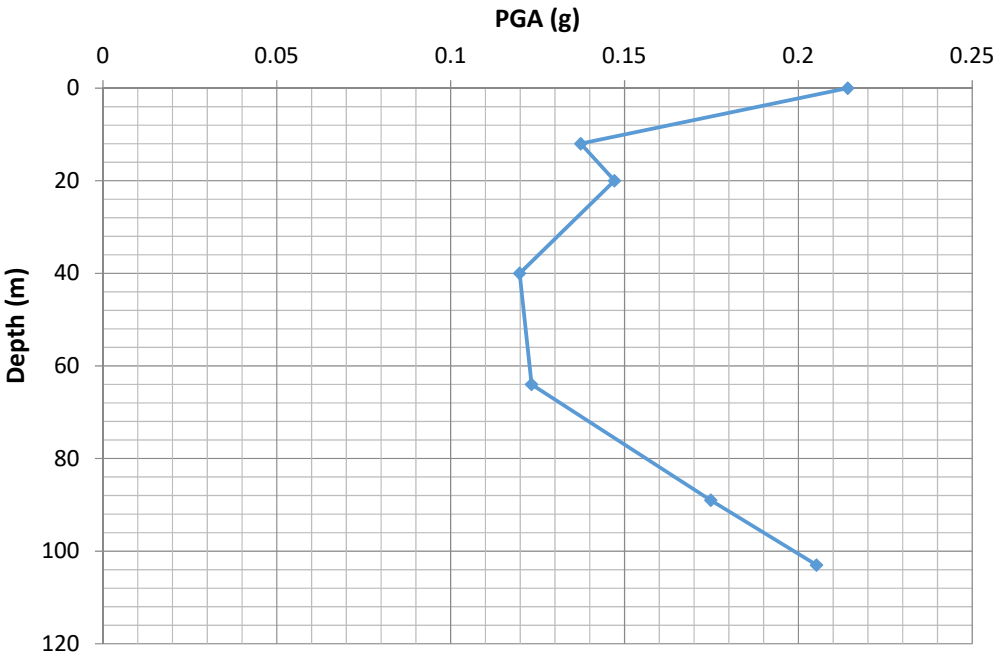

Fig. 4.22 PGA versus depth

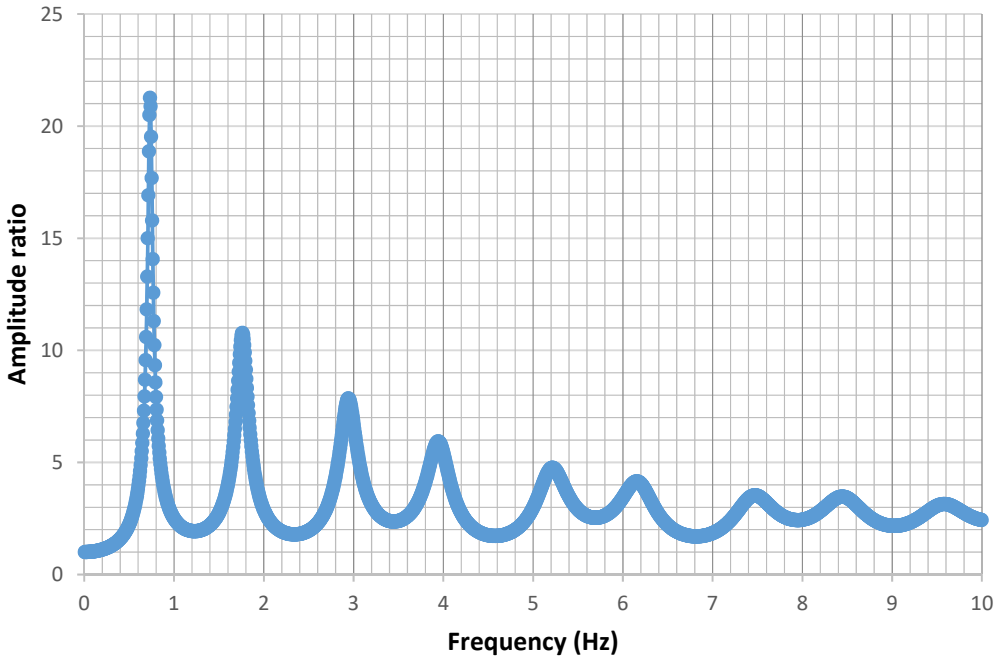

Fig.4 .23 Amplitude versus frequency curve

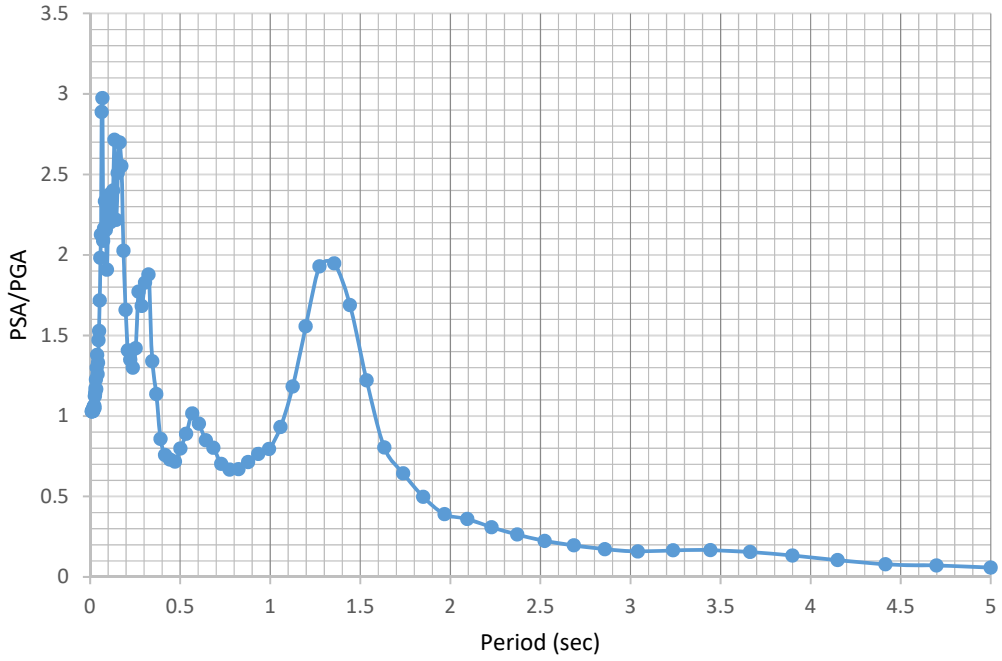

Fig 4.24 Normalized PSA versus period relation

4.2.7 Northridge earthquake

The initial Northridge quake shook with a staggering Richter magnitude of 6.9, and lasted for more than 20 seconds. The earthquake occurred along a "blind" thrust fault, close to the San Andreas fault. The outcome resulted in one of the most financially destructive natural disasters in American history.

Figure 4.25 shows the earthquake records of Northridge on ground surface and in the bedrock. Acceleration value reaches from 0.4 to 0.15 here.

In the Northridge earthquake PGA value has reached to approximately 0.4g. Figure 4.27 shows amplitude ratio versus frequency relation. From the figure, it can be seen that the predominant frequency is around 1 Hz. Figure 4.28 shows normalized PSA versus period relation.

4.2.8 Parkfield earthquake

Parkfield earthquake is a name given to various large earthquakes that occurred in the vicinity of the town of Parkfield, California, United States. The San Andreas fault runs through this town, and six successive magnitude 6 earthquakes occurred on the fault at unusually regular intervals, between 12 and 32 years apart (with an average of every 22 years), between 1857 and 1966. The most recent significant earthquake to occur here happened on September 28, 2004. Figure 4.29 shows the earthquake records of Parkfield on ground surface and in the bedrock. PGA value of Parkfield earthquake is approximately 0.33g after ground Improvement.

In the amplitude ratio versus frequency relation, from the figure, it can be seen that the predominant frequency is around 1 Hz. Figure 4.32 shows normalized PSA versus period relation.

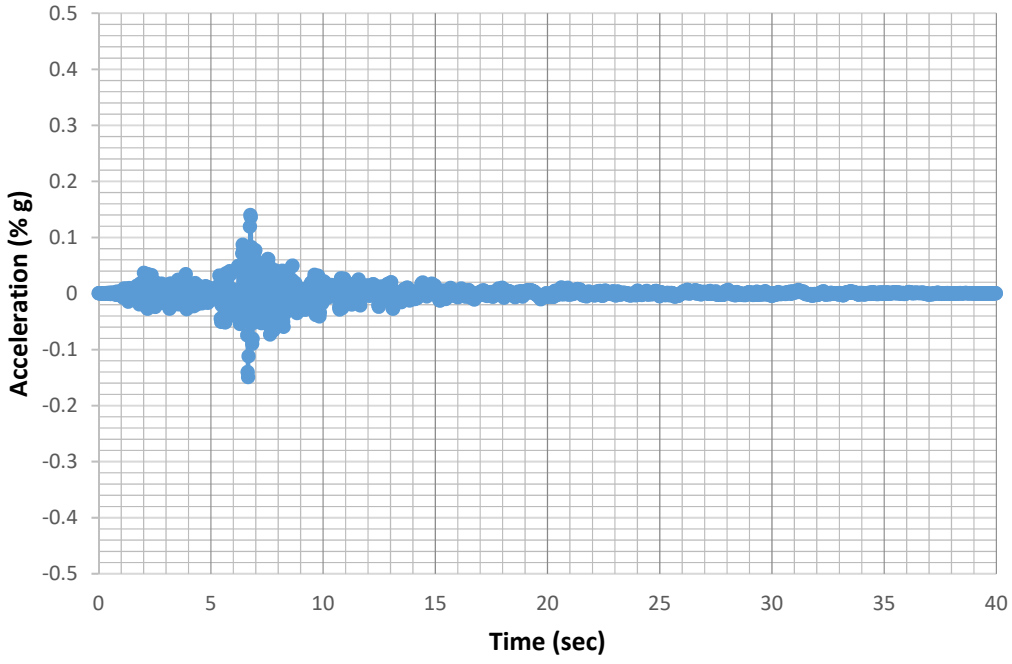

Fig 4.25(a) Time Histories of Northridge Earthquake at bedrock

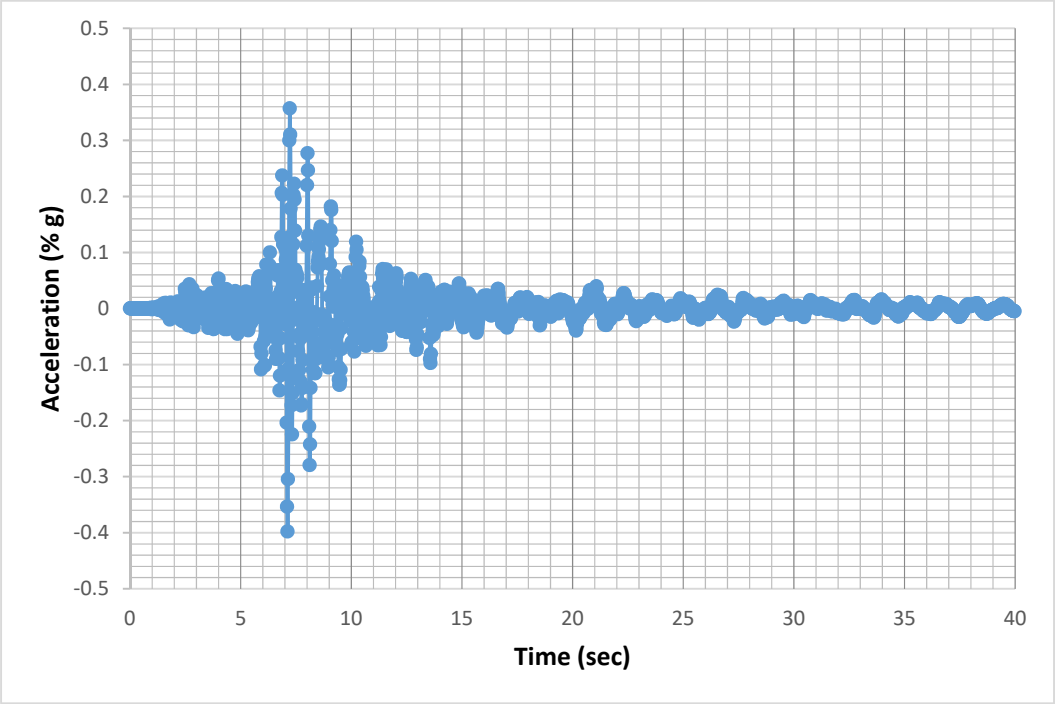

Fig 4.25(b) Time Histories of Northridge Earthquake at surface

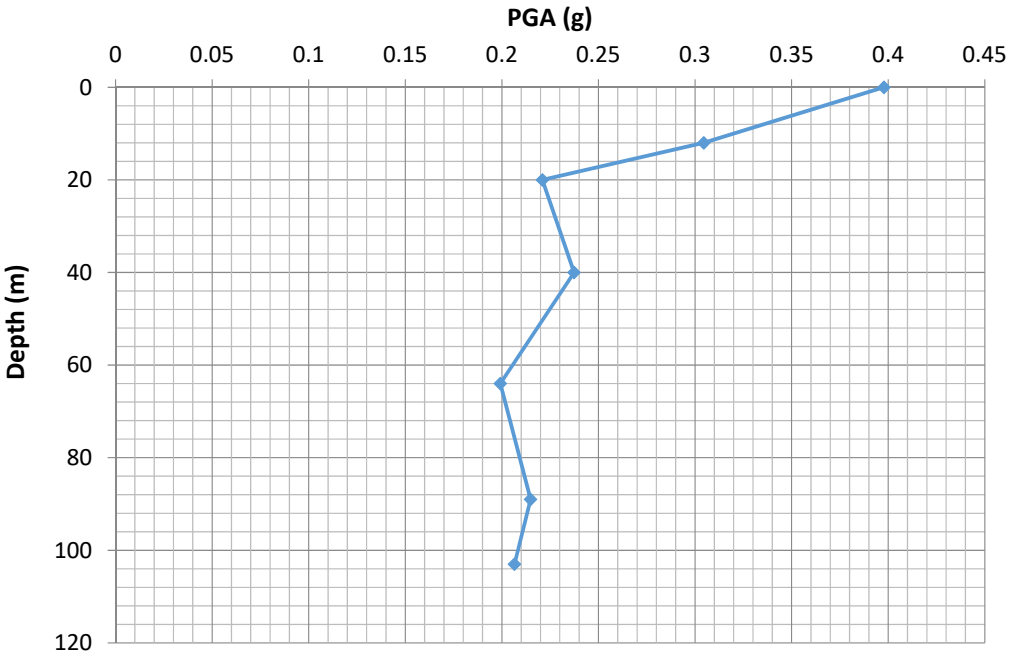

Fig 4.26 PGA versus depth

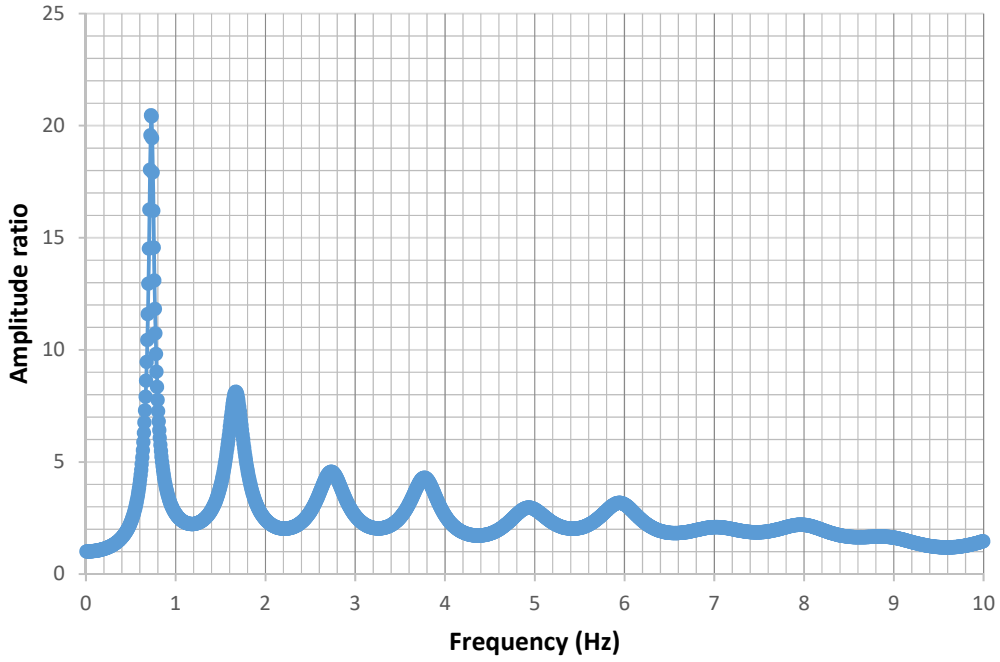

Fig 4.27 Amplitude versus frequency curve

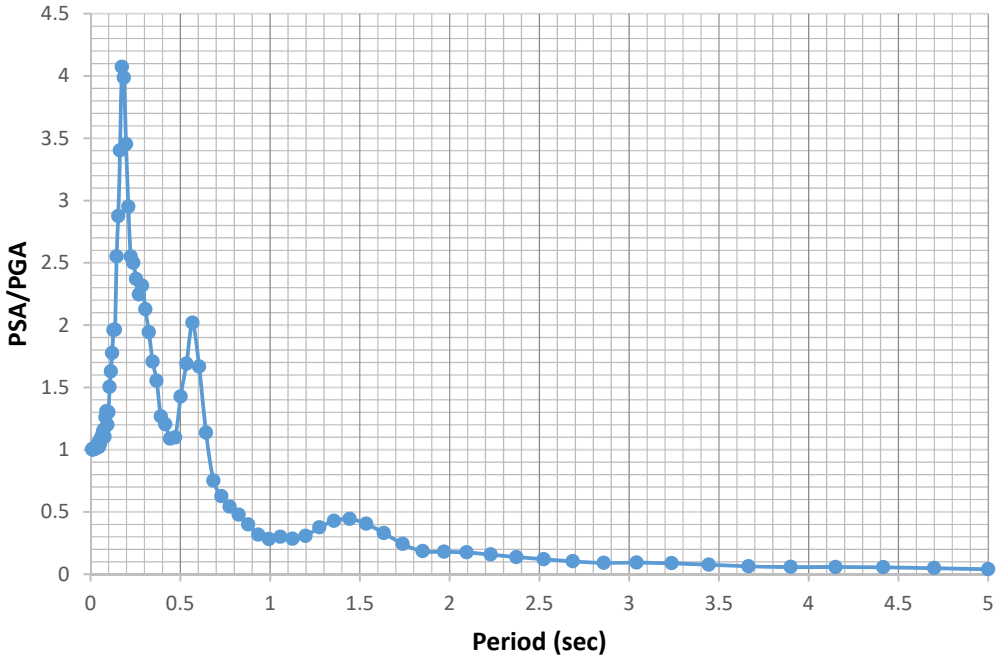

Fig 4.28 Normalized PSA versus period relation

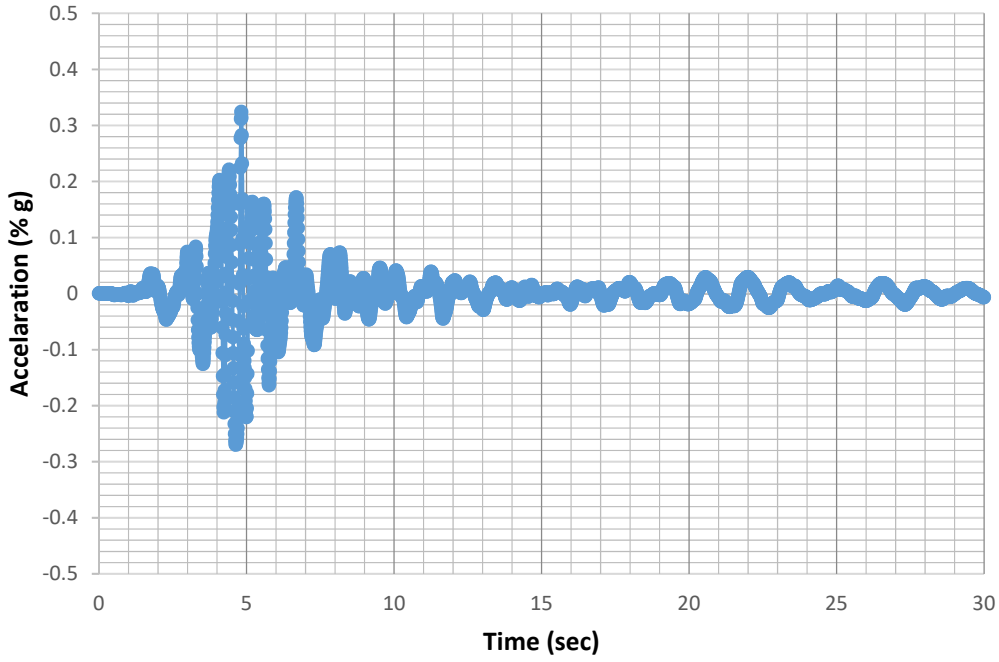

Fig 4.29(a) Time Histories of Parkfield Earthquake at surface

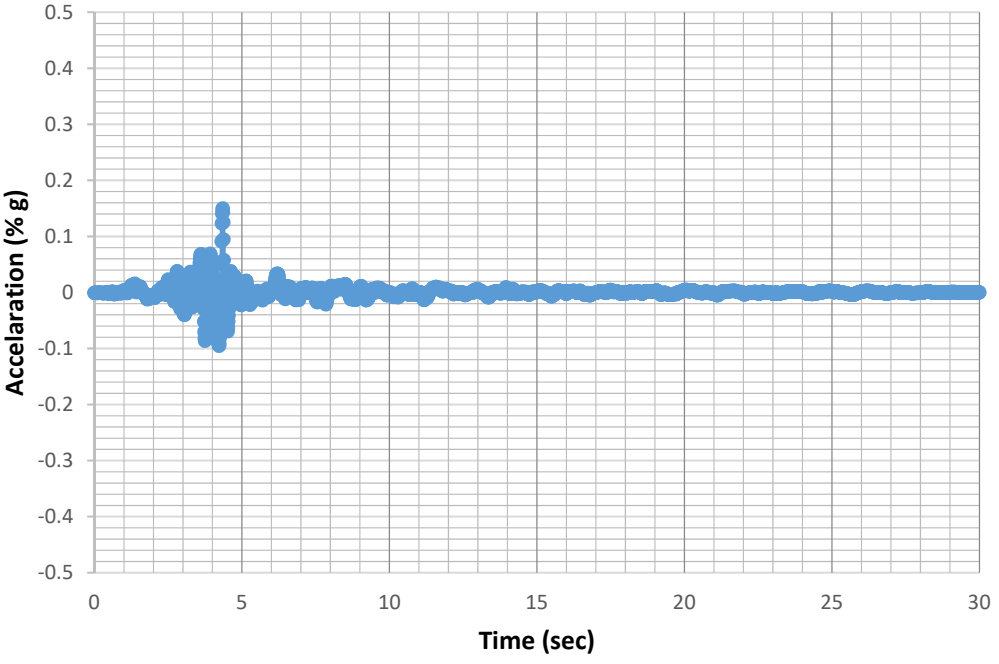

Fig 4.29(b) Time Histories of Parkfield Earthquake at bedrock

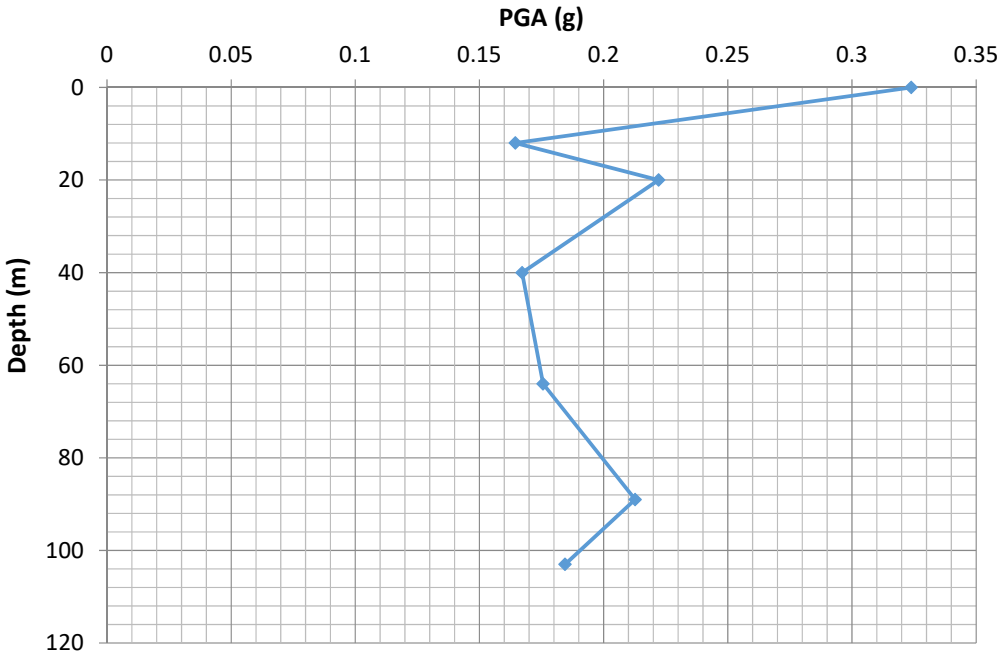

Fig 4.30 PGA versus depth

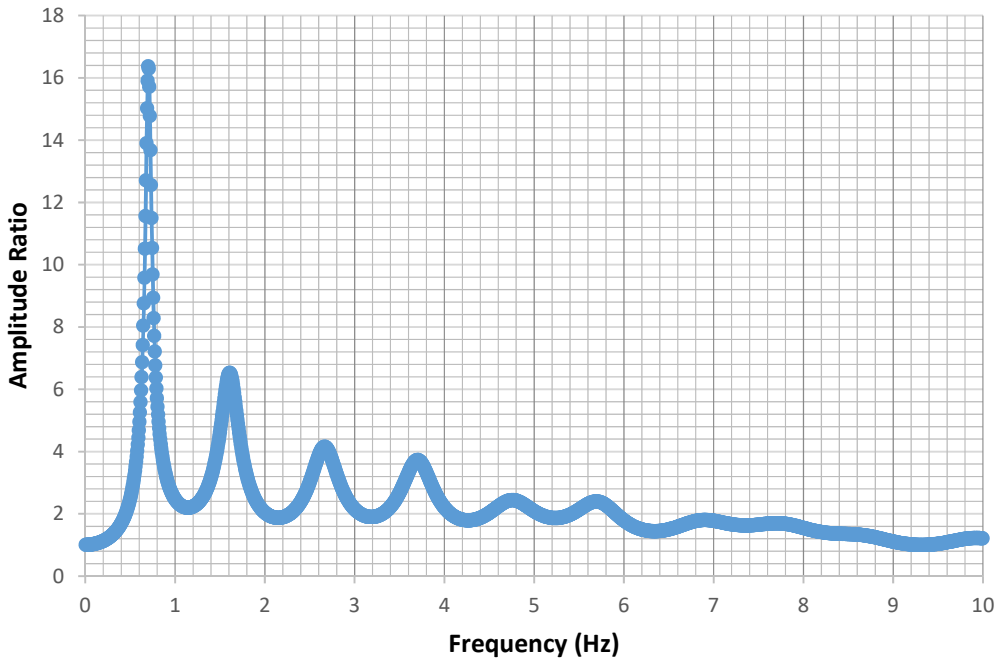

Fig 4.31 Amplitude versus frequency curve

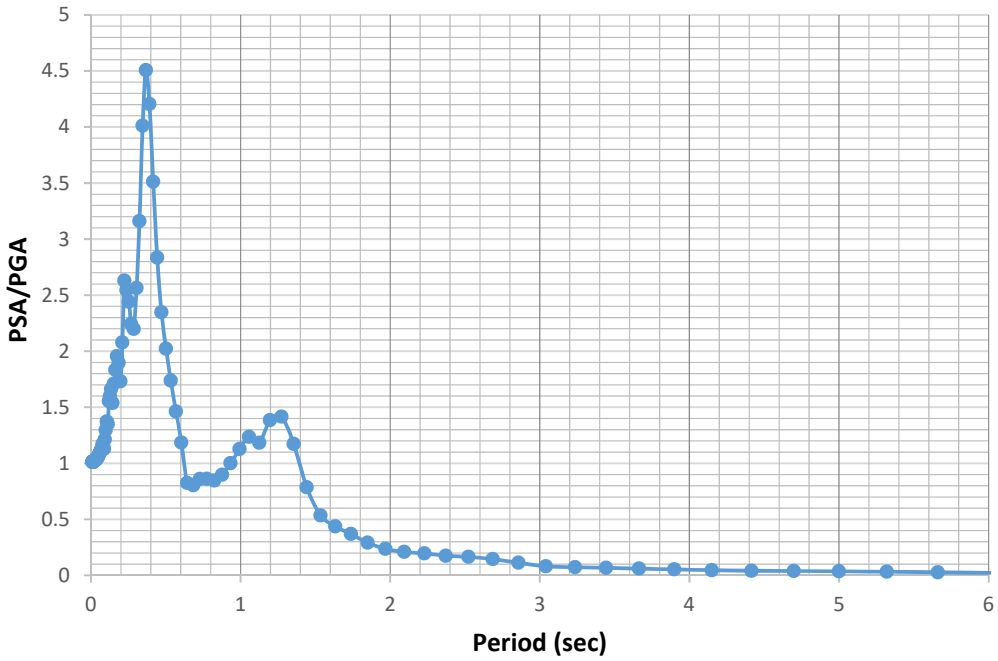

Fig 4.32 Normalized PSA versus period relation

4.2.9 Combination of all earthquakes before ground improvement

Combining all the graphs found from all the earthquakes before ground improvement we see before ground improvement in figure 4.33, the PSA value ranges between 0.6 to 1.62. Nahanni earthquake gives the maximum amplitude ratio of around 22 in figure 4.34 Before ground improvement in figure 4.35, Coyote earthquake gives the maximum value of around 2.48 and Nahanni earthquake gives the minimum value of around 1.58. When we combined all the earthquakes in figure 3.36 before ground improvement, the PGA value ranges between 0.2g to 0.4g. Nahanni earthquake gives the minimum value and Northridge the maximum. The mean values are also shown along with their standard deviation. Before ground improvement, the mean PGA, PSA, Amplitude ratio and normalized PSA value are 0.32g, 0.6, 12 and 2 respectively.

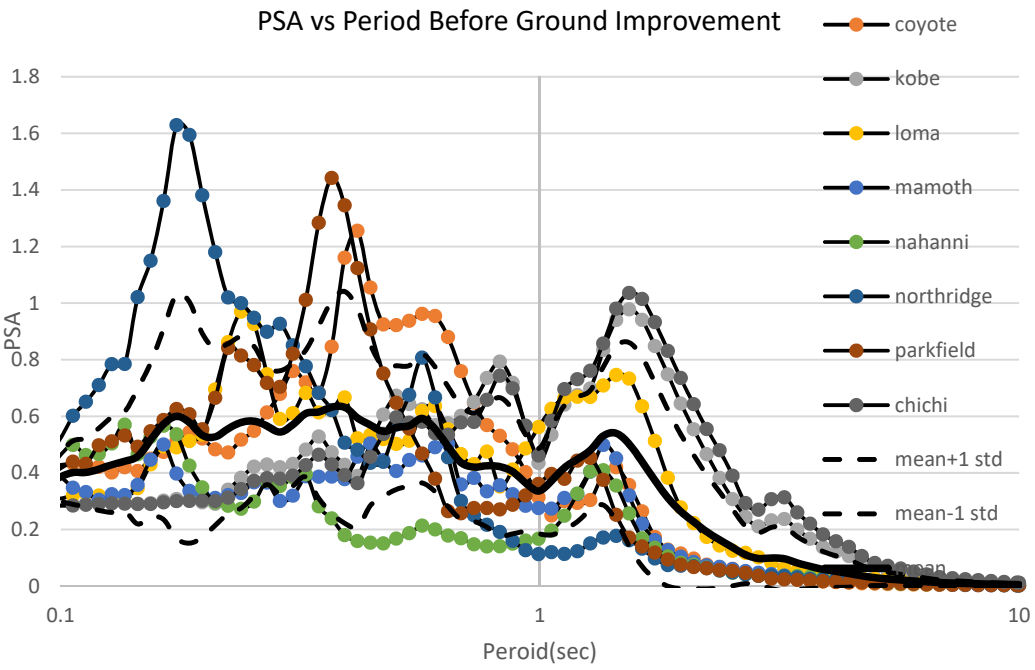

Fig 4.33 Combined PSA versus period relation

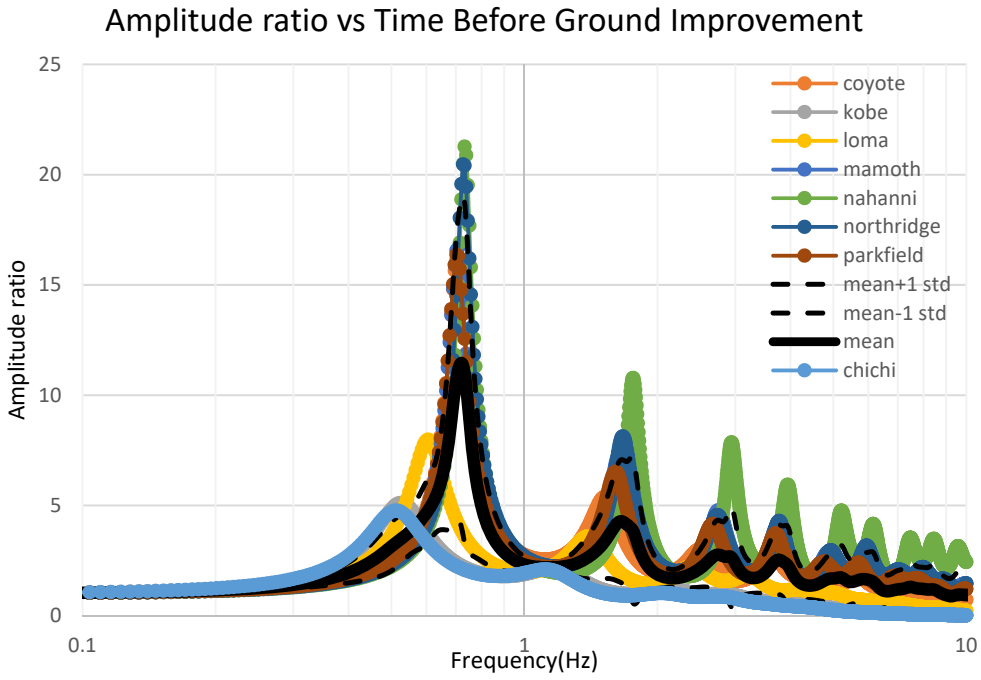

Fig 4.34 Combined Amplitude ratio versus Frequency

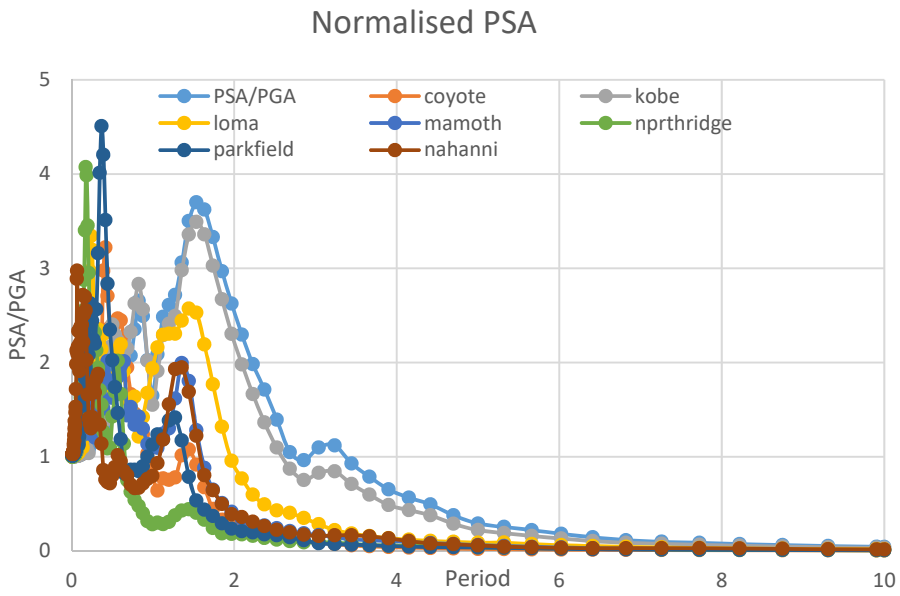

Fig 4.35 Combined PSA/PGA vs Period

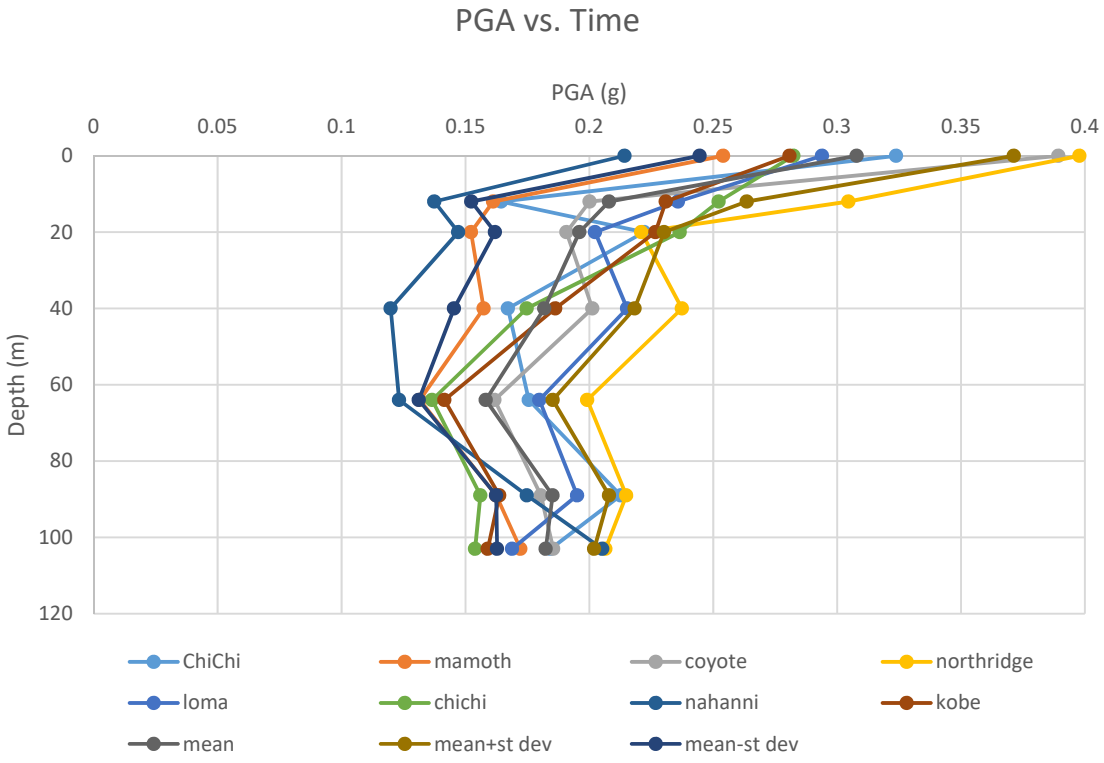

Fig 4.36 Combined PGA versus depth

4.3 Site Response Analysis After Ground Improvement

Figure 4.37 shows the acceleration diagram at surface and at bedrock simultaneously before ground improvement. Table 4.2 shows the soil model used for the current analysis after the soil improvement. The top layer consists of silty fine sand of velocity 1100 m/s and the thickness of the layer is 20m. The other layers are also silty fine sand with different thickness and shear wave velocity shown in the table below. The data have been obtained from Ruppur Nuclear Powerplant site.

Table 4.2 Soil Model After Ground Improvement

Layer	Layer name	Depth(m)	Thickness (m)	Unit wt (KN/m^3)	Shear wave velocity (m/s)
1	Silty fine sand	0-20	20	16	1100
2	Silty fine sand	20-22	2	19	600
3	Silty fine sand	22-23	1	17	450
4	Silty fine sand	23-25	2	16	350
5	Silty fine sand	25-40	15	16	250
6	Silty fine sand	40-64	24	16	360
7	Silty fine sand	64-89	25	16	360
8	Silty fine sand	89-103	14	17	410
9	Silty fine sand	103-120	17	18	640

4.3.1 Chi-Chi earthquake

1D site response analysis has been carried out using the soil model as shown in Table 4.1 and using Chi-Chi earthquake (bedrock) as input. Figure 4.37 shows the earthquake records of ChiChi on ground surface and in the bedrock. PGA value is near 0.2g shown in figure 4.38.

Amplitude ration in figure 4.39 is 4.0 with the predominant frequency is around 0.5 Hz. Figure 4.40 shows normalized PSA versus period relation.

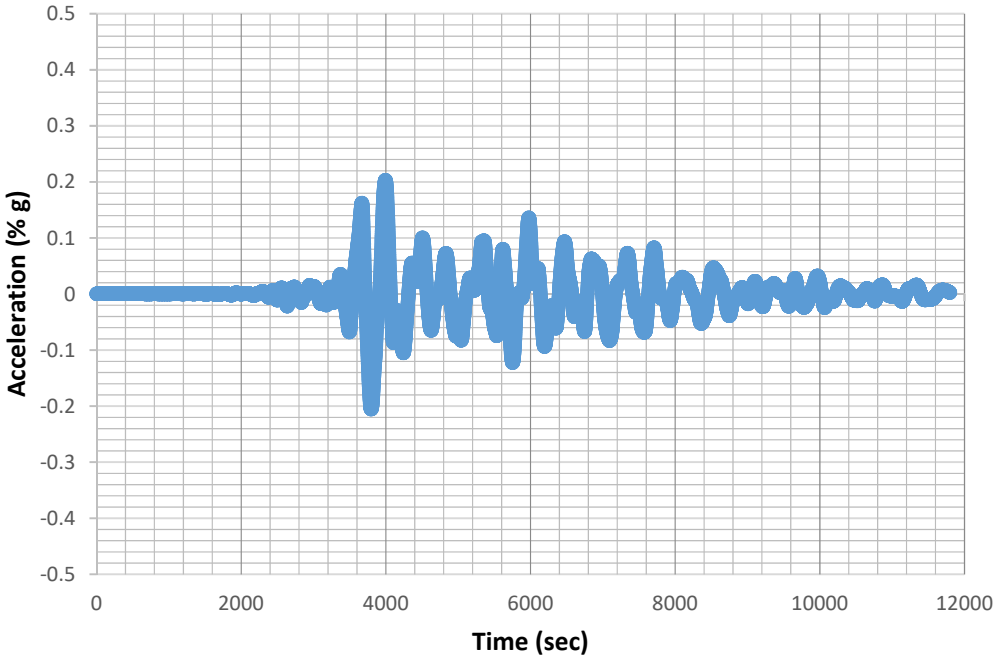

Fig 4.37(a) Time Histories of ChiChi Earthquake at surface

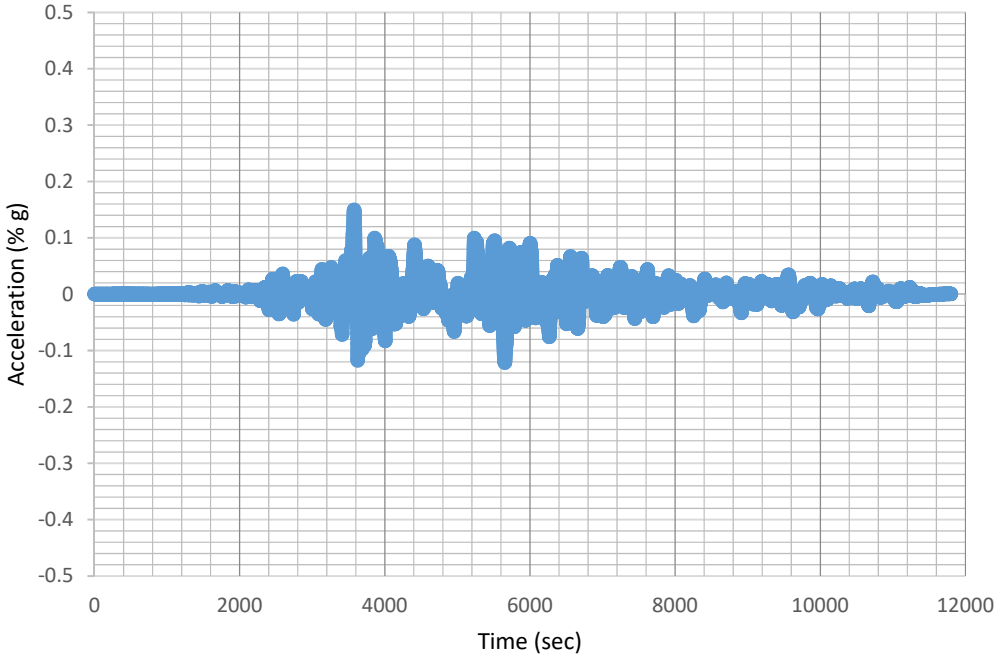

Fig 4.37(b) Time Histories of ChiChi Earthquake at bedrock

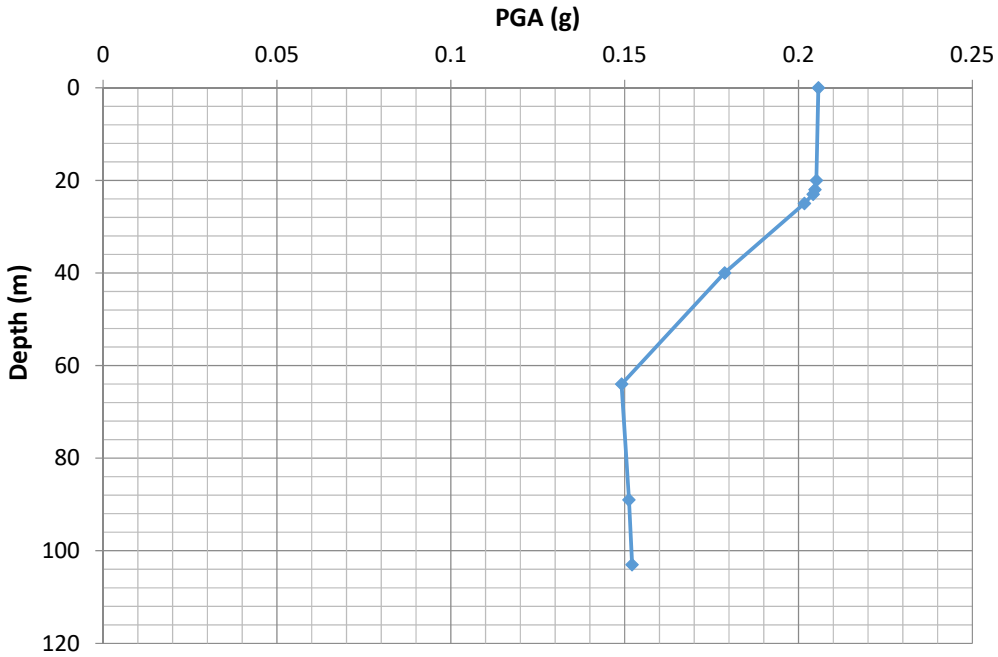

Fig 4.38 PGA versus depth

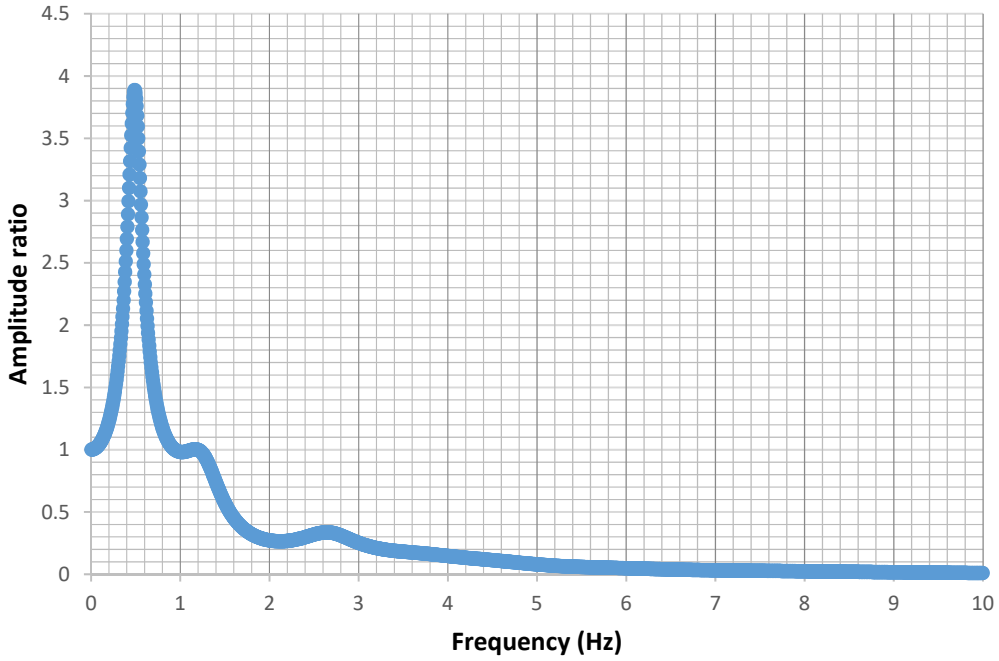

Fig 4.39 Amplitude ratio versus frequency curve

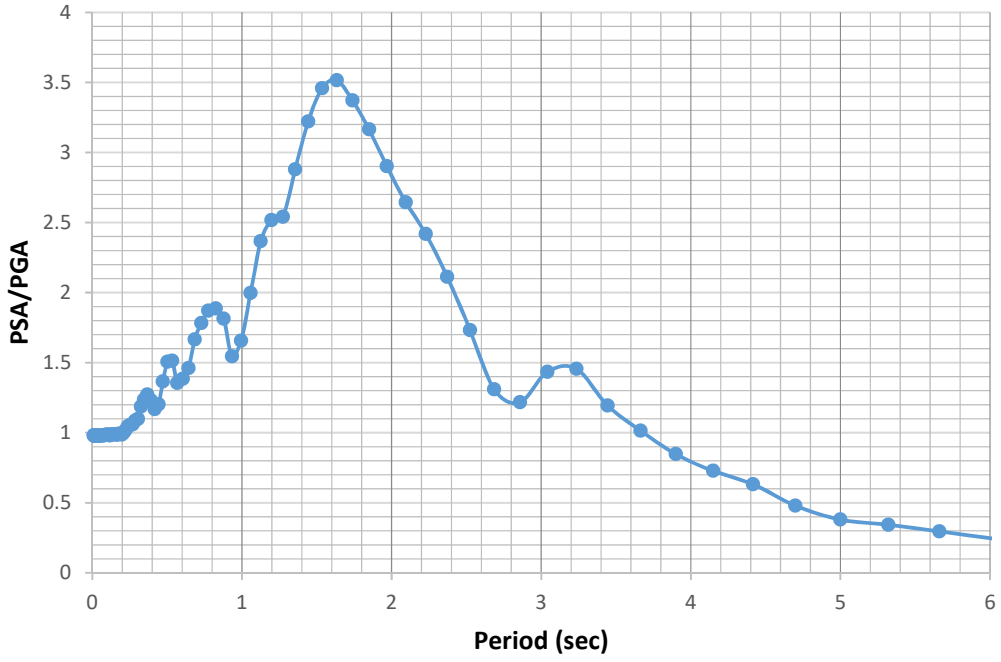

Fig 4.40 Normalized PSA versus period relation

4.3.2 Coyote earthquake

Coyote earthquake after ground improvement shows almost same value on ground surface and in the bedrock. The figure shows the value is approximately 0.18 in figure 4.41.

Figure 4.42 shows the graph of depth versus PGA. PGA value is 0.15g here.

Figure 4.43 shows amplitude ratio versus frequency relation. From the figure, it can be seen that the predominant frequency is around 1 Hz. Figure 4.44 shows normalized PSA versus period relation.

4.3.3 Kobe earthquake

After ground improvement acceleration value is 0.2 at surface and at bedrock it's a little less, around 0.15. Figure 4.46 shows the graph of depth versus PGA. PGA value has reached to approximately 0.18g here. Figure 4.47 shows amplitude ratio versus frequency relation. From the figure, it can be seen that the predominant frequency is around 1 Hz. Figure 4.48 shows normalized PSA versus period relation.

4.3.4 Loma Girloy earthquake

Earthquake records of Loma Girloy on ground surface and in the bedrock is shown in the figure 4.49.

Figure 4.50 shows the graph of depth versus PGA. PGA value has reached to approximately 0.16g here. Figure 4.51 shows amplitude ratio versus frequency relation. From the figure, it can be seen that the predominant frequency is around 1 Hz. Figure 4.52 shows PSA/PGA versus period relation.

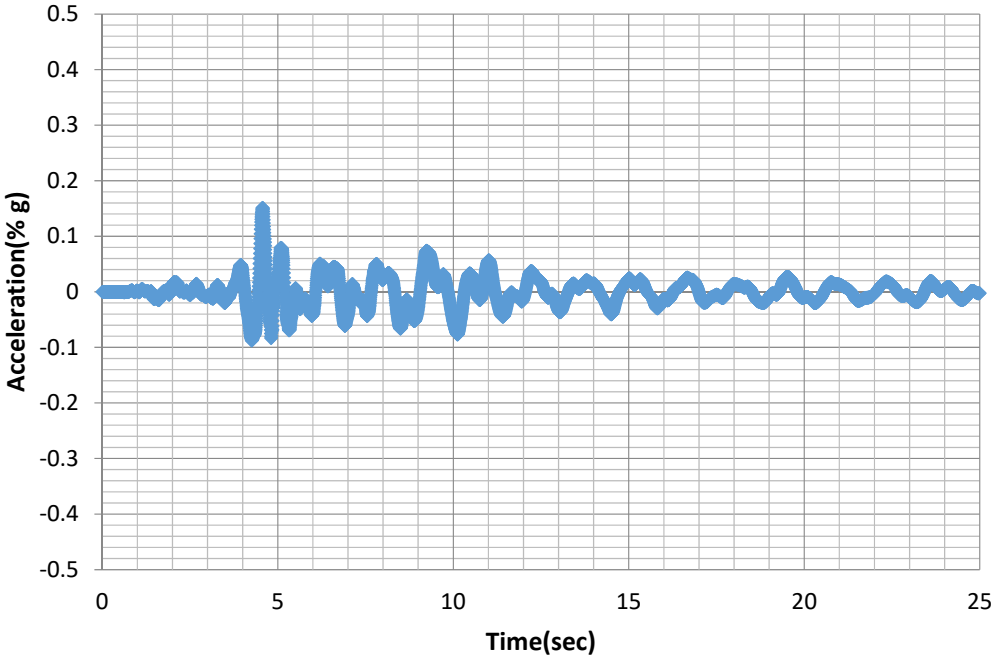

Fig 4.41(a) Time Histories of Nahanni Earthquake at surface

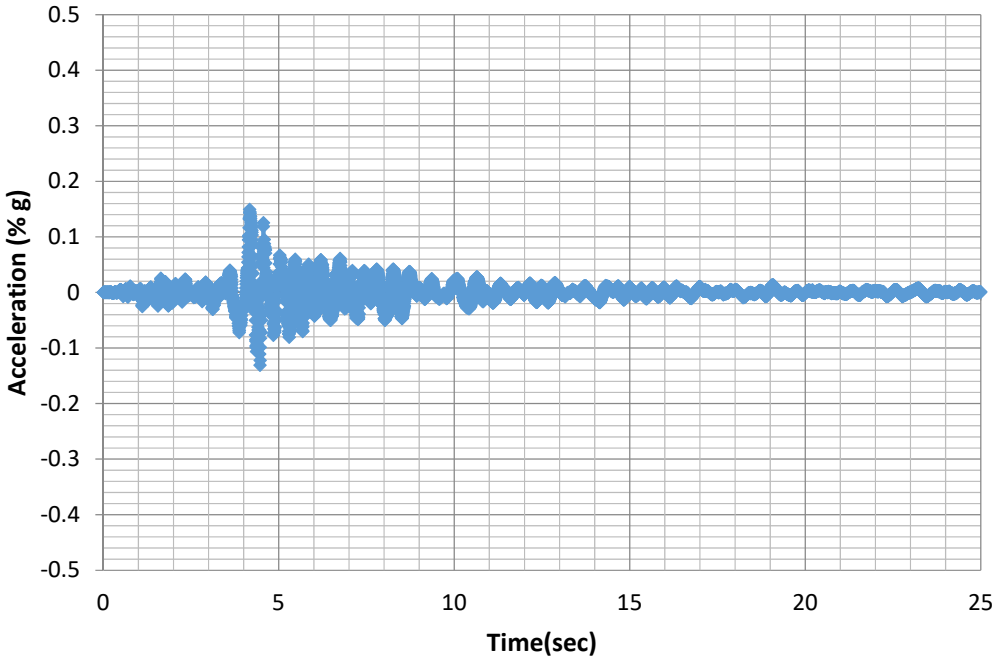

Fig 4.41(b) Time Histories of Nahanni Earthquake at bedrock

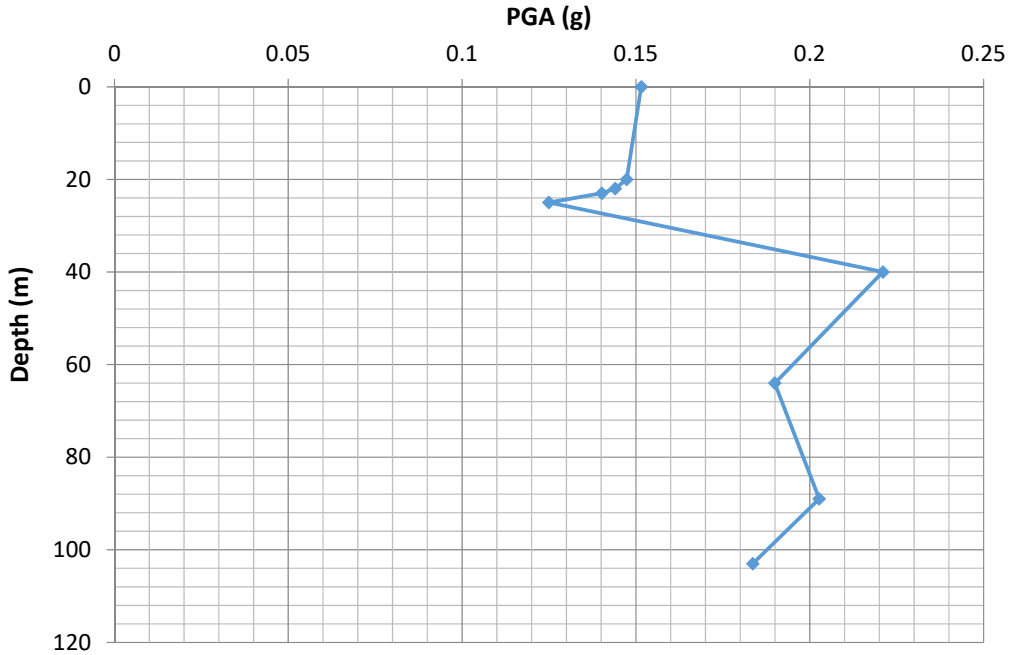

Fig 4.42 PGA versus depth

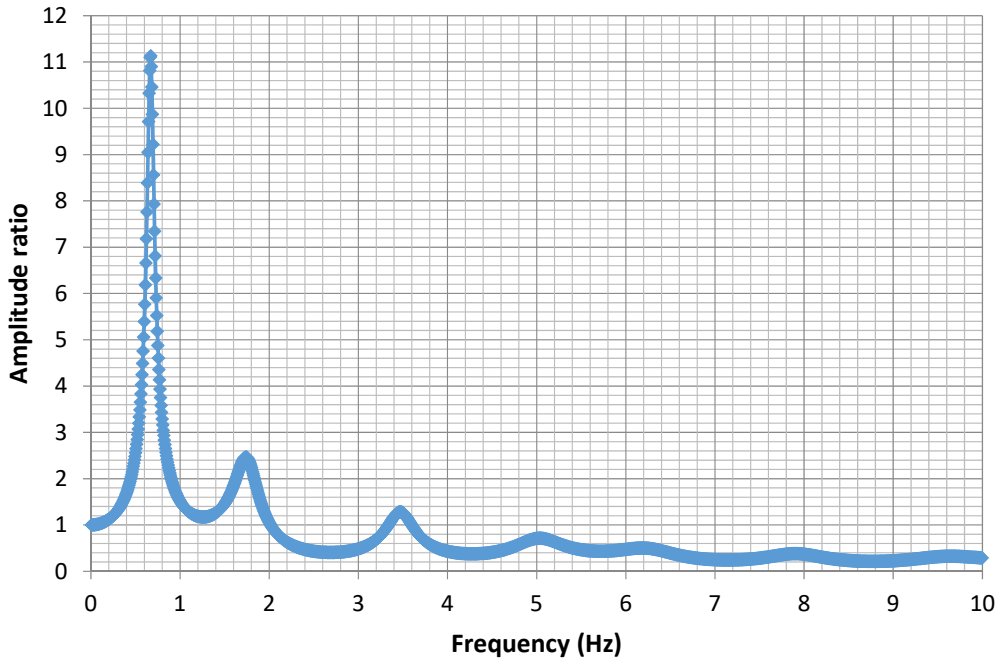

Fig. 4.43 Amp ratio vs. frequency graph

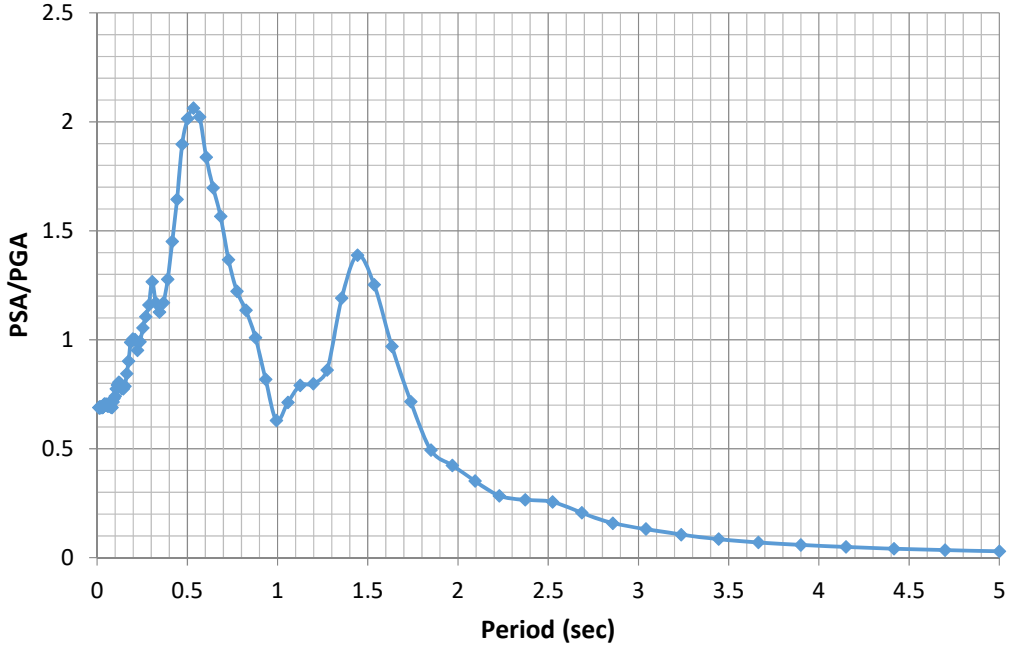

Fig 4.44 Normalized PSA versus period relation

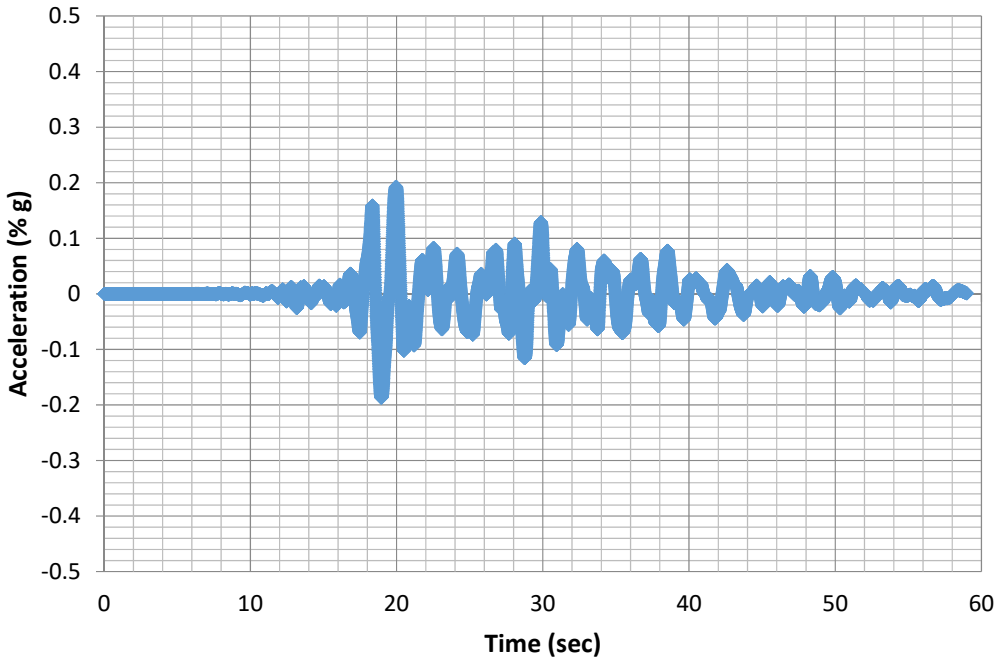

Fig 4.45(a) Time Histories of Nahanni Earthquake at surface

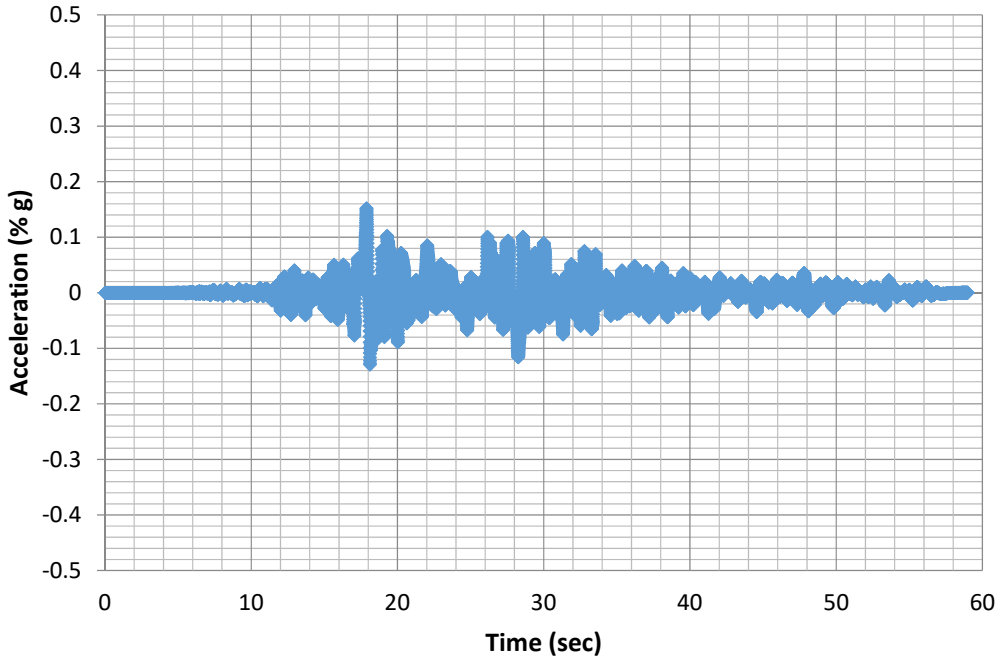

Fig 4.45(b) Time Histories of Nahanni Earthquake at bedrock

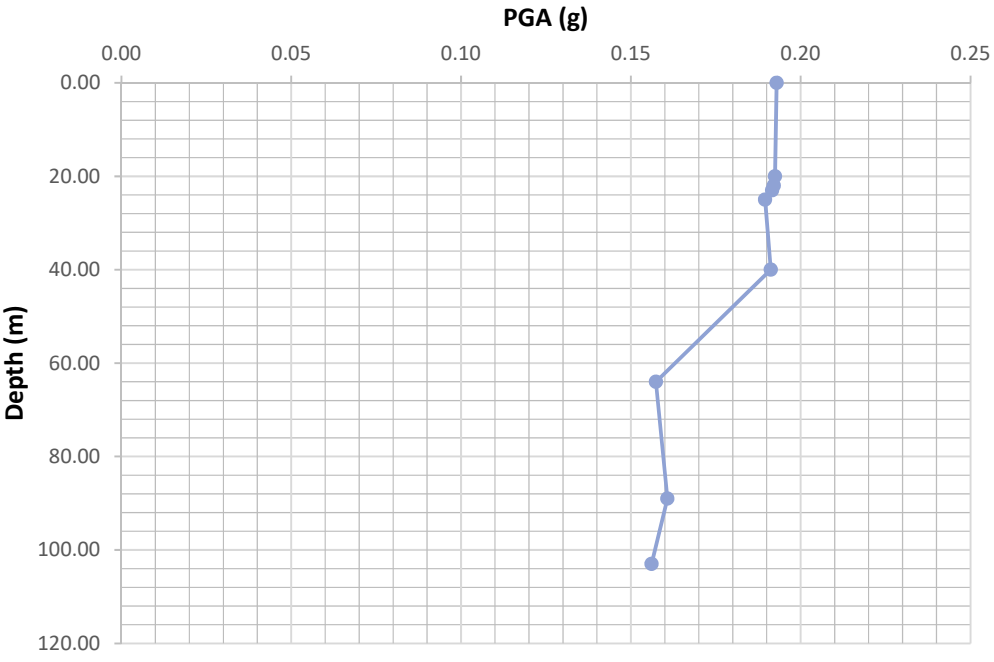

Fig 4.46 PGA versus depth

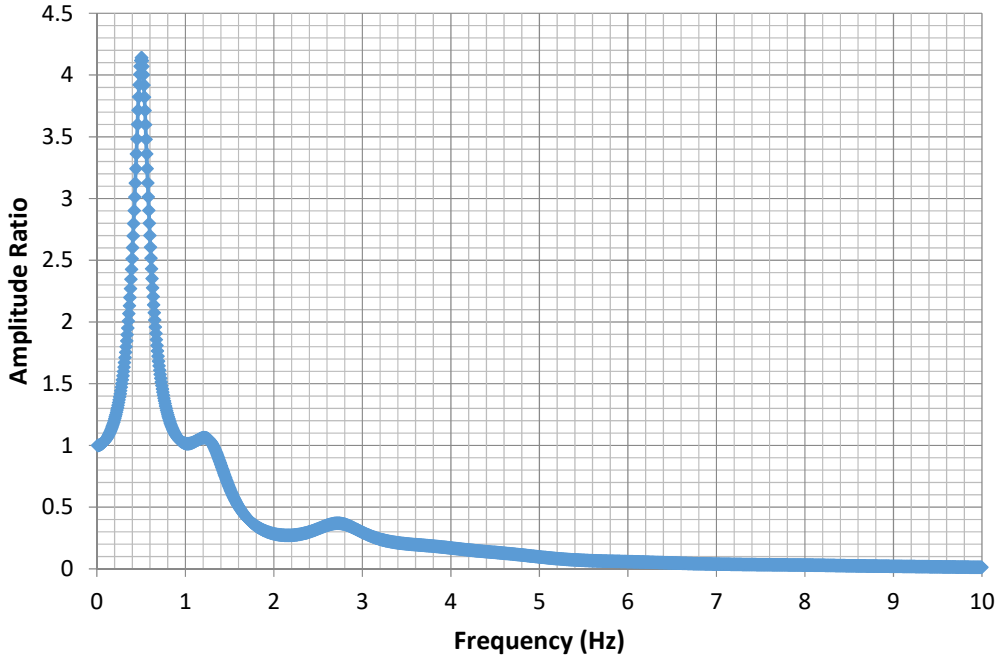

Fig 4.47 Amplitude ratio versus frequency curve

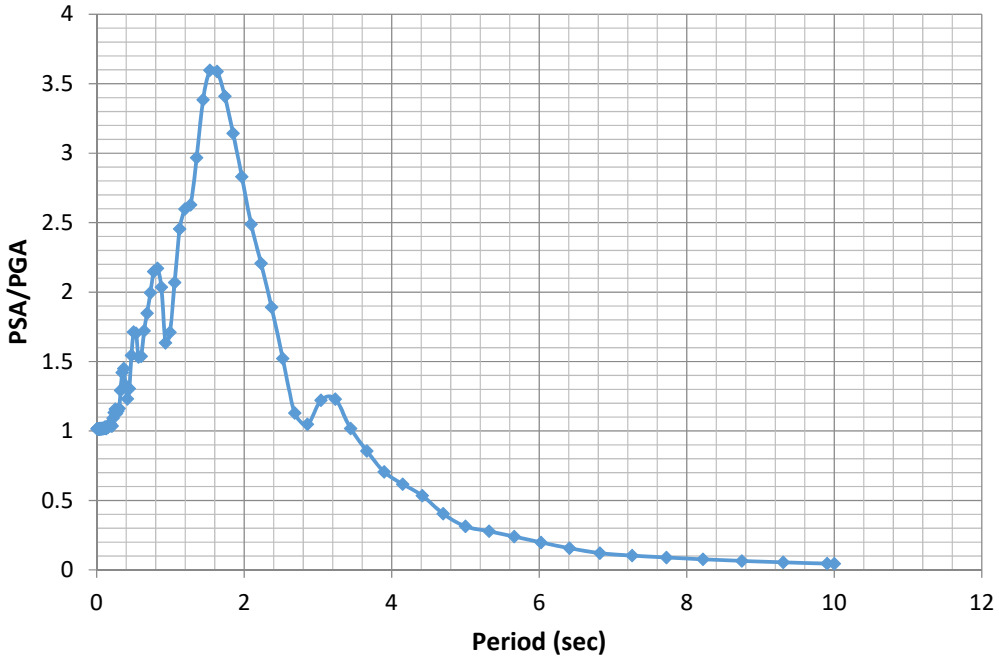

Fig 4.48 Normalized PSA versus period relation

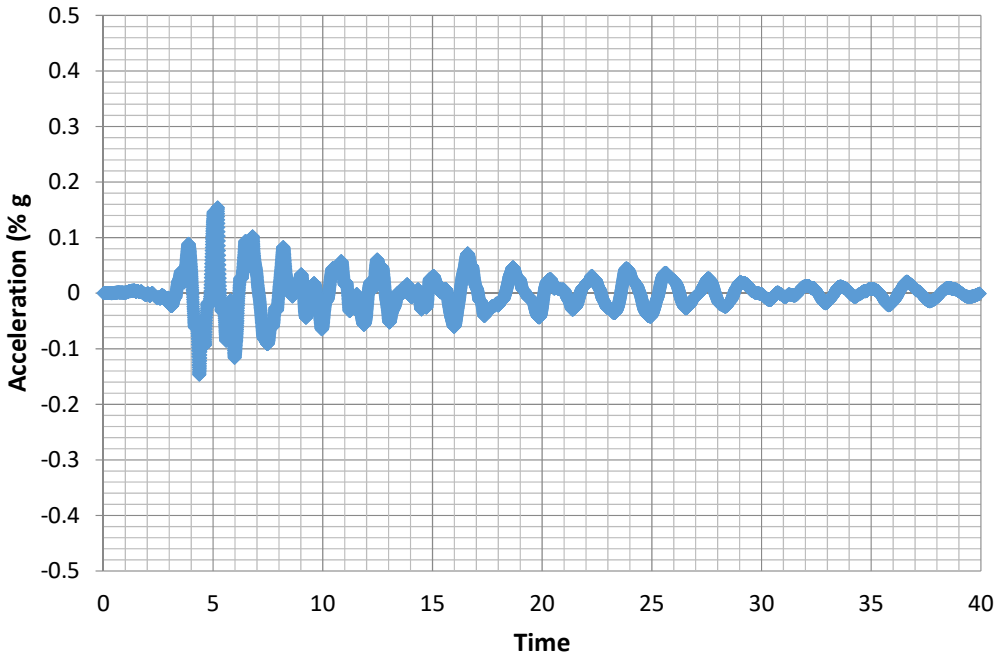

Fig 4.49(a) Time Histories of Loma Girloy Earthquake at surface

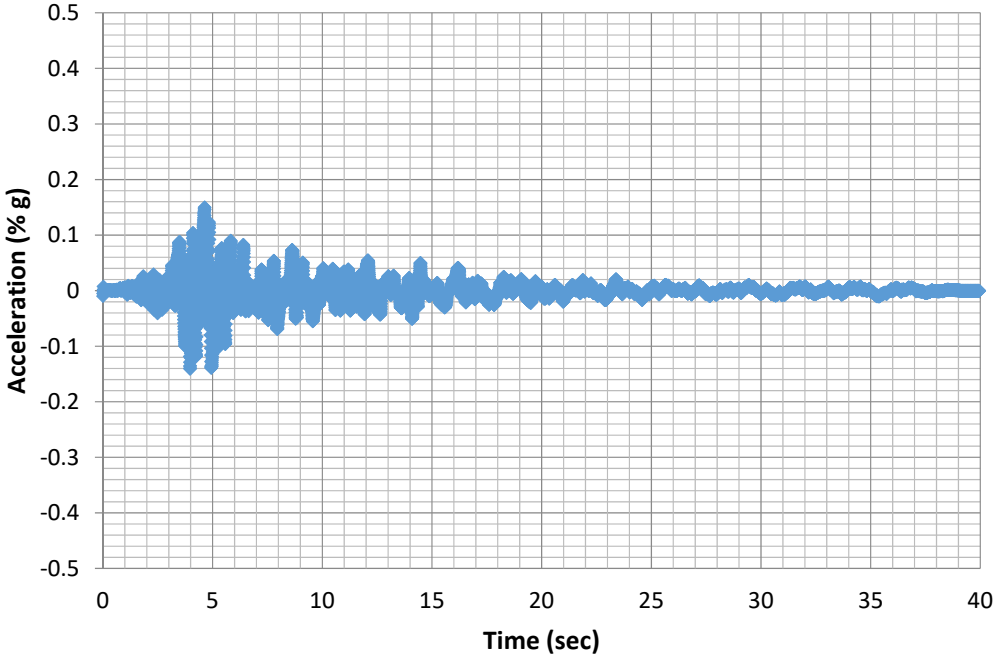

Fig 4.49(b) Time Histories of Loma Girloy Earthquake at bedrock

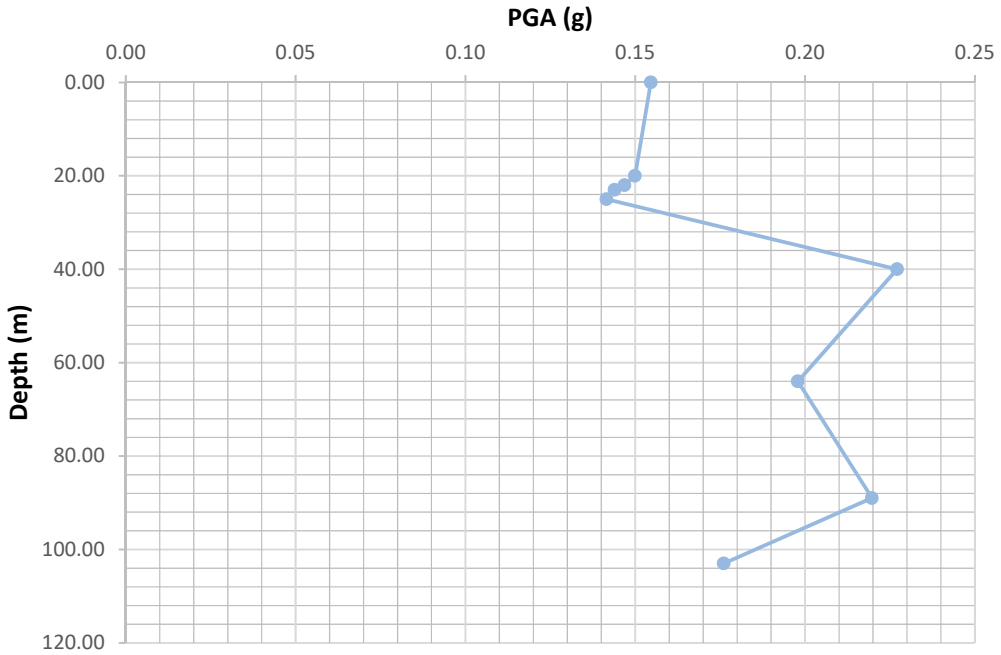

Fig 4.50 PGA versus depth

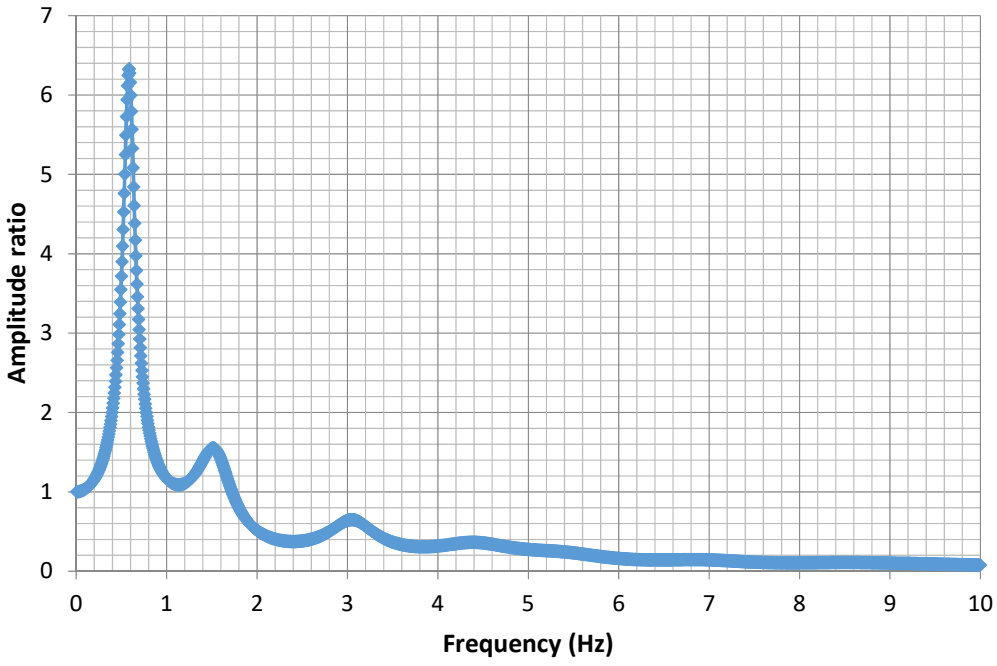

Fig 4.51 Amplitude versus frequency curve

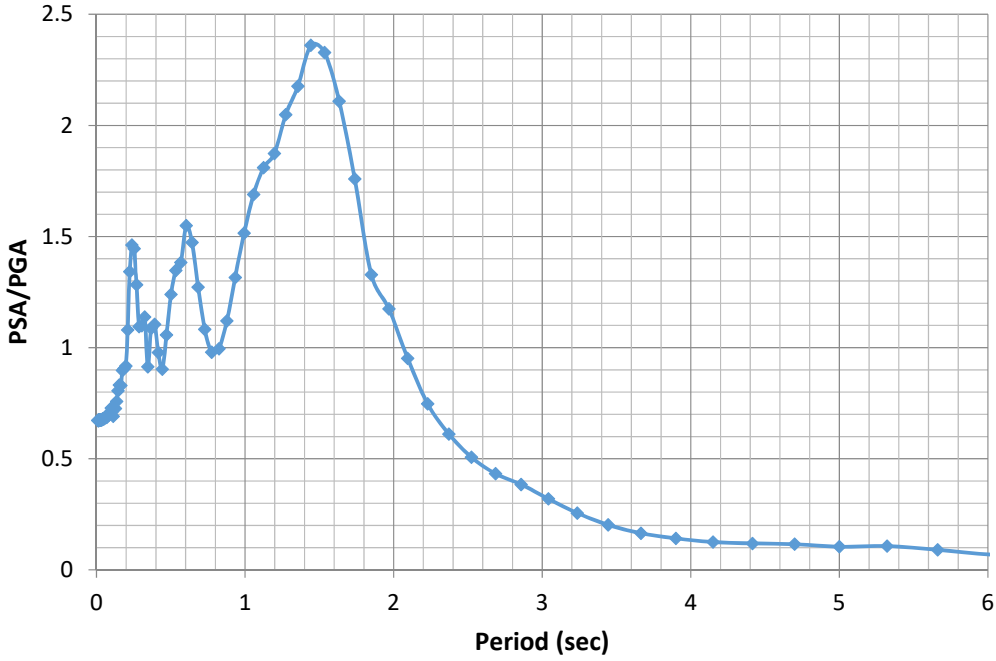

Fig 4.52 PSA/PGA versus period relation

4.3.5 Mammoth earthquake

Earthquake records of Mammoth on ground surface and in the bedrock is shown in the figure 4.53. At bedrock the value of acceleration increases than at surface. Figure 4.54 shows the graph of depth versus PGA. PGA value has reached to approximately 0.26g here. Figure 4.55 shows amplitude ratio versus frequency relation. From the figure, it can be seen that the predominant frequency is around 1 Hz. Figure 4.56 shows PSA/PGA versus period relation.

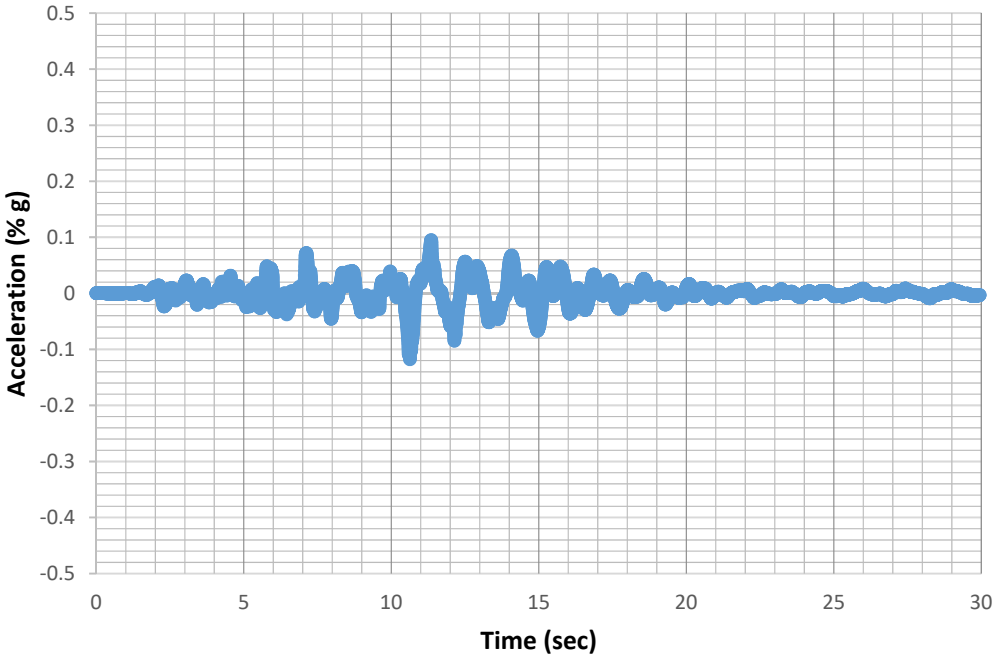

Fig 4.53(a) Time Histories of Mammoth Earthquake at surface

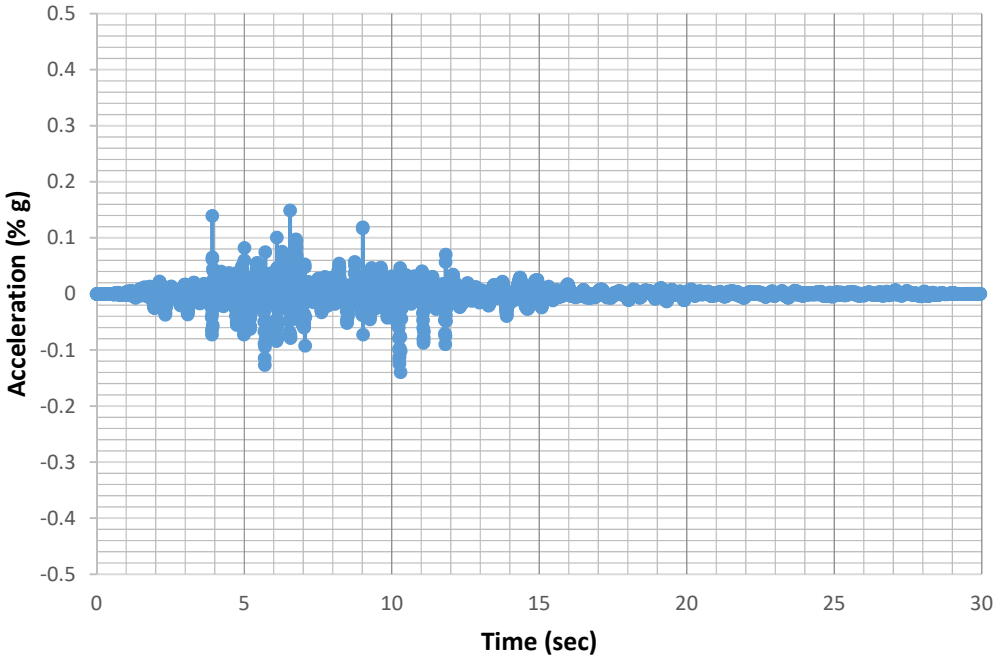

Fig 4.53(b) Time Histories of Mammoth Earthquake at bedrock

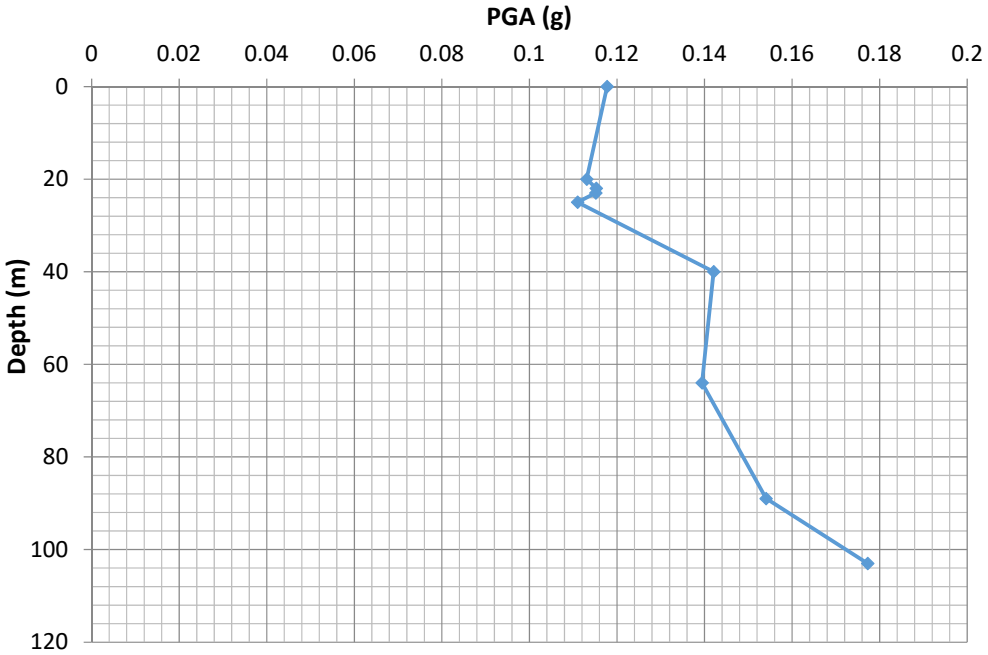

Fig 4.54 PGA versus depth

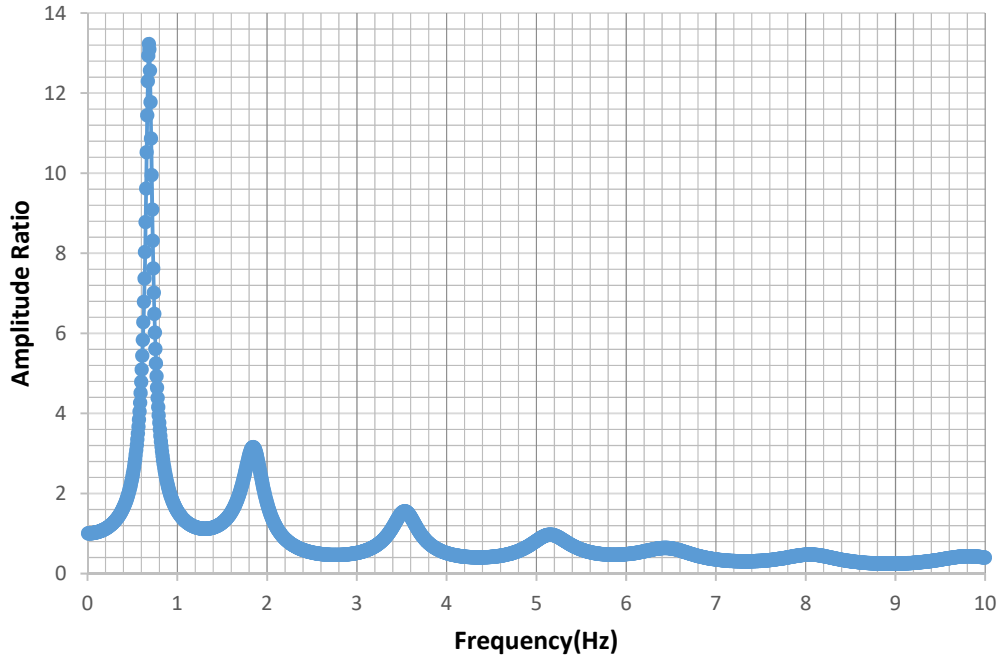

Fig 4.55 Amplitude ratio versus frequency curve

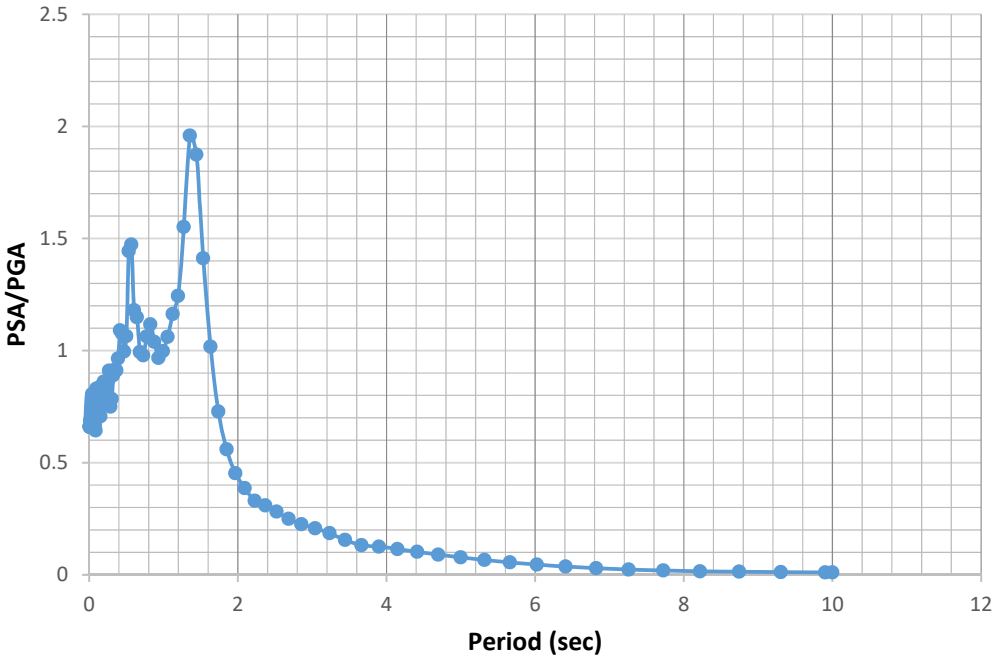

Fig 4.56 PSA/PGA versus period relation

4.3.6 Nahanni earthquake

Earthquake records of Nahanni on ground surface and in the bedrock is shown in figure 4.57. Figure 4.58 shows the graph of depth versus PGA. PGA value has reached to approximately 0.18g here. Figure 4.59 shows amplitude ratio versus frequency relation. From the figure, it can be seen that the predominant frequency is around 1 Hz. Figure 4.60 shows normalized PSA versus period relation.

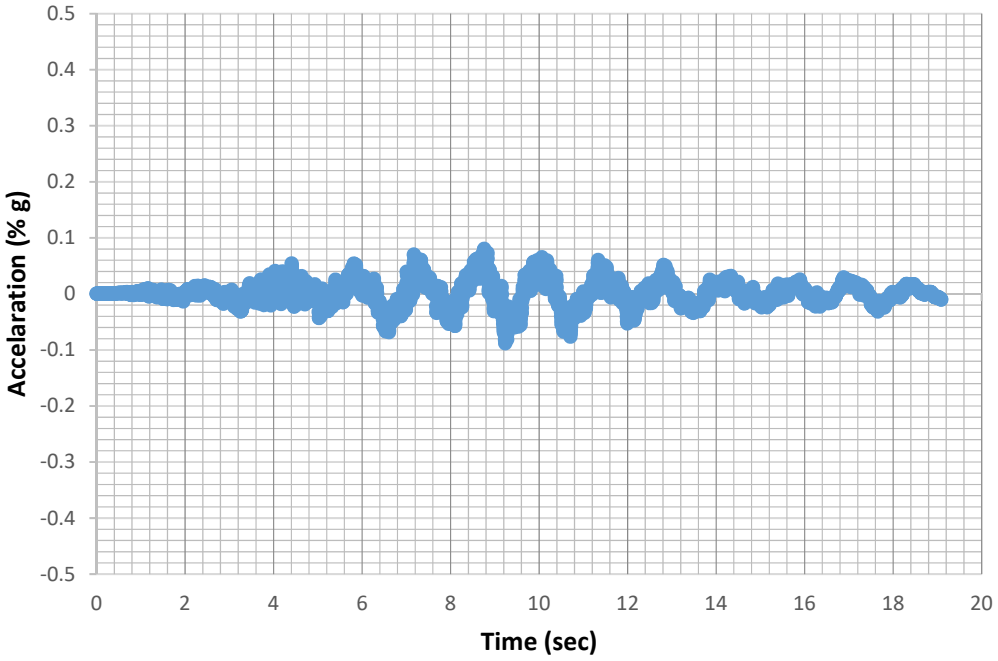

Fig 4.57(a) Time Histories of Nahanni Earthquake at surface

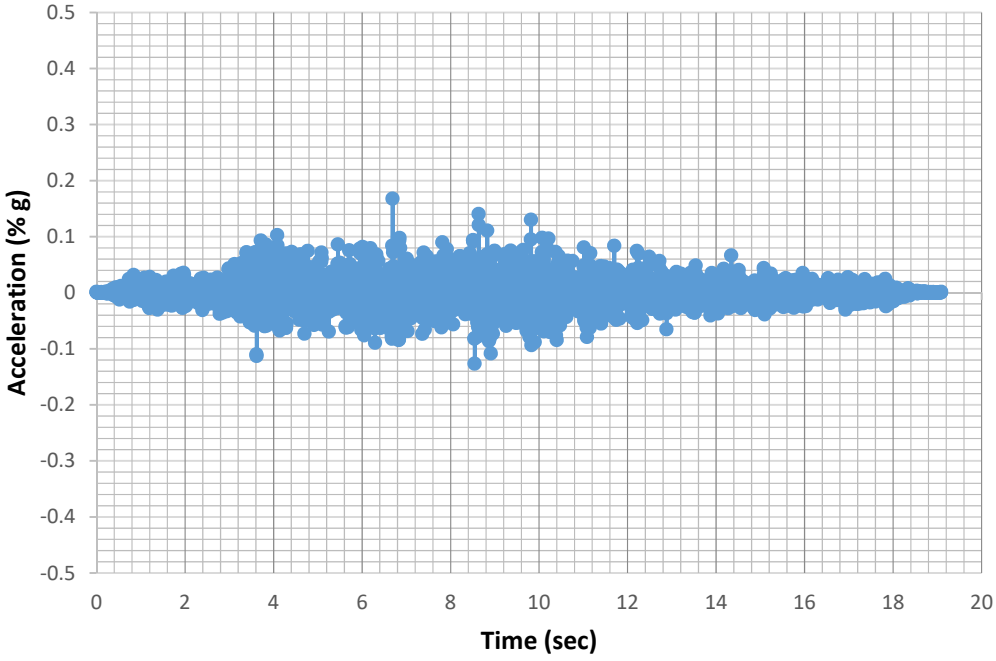

Fig 4.57(b) Time Histories of Nahanni Earthquake at bedrock

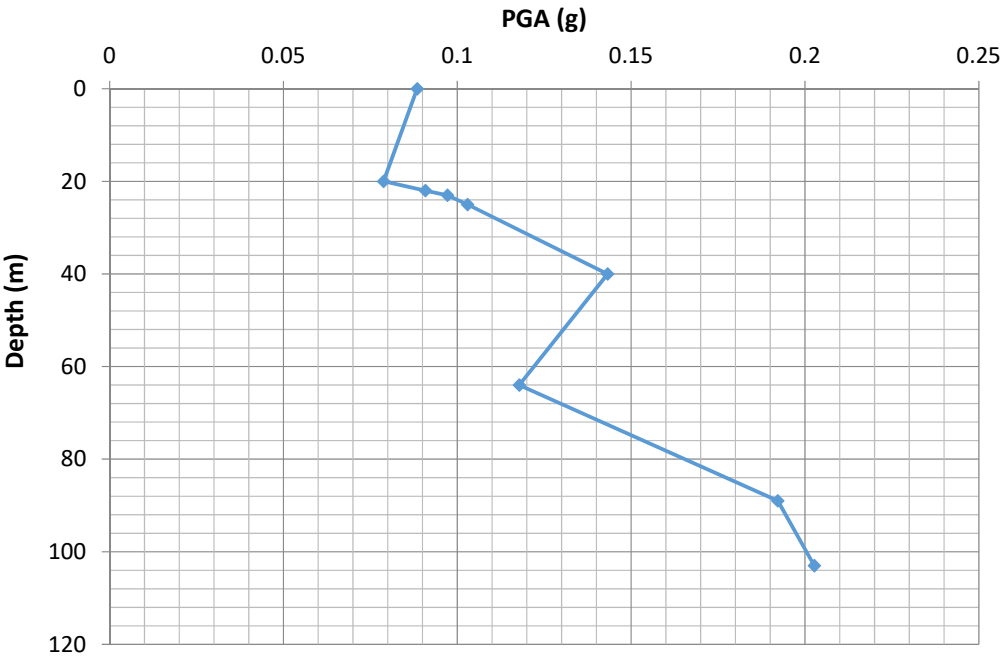

Fig: 4.58 PGA versus depth

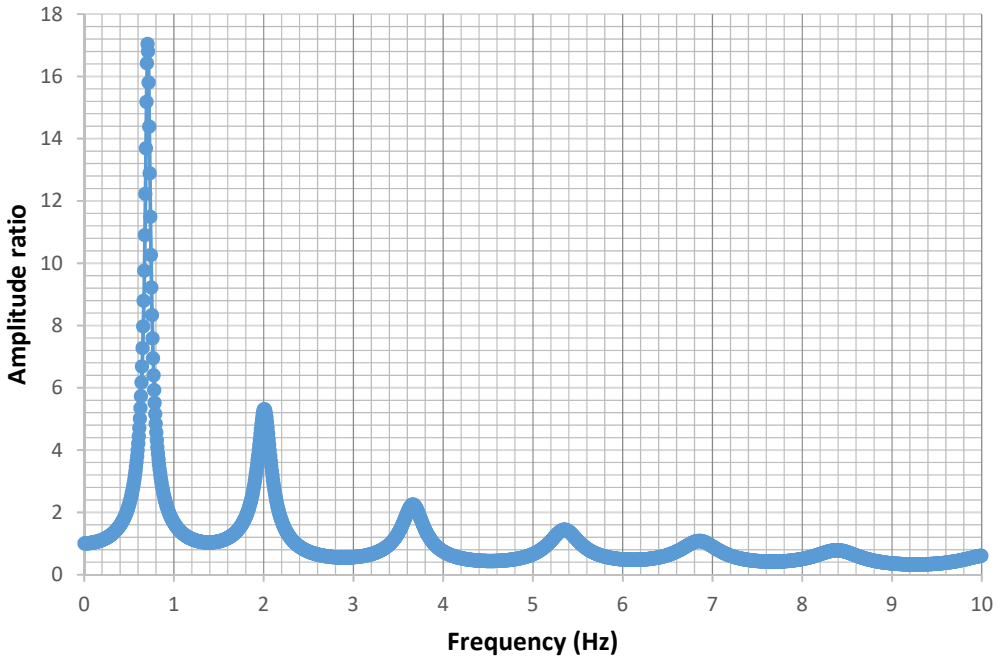

Fig 4.59 Amp ratio vs. Frequency Graph

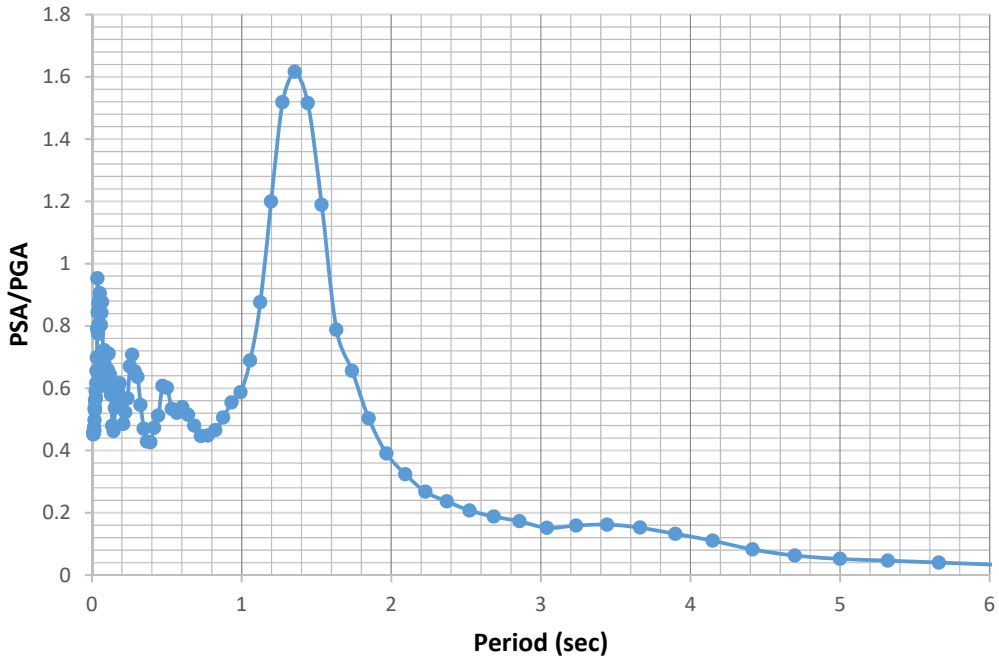

Fig 4.60 Normalized PSA versus period relation

4.3.7 Northridge earthquake

Northridge earthquake on ground surface and in the bedrock shows the acceleration value. Figure 4.62 shows the graph of depth versus PGA. PGA value has reached to approximately 0.4g here. Figure 4.63 shows amplitude ratio versus frequency relation. From the figure, it can be seen that the predominant frequency is around 1 Hz. Figure 4.64 shows PSA/PGA versus period relation.

4.3.8 Parkfield earthquake

Earthquake records of Parkfield on ground surface and in the bedrock shows the acceleration value increases from surface to bedrock. Figure 4.66 shows the graph of depth versus PGA. PGA value has reached to approximately 0.12g here.

Figure 4.67 shows amplitude ratio versus frequency relation. From the figure, it can be seen that the predominant frequency is around 1 Hz. Figure 4.68 shows PSA/PGA versus period relation.

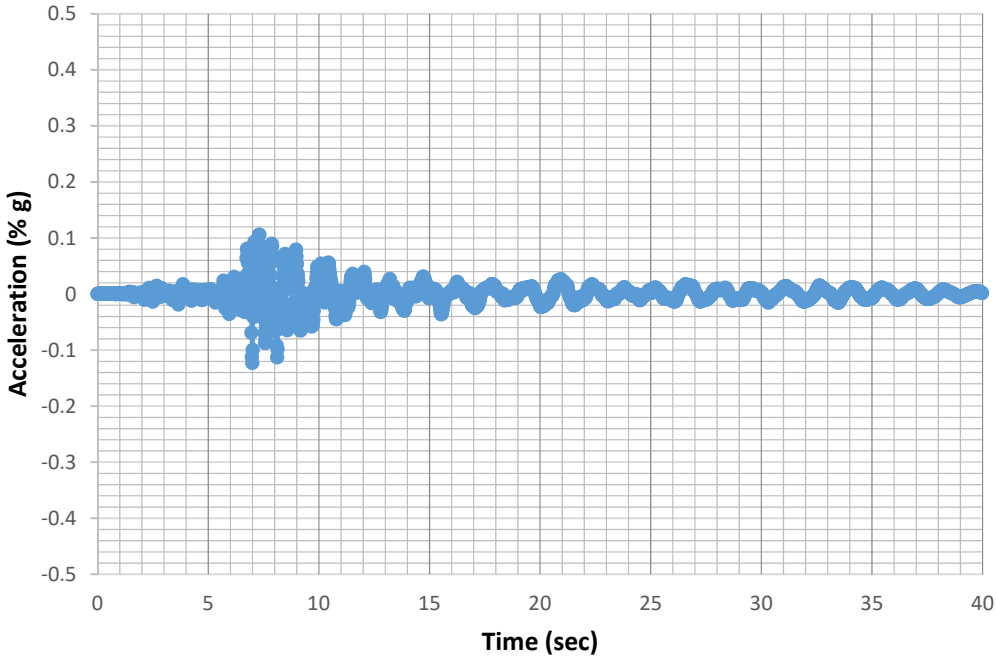

Fig 4.61(a) Time Histories of Northridge Earthquake at surface

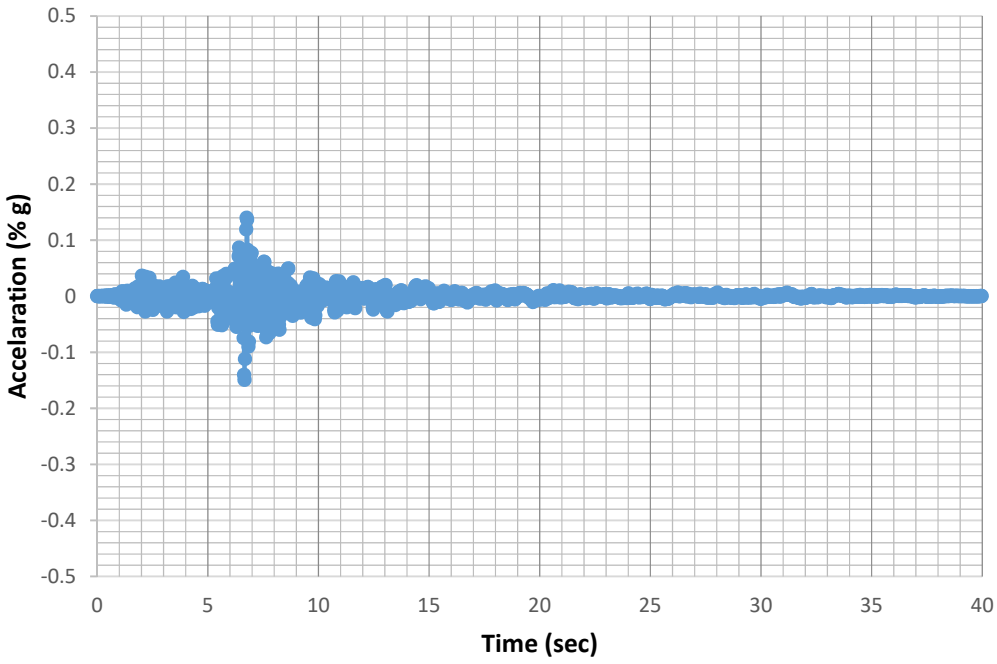

Fig 4.61(b) Time Histories of Northridge Earthquake at bedrock

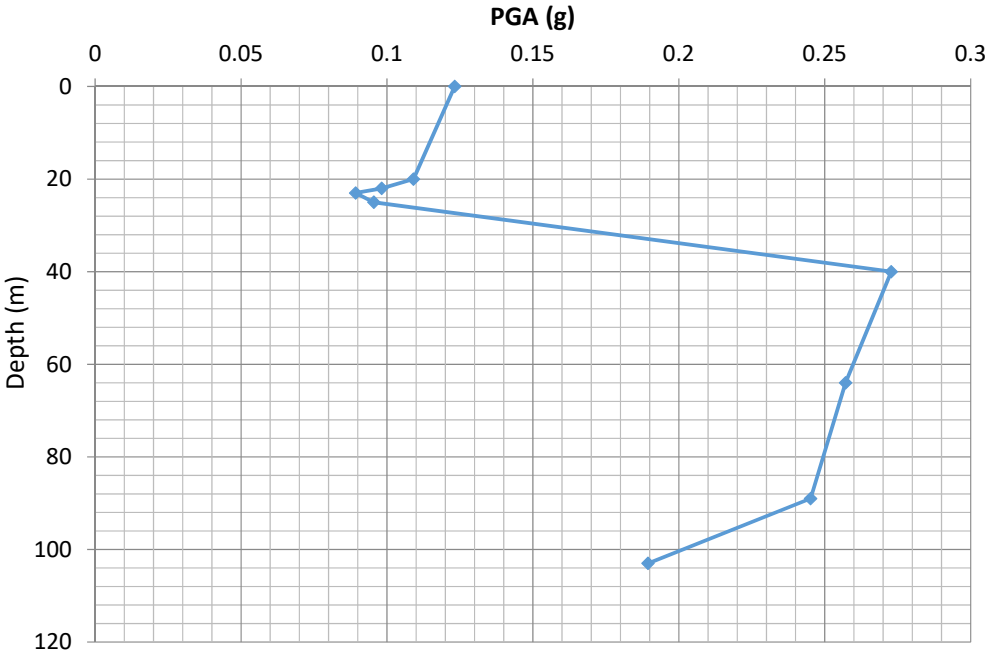

Fig 4.62 PGA versus depth

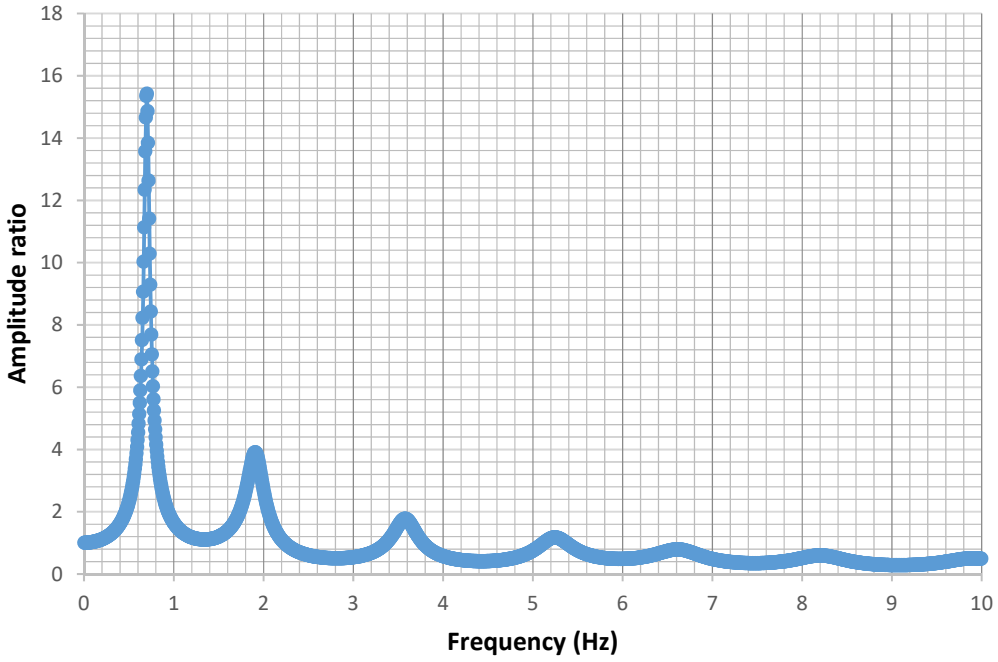

Fig 4.63 Amplitude versus frequency curve

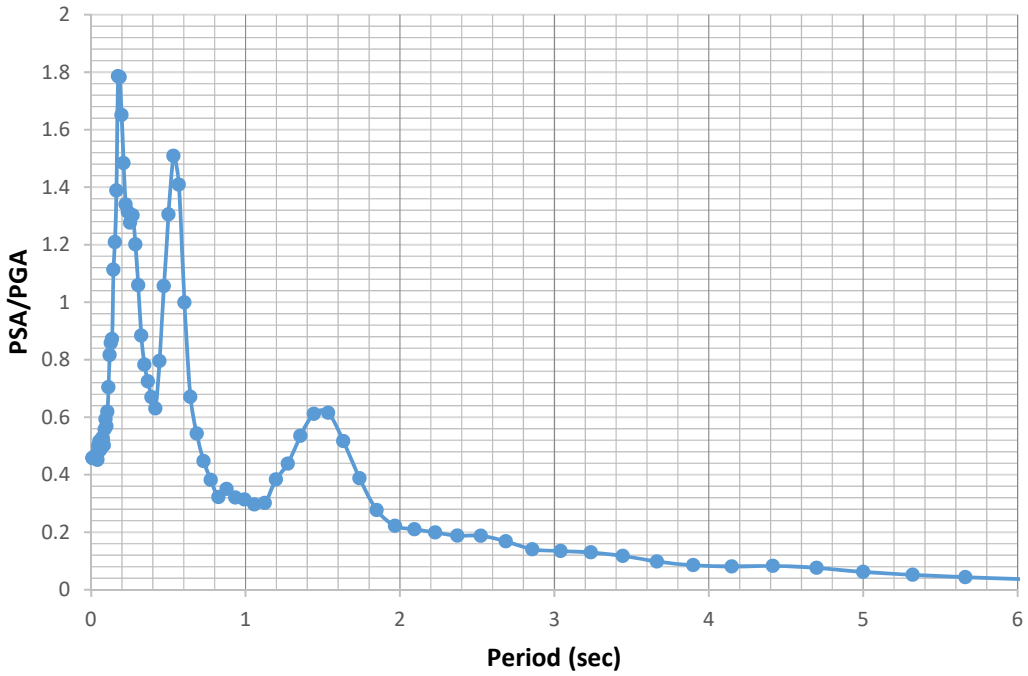

Fig 4.64 PSA/PGA versus period relation

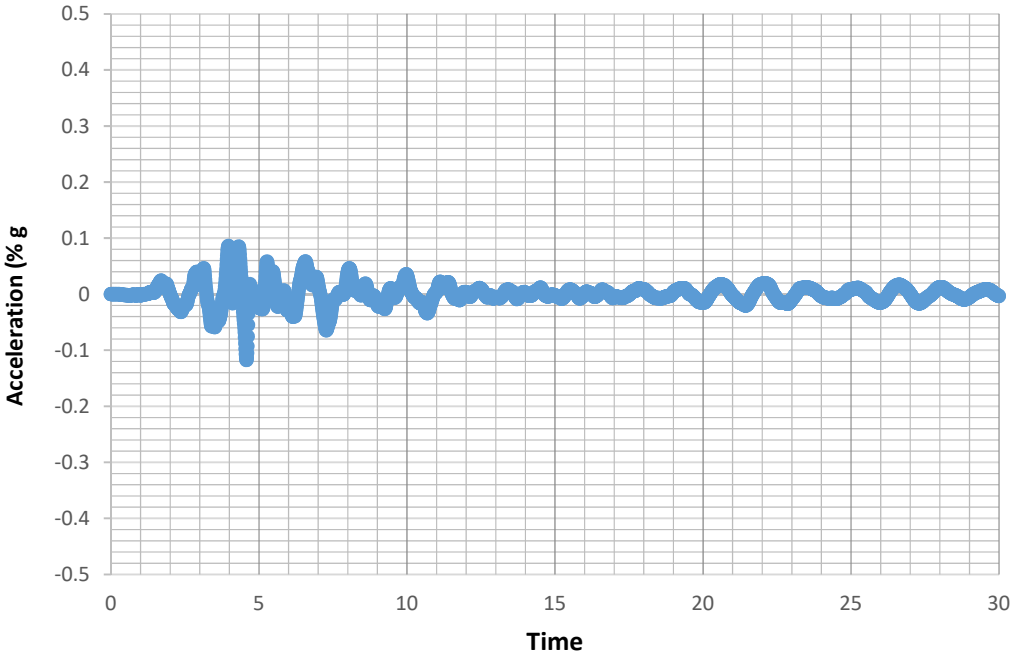

Fig 4.65(a) Time Histories of Parkfield Earthquake at surface

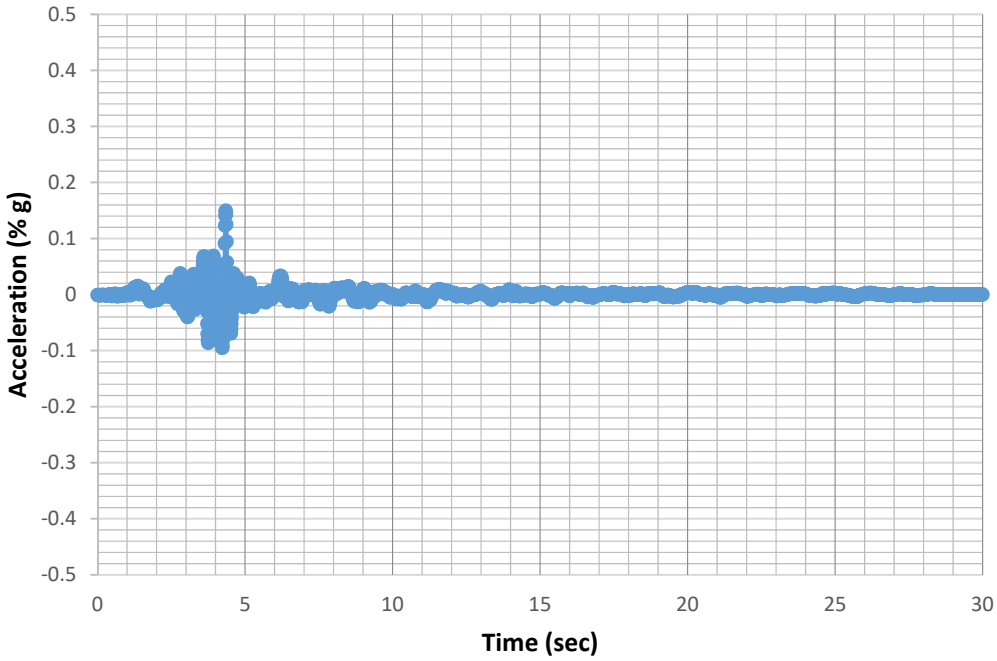

Fig 4.65(b) Time Histories of Parkfield Earthquake at bedrock

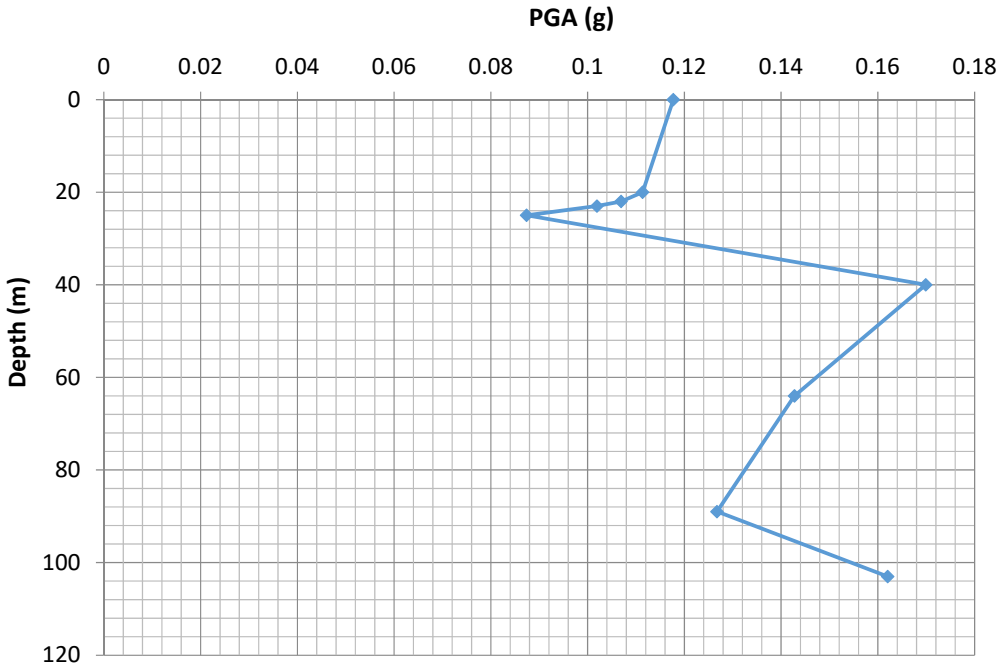

Fig 4.66 PGA versus depth

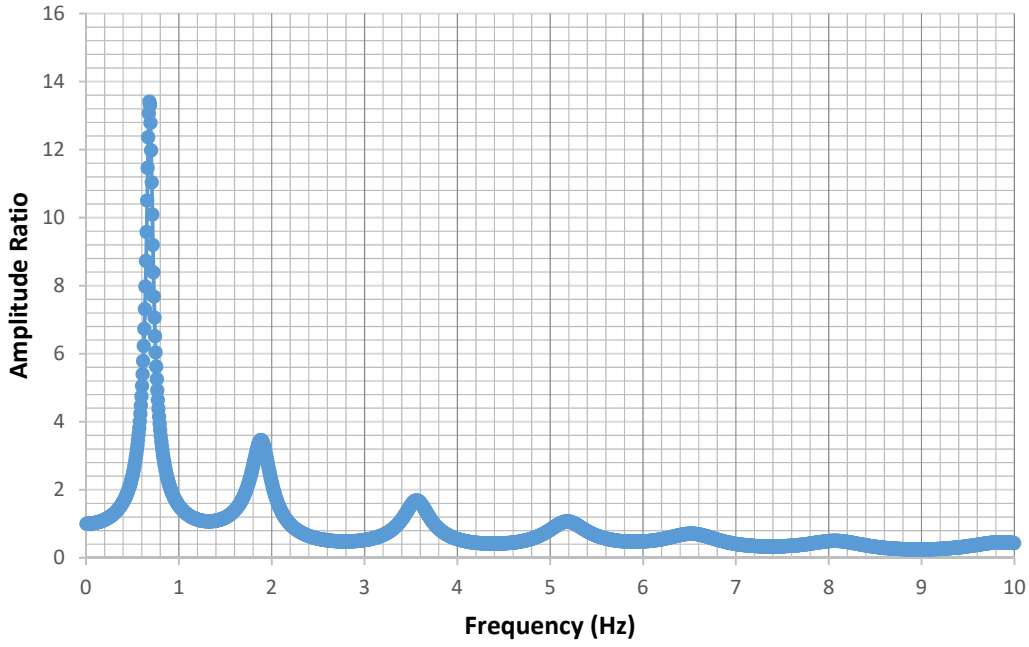

Fig 4.67 Amplitude versus frequency curve

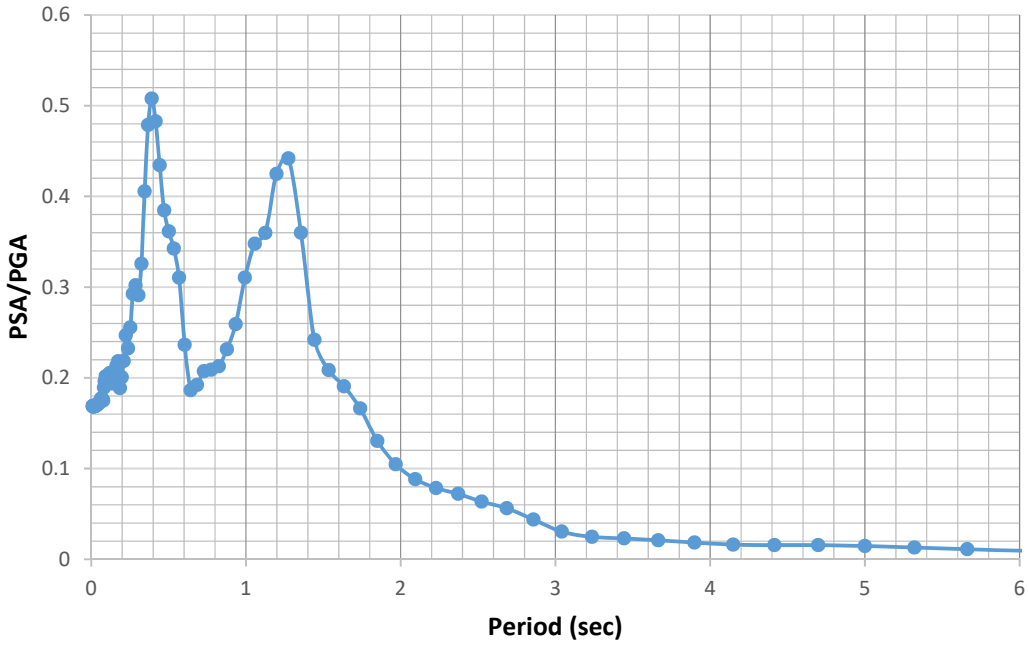

Fig 4.68 PSA/PGA versus period relation

4.3.9 Combination of all earthquakes after ground improvement

Combining all the graphs found from all the earthquakes after ground improvement, the interpretation is as below:

In figure 4.69 we see after ground improvement, the value varies from 0.75 to 0.2. The graph shows the value increases from ChiChi to Nahanni earthquake.

Nahanni earthquake gives the maximum amplitude ratio of around 17 in figure 3.70.

Figure 4.71 shows after ground improvement, Coyote earthquake gives the maximum vale of around 1.4 and Nahanni earthquake gives the minimum value of around 0.9.

When we combined all the earthquakes in figure 4.72 before ground improvement, the PGA value ranges between 0.08g to 0.22g. Nahanni earthquake gives the minimum value and ChiChi the maximum.

The mean and standard deviation is also shown in figure 4.69 & figure 4.70. We can see all the earthquakes data are near the mean value.

4.4 Comparison of Before and After Ground Improvement

PGA is calculated using attenuation function that describes the correlation between the local ground movement intensity the earthquake magnitude and the distance from the earthquake's epicenter prepared.

Figure 4.73 compares the change in PGA value before & after ground improvement. PGA value determines the risk of an earthquake. After ground improvement the value drastically reduces to 0.15g from 0.30g in surface.

Amplitude ratio is around 12 before ground improvement and it decreases to around 9 after ground improvement in figure 4.74. Frequency is around 0.5 Hz. Figure 4.75 shows two peak values of PSA and here also after improvement the value decreases to 0.4 from 0.7. Figure 4.76 shows a little change in the peak value from before to after ground improvement.

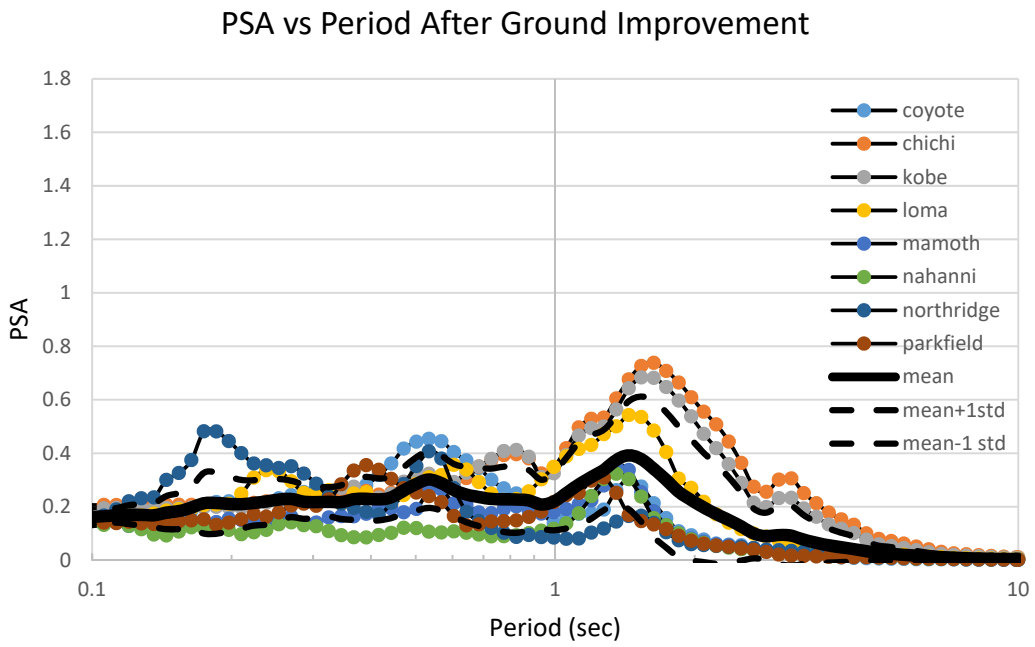

Fig 4.69 Combined PSA versus period relation

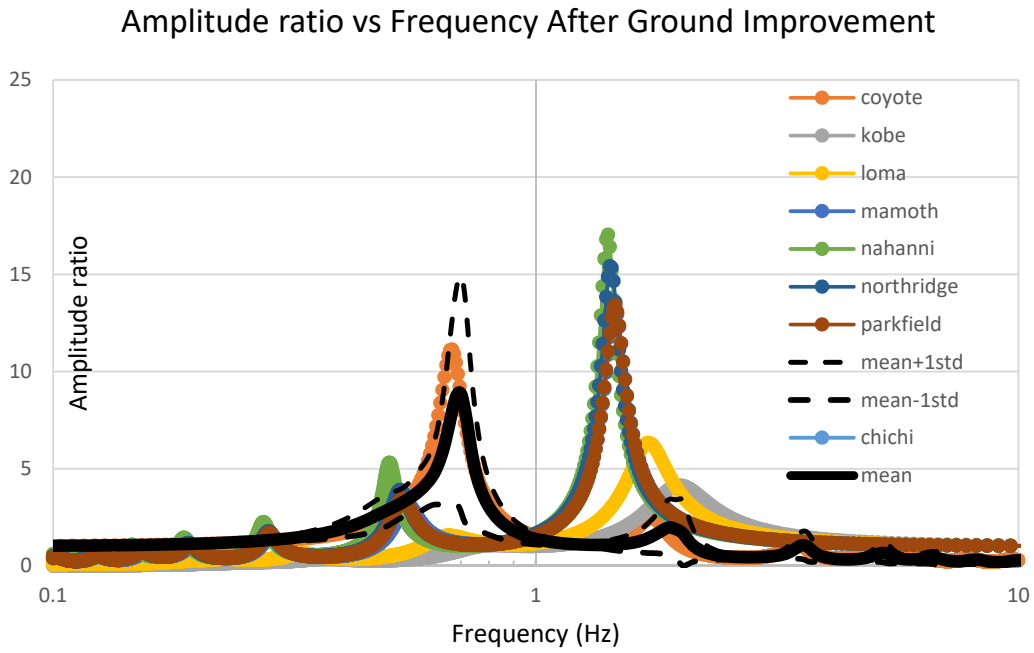

Fig 4.70 Combined Amplitude ratio versus time

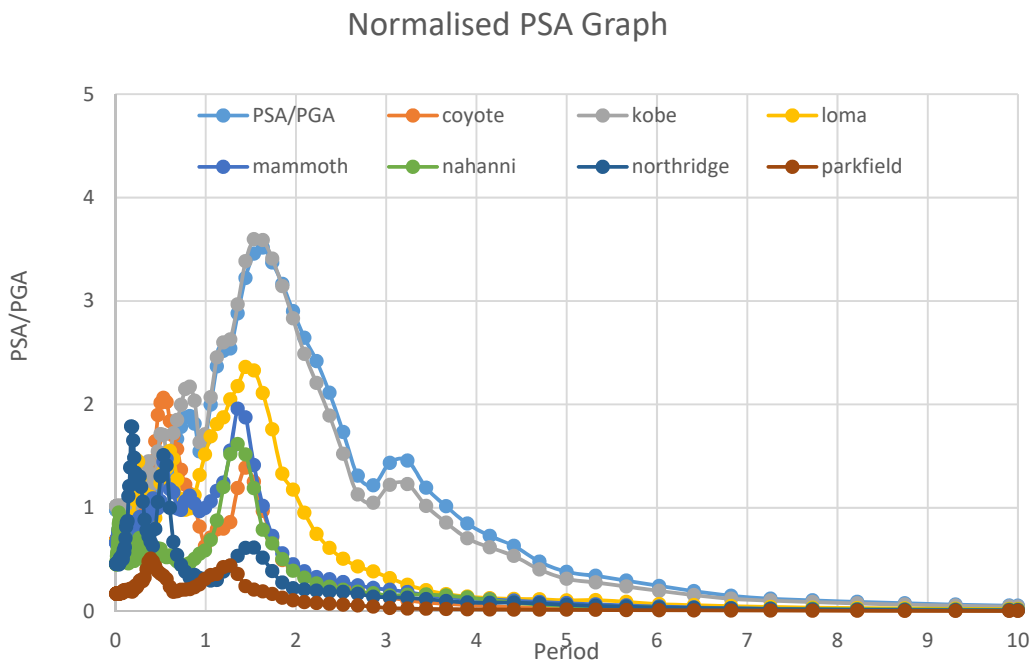

Fig 4.71 Combined PSA/PGA vs Period

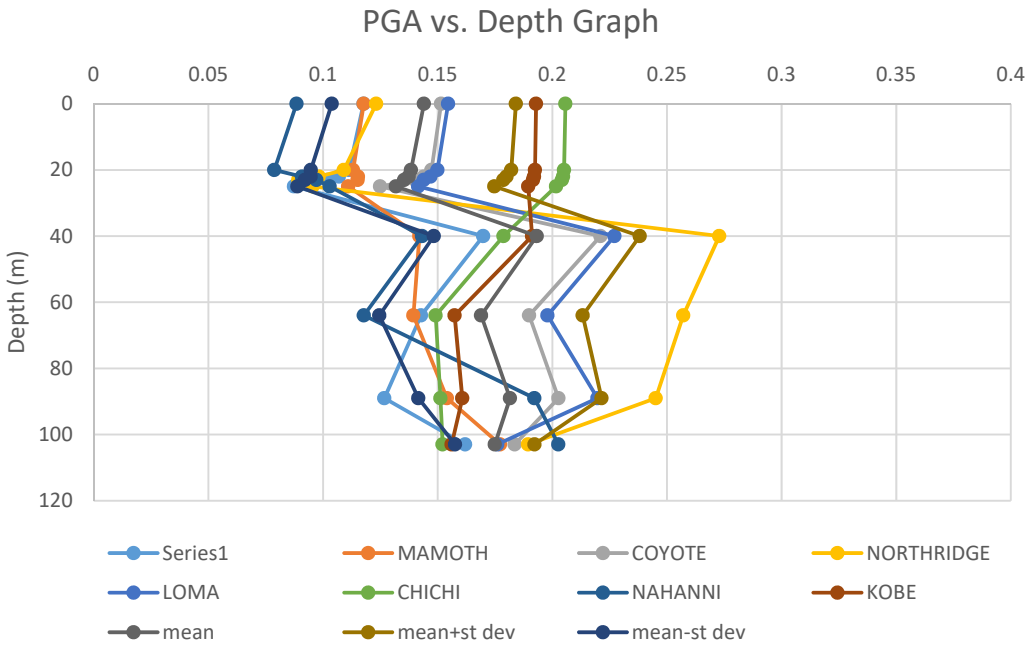

Fig 4.72 Combined PGA versus depth

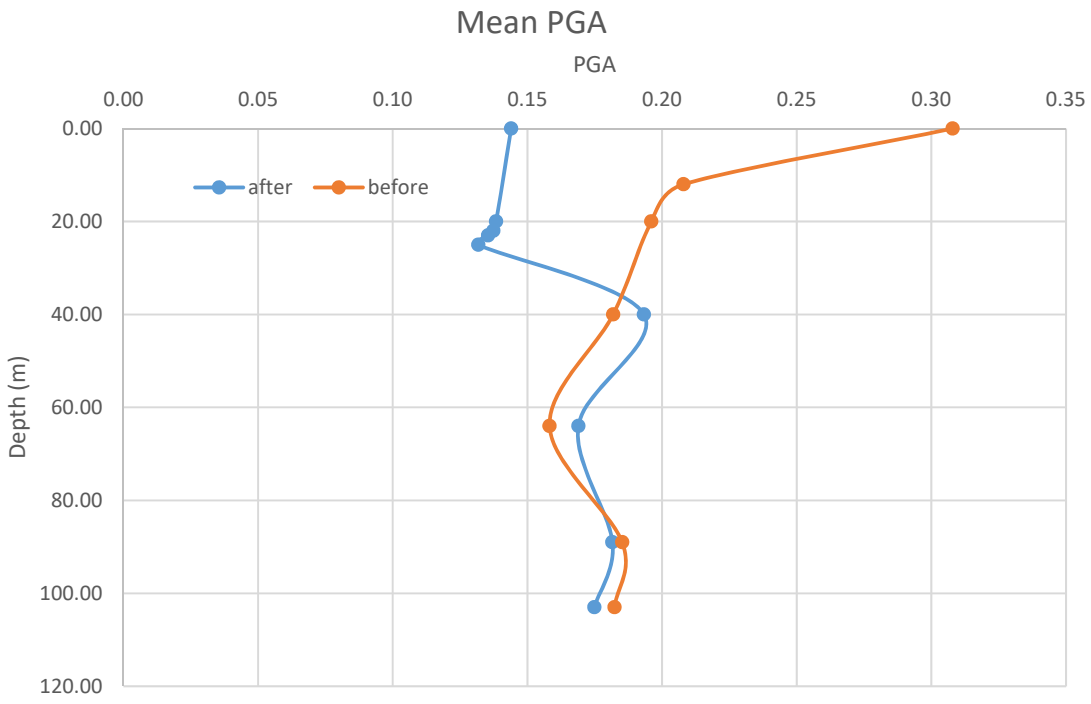

Fig 4.73 Comparison of mean PGA before and after ground improvement

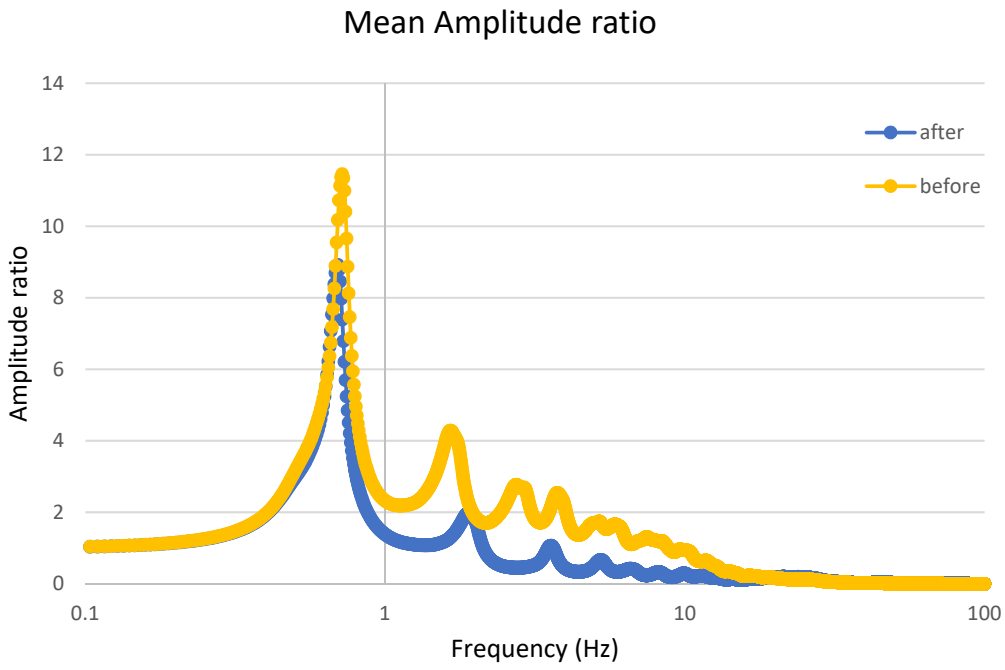

Fig 4.74 Comparison of mean amplitude ratio before and after ground improvement

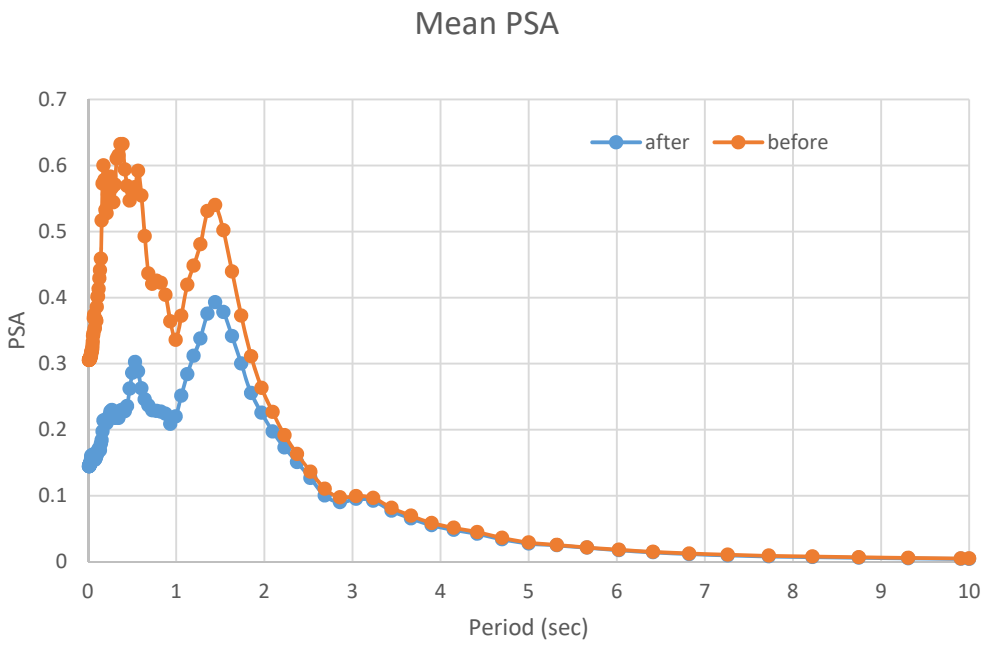

Fig 4.75 Comparison of mean PSA before and after ground improvement

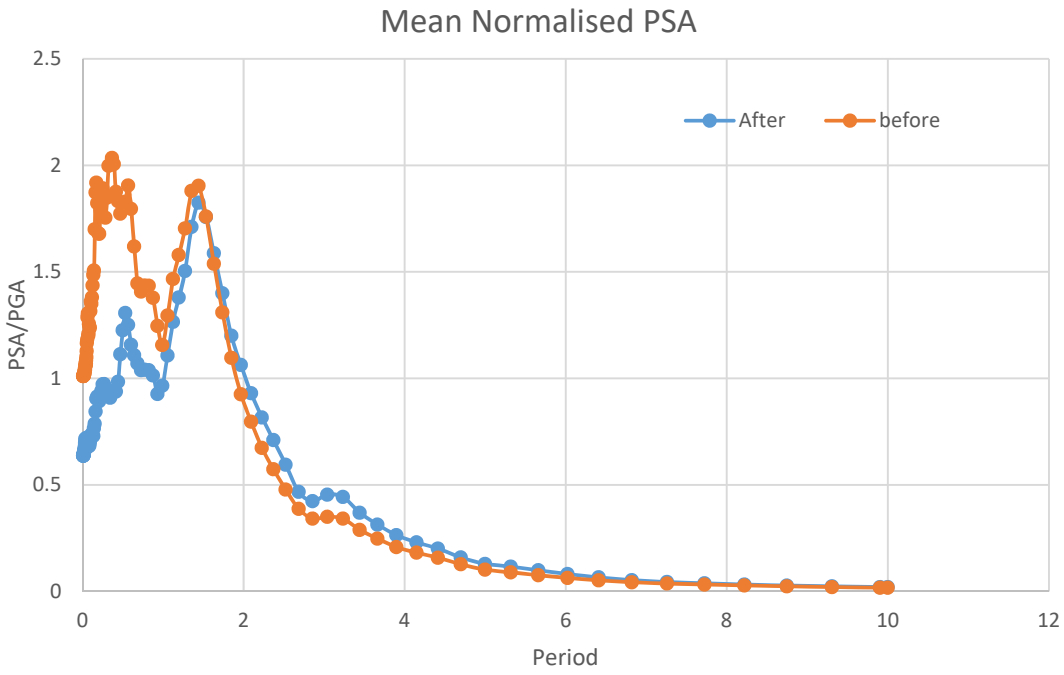

Fig 4.76 Comparison of mean PSA/PGA before and after ground improvement

4.5 Summary:

From the detailed site specific analysis, it has been observed that after ground improvement the maximum PSA value has been found in Chichi earthquake and minimum in Nahanni earthquake. While before ground improvement Mammoth earthquake gave the maximum PSA and Nahanni was still the minimum. Ground improvement caused Kobe earthquake to give the minimum amplitude ratio and Nahanni the maximum. But before ground improvement Mammoth earthquake gave the maximum amplitude ratio and Nahanni earthquake the minimum. In case of PGA value, after ground improvement the mean PGA value changed significantly of all the earthquakes. The value changed to 0.15g from 0.30g. Amplitude ratio & peak surface acceleration are two important parameters for structural safety during earthquake and ground improvement decreased both of the values thus increased the safety of the structure.

CHAPTER FIVE
CONCLUSIONS AND RECOMMENDATIONS

5.1 Conclusions

This study has described many of the important and practical developments designed to improve the quality of equivalent linear site response analysis. The high degree of damage is essential due to the transfer of large accelerations to high rise buildings by soil amplification. Ground Improvement is a very significant way to reduce the risk and decrease the amplitude ratio. The structural safety can be increased in a significant way with ground improvement.

The analysis has been run in two separate soil model after and before soil improvement. The shear wave velocity has been presented in the tables. Various important parameters i.e Peak Ground Acceleration (PGA), Amplitude Ratio, Peak Surface Acceleration (PSA) were determined with graphical representation in different conditions.

For the evaluation of PGA values, the site characterization has to be done and large amount of geological, seismological and geotechnical data have been studied. The treated soil gain greater stiffness and strength, reduce compressibility, and lower hydraulic conductivity and becomes effective to provide support for overlaying structures and to reduce seismic hazards.

(1) After combining all the earthquake's mean value, PGA value has been significantly changed from 0.3g to 0.15g after improvement. This change has been occurred as shear wave velocity has been increased and soil property has been converted to rock property. According to BNBC, PGA value in rock is 0.15g.

(2) Peak value of amplitude ratio in the combined graph decreased after soil improvement. Though the frequency has been almost same.

(3) Ground response analysis has been performed to obtain representative response spectra at the ground surface based on the time histories. In the Response spectra (PSA) graph the peak value has been decreased after ground improvement. In Chapter two, figure 2.4 the response spectra according to BNBC gives peak value in first one second, where in chapter four, the analysis shows peak value within the first two second.

5.2 Recommendations for future Research

The testing program and empirical analysis have been conducted under the present study led to many questions and subsequent future research interests. The areas of future research have been listed below followed by brief comments:

a) A study may be undertaken to prepare guidelines for mitigation of seismic hazards of reclaimed areas.

b) A study may be conducted to determine the suitable ground improvement techniques for such areas.

c) The correlation developed from the present study is done by using eight earthquakes data. Using more data correlation can be refined.

d) Ground response analysis may be performed in the reclaimed areas of Bangladesh.

e) A study may be conducted to make a GIS Map of Bangladesh based on shear wave velocity.

References

Ali, M.H. and Choudhury, J.R. (1992), Tectonics and earthquake occurrence in Bangladesh, 36th annual convention of the institute of engineers, Bangladesh, Dhaka,1: pp. 4-8.

BNBC (1993). Bangladesh National Building Code, 1993. Housing and Building Research Institute. (HBRI) and Bangladesh Standard Testing Inst.(BSTI), Bangladesh.

BSSC (2000), Building Seismic Safety Council, USA, NEHRP Recommended Provisions for Seismic Regulations for new Buildings and Other Structures.

Bolt, B.A. (1987), Seismic Strong Motion Synthetics, Academic Press, Orlando.

GSB (1991), Final report by the Committee of Experts on Earthquake Hazard Minimization, Geological Survey of Bangladesh.

Hashash, Y., Park, D. and Tsai, C. C., Philips, C. and Groholski, D.R. (2016), DEEPSOIL 1-D Wave Propagation Analysis Program for Geotechnical Site Response Analysis of Deep Soil Deposits, Version 6.1, Tutorial and User Manual, University of Illinois at Urbana- Campaign.

Kramer, S. L. (1996), Geotechnical earthquake engineering. Upper Saddle River, N.J.: Prentice Hall.

Kottke, A. R., and Rathje E. M. (2008), Technical Manual for Strata, Pacific Earthquake Engineering Research Center.

Majdeddin S. and Hossaini MM, (2010), Comparative study on the equivalent linear and the fully nonlinear site response analysis approaches, Saudi Society for Geosciences.

Sharifuddin, M. and Ansary, M.A, (2001), Earthquake Hazard Analysis for Bangladesh, Bangladesh University of Engineering and Technology (BUET).

Zalachoris G. and Rathje E.M, (2015), Evaluation of One-Dimensional Site Response Techniques Using Borehole Arrays, ASCE.